NASA Reference Publication 1337

January 1994

Present State of Knowledge of the Upper Atmosphere 1993: An Assessment Report

Report to Congress

M. J. Kurylo,
J. A. Kaye,
R. F. Hampson,
and A. M. Schmoltner

NASA Office of Mission to Planet Earth
Science Division
Washington, D.C.

Preface

NASA has relied heavily on the entire scientific community, national and international, in its effort to provide a better understanding of the upper atmosphere and its perturbation in response to natural phenomenon and human activities. The lists of contributors to the individual sections in this report are given in Section G. We are indebted to those who gave their time and knowledge.

Michael J. Kurylo

Jack A. Kaye

Robert F. Hampson

Anne-Marie Schmoltner

PRECEDING PAGE BLANK NOT FILMED

TABLE OF CONTENTS

PRECEDING PAGE BLANK NOT FILMED

PAGE N INTENTIONALLY BLANK

SECTION D:
CONCENTRATIONS, LIFETIMES, AND TRENDS OF CHLOROFLUOROCARBONS (CFCS), HALONS, AND RELATED MOLECULES IN THE ATMOSPHERE

SECTION E:
THE ATMOSPHERIC EFFECTS OF STRATOSPHERIC AIRCRAFT: INTERIM ASSESSMENT REPORT OF THE NASA HIGH-SPEED RESEARCH PROGRAM

SECTION F:
CHEMICAL KINETICS AND PHOTOCHEMICAL DATA FOR USE IN STRATOSPHERIC MODELING 69

SECTION A

INTRODUCTION

In compliance with the Clean Air Act Amendments of 1990, Public Law 101-549, the National Aeronautics and Space Administration (NASA) has prepared this Report on the state of our knowledge of the Earth's upper atmosphere, and particularly, of stratospheric ozone. The Report for the year 1993 presents new findings since the last Report in 1990 and is printed in two parts. Part I (Research Summaries) summarizes the objectives, status, and accomplishments of the research tasks supported under NASA's Upper Atmosphere Research Program (UARP) and Atmospheric Chemistry Modeling and Analysis Program (ACMAP). It consists of two documents, the NASA UARP Research Summaries 1990-1991, issued in January 1992, and the NASA UARP and ACMAP Research Summaries 1992-1993, which will be issued in early 1994. Part II (this document) presents summaries of several scientific assessments of our current understanding of the chemical composition and physical structure of the stratosphere, in particular how the abundance and distribution of ozone is predicted to change in the future. These reviews include: (Section B) "Scientific Assessment of Ozone Depletion: 1991"; (Section C) "Methyl bromide and the Ozone Layer: A Summary of Current Understanding", published in 1992; (Section D) "Concentrations, Lifetimes, and Trends of Chlorofluorocarbons (CFCs), Halons, and Related Molecules in the Atmosphere"; (Section E) "The Atmospheric Effects of Stratospheric Aircraft: Interim Assessment Report of the NASA High-Speed Research Program"; (Section F) "Chemical Kinetics and Photochemical Data for Use in Stratospheric Modeling"; and (Section G) a list of the contributors to this Report.

For over two decades scientists have postulated that certain pollutants directly associated with human activity could cause harmful effects by reducing the amount of stratospheric ozone. Initial concerns focused on supersonic aircraft emissions of NO and NO_2, and then shifted to the issue of chlorine loading of the stratosphere from CFCs. Now there is compelling evidence that human activity can, in fact, change the atmospheric environment on a global scale. In recognition of the importance of understanding such perturbations, Congress directed NASA in June 1975 to "develop and carry out a comprehensive program of research, technology, and monitoring of the phenomena of the upper atmosphere so as to provide for an understanding of and to maintain the chemical and physical integrity of the Earth's upper atmosphere."

Responding to this Congressional mandate, NASA implemented a long-range scientific research program, conducted through UARP and ACMAP, aimed at developing a comprehensive understanding of processes in the upper atmosphere. In the near-term NASA has the responsibility of providing triennial reports to Congress and concerned regulatory agencies on the status of upper atmospheric research, including scientific assessments of potential effects of human activities on the atmosphere, and particularly, on stratospheric ozone.

Many governments around the world, including the United States, have recognized that the ozone layer must be protected in order to protect human health and aquatic and terrestrial ecosystems from damage due to enhanced levels of ultraviolet radiation. In particular, it was recognized that the use of chemicals containing chlorine (in the form of chlorofluorocarbons, CFCs, and hydrochlorofluorocarbons, HCFCs) and bromine (mainly in the form of halons and methyl bromide) constitute a potential threat to the ozone layer. More than twenty nations, including the United States, signed the Vienna Convention for the Protection of the Ozone Layer in Vienna, Austria, in 1985, and the Montreal Protocol on Substances that Deplete the Ozone Layer, in Montreal, Canada, in 1987. Subsequent amendments (London, UK, 1990 and

Copenhagen, Denmark, 1992) strengthened the Montreal Protocol by calling for an accelerated CFC phaseout schedule and added to the list of regulated compounds. The Vienna Convention and the Montreal Protocol both call for all regulatory decisions to be based on a scientific understanding of the issues, and specifically the Montreal Protocol called for international scientific assessments at least every four years.

The 1991 scientific assessment was coordinated by NASA, the National Oceanic and Atmospheric Administration (NOAA), the United Kingdom Department of the Environment (DOE), the United Nations Environment Program (UNEP), and the World Meteorological Organization (WMO). The executive summary and scientific summaries of the assessment chapters are reproduced in Section B.

The understanding of the atmospheric science of methyl bromide was reviewed (see Section C). The impact of methyl bromide on the ozone layer was determined to be significant since bromine, on an atom by atom basis, is 30-60 times more efficient than chlorine in destroying ozone. 25±10% of the methyl bromide emissions are estimated to be anthropogenic, stemming in large part from the its use as a fumigant for soils, commodities, and structures.

The report "Concentrations, Lifetimes, and Trends of Chlorofluorocarbons (CFCs), Halons, and Related Molecules in the Atmosphere" was prepared to assess the status of our knowledge of the atmospheric lifetimes of the title molecules. The executive summary and chapter summaries are included here as section D. The report provides critical analyses of all the information needed to determine lifetimes with two complementary techniques. Lifetimes can be inferred from observed concentrations and estimated emission rates using an atmospheric model. They can also be calculated from atmospheric chemistry/transport models using detailed knowledge of the processes associated with their atmospheric chemistry, including absorption cross sections and chemical destruction. Specific material included in the report for the title molecules are tropospheric and stratospheric concentrations, estimated production and emission rates, inference of lifetimes using atmospheric models, spectroscopy, kinetics, and aqueous phase chemistry, and simulation with multi-dimensional atmospheric chemistry/transport models. This report, prepared with extensive national and international input, will be published as a NASA Reference Publication in 1994.

The environmental impact of proposed high-speed, i.e. supersonic, civil transport aircraft on the ozone layer is also being investigated. An interim assessment report from NASA's High Speed Research Program was issued in June 1993, and the executive summary and chapter summaries are included in this Report as Section E. The possible impact of the entire range of effluents from the aircraft was considered using improved assessment models and detailed fleet emission scenarios. The emphasis was on the effects of NO_x and H_2O on the atmospheric ozone content, as well as increases in particle surface area caused by the effluents of aircraft which is of concern due to the importance of heterogeneous chemistry on sulfate aerosols.

The biennial review of the status of kinetics and photochemistry by the NASA Panel for Data Evaluation is an important document for the atmospheric sciences community. It provides a regular focus that brings together the laboratory measurements and the theoretical studies and establishes a reference standard for atmospheric modeling. The most recent recommendations of this panel are published as Report JPL 92-20 "Chemical Kinetics and Photochemical Data for Use in Stratospheric Modeling," and pertinent sections are included as Section F in this Report.

The contributors to all of the above are listed in Section G.

SECTION B

SCIENTIFIC ASSESSMENT OF OZONE DEPLETION: 1991

EXECUTIVE SUMMARY

RECENT MAJOR SCIENTIFIC FINDINGS

Over the past few years, there have been highly significant advances in the understanding of the impact of human activities on the Earth's stratospheric ozone layer and the influence of changes in chemical composition on the radiative balance of the climate system. Specifically, since the last international scientific review (1989), there have been five major advances:

- **Global Ozone Decreases**: Ground-based and satellite observations continue to show decreases of total column ozone in winter in the northern hemisphere. For the first time, there is evidence of significant decreases in *spring and summer* in both the northern and southern hemispheres at middle and high latitudes, as well as in the southern winter. No trends in ozone have been observed in the tropics. These downward trends were larger during the 1980s than in the 1970s. The observed ozone decreases have occurred predominantly in the *lower* stratosphere.

- **Polar Ozone:** Strong Antarctic ozone holes have continued to occur and, in four of the past five years, have been deep and extensive in area. This contrasts to the situation in the mid-1980s, where the depth and area of the ozone hole exhibited a quasi-biennial modulation. Large increases in surface ultraviolet radiation have been observed in Antarctica during periods of low ozone. While no extensive ozone losses have occurred in the Arctic comparable to those observed in the Antarctic, localized Arctic ozone losses have been observed in winter concurrent with observations of elevated levels of reactive chlorine.

- **Ozone and Industrial Halocarbons:** Recent laboratory research and re-interpretation of field measurements have strengthened the evidence that the Antarctic ozone hole is primarily due to chlorine- and bromine-containing chemicals. In addition, the weight of evidence suggests that the observed middle- and high-latitude ozone losses are largely due to chlorine and bromine. Therefore, as the atmospheric abundances of chlorine and bromine increase in the future, significant additional losses of ozone are expected at middle latitudes and in the Arctic.

- **Ozone and Climate Relations:** For the first time, the observed global lower-stratospheric ozone depletions have been used to calculate the changes in the radiative balance of the atmosphere. The results indicate that, over the last decade, the observed ozone depletions would have tended to cool the lower stratosphere at middle and high latitudes. Temperature data suggest that some cooling indeed has taken place there. The observed lower-stratospheric ozone changes and calculated temperature changes would have caused a decrease in the radiative forcing of the surface-troposphere system in the middle- to high-latitudes that is larger in magnitude than that predicted for the CFC increases over the last decade. In addition, the ozone depletion may indeed have offset a significant fraction of the radiative forcing due to increases of all greenhouse gases over the past decade.

- **Ozone Depletion and Global Warming Potentials (ODPs and GWPs):** A new semi-empirical, observation-based method of calculating ODPs has better quantified the role of polar processes in this index. In addition, the direct GWPs for tropospheric, well-mixed, radiatively active species have been recalculated. However, because of the incomplete understanding of tropospheric chemical processes, the indirect GWP of methane has not, at present, been quantified reliably. Furthermore, the concept of a GWP may prove inapplicable for the very short-lived, inhomogeneously mixed gases, such as the nitrogen oxides. Hence, many of the *indirect* GWPs reported in 1990 by the Intergovernmental Panel on Climate Change (IPCC) are likely to be incorrect.

SUPPORTING EVIDENCE AND RELATED ISSUES

Global Ozone

- Independent observations from the ground-based Dobson and M-83/124 instruments and the TOMS satellite instrument all show, for the first time, that there are significant decreases in total-column ozone, after accounting for known natural variability, in winter and now in spring and summer in both the northern and southern hemispheres at middle and high latitudes, but not in the tropics. The following table illustrates some of these points.

Total Ozone Trends (% per decade with 95% confidence limits)

	TOMS: 1979-91			Ground-based: 26°N - 64°N	
Season	45°S	Equator	45°N	1979-1991	1970-1991
Dec-Mar	-5.2 ± 1.5	+0.3 ± 4.5	-5.6 ± 3.5	-4.7 ± 0.9	-2.7 ± 0.7
May-Aug	-6.2 ± 3.0	+0.1 ± 5.2	-2.9 ± 2.1	-3.3 ± 1.2	-1.3 ± 0.4
Sep-Nov	-4.4 ± 3.2	+0.3 ± 5.0	-1.7 ± 1.9	-1.2 ± 1.6	-1.2 ± 0.6

- There is strong *combined* observational evidence from balloonsondes, ground-based Umkehr, and the SAGE satellite instruments that, over the past decade, annual-average ozone has decreased in the middle- and high-latitude stratosphere below 25 km (about 10% near 20 km).

- Ozone losses in the upper stratosphere have been observed by ground-based Umkehr and SAGE satellite instruments. Changes in the shape of the vertical distribution of ozone near 40 km are qualitatively consistent with theoretical predictions, but are smaller in magnitude.

- Measurements indicate that ozone levels in the troposphere up to 10 km above the few existing balloonsonde stations at northern middle latitudes have increased by about 10% per decade over the past two decades. However, the data base for ozone trends in the upper troposphere, where it is an effective greenhouse gas, are sparse and inadequate for quantifying its contribution to the global radiative balance. It should be noted that the response of ozone in the upper troposphere is particularly sensitive to oxides of nitrogen injected by aircraft.

- The temperature record indicates that a small cooling (about 0.3°C per decade, globally averaged) has occurred in the lower stratosphere over the last two decades, which is in the sense of that expected from the observed ozone change.

- Increases continue in the atmospheric abundances of source gases that affect ozone and the radiative balance. Although methane has continued to increase in the atmosphere, the rate of increase has slowed, for reasons that are not understood. Methyl bromide is the major contributor to stratospheric bromine (15 pptv). The sources of methyl bromide are not well characterized; however, significant anthropogenic emissions have been suggested.

- Recent laboratory studies have identified key heterogeneous reactions and have allowed a more-quantitative assessment of the role of global stratospheric sulfate aerosols in leading to enhanced abundances of reactive chlorine species.

- Limited observations suggest that the abundance of chlorine monoxide (ClO) in the lower stratosphere at northern middle latitudes is greater than that predicted by models containing only currently known gas-phase chemistry, and the observed seasonal and latitudinal dependences are inconsistent with those predicted. Some new studies that incorporate currently known heterogeneous processes provide an improved simulation for some observed gases, such as ClO and nitric acid.

- Present models containing only gas-phase processes cannot simulate the observed seasonal ozone depletions at middle and high latitudes. However, models incorporating currently known heterogeneous processes on sulfate aerosols predict substantially greater ozone depletion (e.g., a factor of 2 - 3 at middle latitudes) from chlorine and bromine compounds compared to models containing only gas-phase processes. Indeed, the heterogeneous models simulate most of the observed trend of column ozone in middle latitudes in summer, but only about half of that in winter.

- There is not a full accounting of the observed downward trends in global ozone. Plausible mechanisms include (i) local heterogeneous chemistry on stratospheric sulfate aerosols (as evidenced by, for example, elevated levels of ClO and the presence of sulfate aerosols at the altitudes of the observed ozone depletion) and (ii) the transport of both ozone-depleted and chemically perturbed polar air to middle latitudes (as evidenced by high levels of reactive chlorine and low levels of reactive nitrogen, which is a characteristic of chemically perturbed polar air). Although other possible mechanisms cannot be ruled out, those involving chlorine and bromine appear to be largely responsible for the ozone loss and are the only ones for which direct evidence exists.

- Since the middle latitude ozone losses are apparently due in large part to chlorine and bromine, greater ozone losses are expected as long as the atmospheric levels of these compounds continue to increase. With the increases in the levels of chlorine and bromine that are estimated for the year 2000, the additional ozone losses during the 1990s are expected to be comparable to those already observed for the 1980s.

- There are numerous ways in which further increases in stratospheric halogen abundances can be reduced. The table below illustrates the effects of reducing the emissions of several types of halocarbons. Four aspects are shown: (i) the change in peak chlorine loading, (ii) the times at which chlorine abundances have decreased back to 2 ppbv (the abundance in the late 1970s, which is when the Antarctic ozone hole started and when the accelerated trends in total-column ozone losses in the northern hemisphere began); (iii) the times at which chlorine abundances have decreased back to 3 ppbv (the abundance in the mid-late 1980s); and (iv) a measure of the cumulative ozone loss for the time period that the chlorine

levels are above 3 ppbv. All of the values in the table are relative to the reference scenario (AA).

- Stratospheric bromine is 30 - 120 times more efficient than stratospheric chlorine in destroying ozone on a per atom basis. Therefore, 1 pptv of stratospheric bromine is equivalent to 0.03 - 0.12 ppbv of stratospheric chlorine.

Scenarios for Reducing Chlorine Emissions

Scenario	Peak Cl (ppbv)	Year at 3 ppbv	Year at 2 ppbv	Integral (Cl>3 ppbv)
AA	**4.1 (ppbv)**	**2027**	**2060**	**22.7 ppbv-yr**
AA3	-0.18	-10 yrs	-7 yrs	-7.6
D	-0.03	0	0	-1.3
D3	-0.10	0	0	-2.9
E	0.00	-7	-3	-2.0 *
E3	-0.03 *	-10	-3	-4.4 *
F20	+0.01	0	0	+0.8
F40	+0.02	+1	0	+1.5
G20	+0.01	+5	+2	+4.2
AA3 + D3	-0.21	-11	-7	-10.4

* These values should be reduced by a factor of about 2 - 3 when evaluating ozone loss rather than chlorine loading.

Definitions of scenarios:

AA: Montreal Protocol (10 yr lag of 10% of CFCs plus CCl_4; no lag for CH_3CCl_3 and Halons). HCFC-22 increases at 3% per year from 1991 to 2020, ramps to 0 by 2040. No substitution of CFCs with HCFCs.

o Non-substitution scenarios:

AA3: 3 year acceleration of CFCs and CCl_4 schedules.
D: 3 year acceleration of CH_3CCl_3 schedule.
D3: CH_3CCl_3 on the accelerated CFC phase-out schedule.
E: HCFC-22 ramp to zero between 2000 and 2020.
E3: HCFC-22 on the accelerated CFC phase-out schedule.

o Substitution scenarios:

HCFC substitutions begin in 1995, no growth to 2000, 3% per year to 2020, ramp to zero by 2030. HCFC-A has a 2 year lifetime, one chlorine, and an ODP of 0.013. HCFC-B has a 20 year lifetime, one chlorine, and an ODP of 0.13.

F20: 20% initial substitution, HCFC-A.
F40: 40% initial substitution, HCFC-A.
G20: 20% initial substitution, HCFC-B.

Polar Ozone

- The Antarctic ozone hole in 1991 was as deep and as extensive in area as those of 1987, 1989, and 1990. The low value of total-column ozone measured by TOMS in early October in 1991 was 110 Dobson units, which is a decrease of about 60% compared to the ozone levels prior to the late 1970s. The previously noted quasi-biennial modulation of the severity of the ozone hole did not occur during the past three years. This apparent lack of variability in recent years may imply that halogen chemistry is becoming dominant over dynamically induced fluctuations on Antarctic ozone depletion.

- Recent laboratory studies of heterogeneous processes, reevaluated field measurements, and modeling studies have strengthened the confidence that the cause of the Antarctic ozone hole is primarily chlorine and bromine emissions.

- High concentrations of ClO have been observed in winter in the Arctic stratosphere between 16 -20 km. These observations have been incorporated into diagnostic models that have calculated localized ozone depletions of about 10% at these altitudes over a period of about a month, which are consistent with concurrent ozone measurements.

Ozone/Climate Relations

- The ozone losses observed in the lower stratosphere over the last decade are predicted to have increased the visible and ultraviolet incoming solar radiation reaching the surface/troposphere system and decreased the downward infrared radiation reaching the surface/troposphere system. For models that allow for the temperature of the stratosphere to adjust to the loss of ozone, the net effect is a decrease in radiative forcing. For middle and high latitudes throughout the year, the magnitude of this decrease may be larger than the predicted increases in the radiative forcing due to the increased abundances of CFCs over the last decade. Indeed, this ozone-induced decrease in radiative forcing could be offsetting a significant fraction of the increased forcing attributed to the increases in the abundances of all greenhouse gases over the same period. Changes in the global annual-average radiative forcing due to the observed ozone depletion are predicted to be comparable in magnitude, but opposite in sign, to those attributed to the CFCs over the last decade.

- Current tropospheric models exhibit large differences in their predictions of changes in ozone, the hydroxyl radical, and other chemically active gases due to emissions of methane, nonmethane hydrocarbons, carbon monoxide, and nitrogen oxides. This arises from uncertainties in the knowledge of background chemical composition and an inadequate understanding of chemical reactions and dynamical processes. Hence, these deficiencies limit the accuracy of predicted changes in the abundance and distribution of tropospheric ozone, which is a greenhouse gas, and in the lifetimes of a number of other greenhouse gases, including the HCFCs and HFCs, which depend upon the abundance of the hydroxyl radical.

Ozone Depletion and Global Warming Potentials (ODPs and GWPs)

- Steady-state and time-dependent ODPs have been recalculated with improved models that have incorporated more-accurate reaction rate coefficients and absorption cross sections and known heterogeneous processes on sulfate aerosols. The numerical values are generally similar to those in previous assessments.

- A new semi-empirical, observation-based method of calculating ODPs has been developed. The resulting values are generally larger (up to a factor of two as compared to some model-

based estimates) for species with long stratospheric lifetimes (e.g., HCFC-22 and HCFC-142b) and slightly smaller for species with short stratospheric lifetimes (e.g., carbon tetrachloride and methyl chloroform). Since this approach utilizes more atmospheric observations and less model calculations in characterizing polar ozone losses, it is considered to be better than standard model ODPs, at least in the polar regions.

- The *direct GWPs* (with five different time horizons: 20, 50, 100, 200, and 500 years) for tropospheric, well-mixed, radiatively active species have been recalculated using updated lifetimes for methane, nitrous oxide, and the halocarbons and following the same methodology of IPCC (1990). With the exception of methane, new GWP results indicate only modest changes from the IPCC values, but uncertainties still exist in these calculations due to limitations in knowledge of the carbon cycle.

- Because of incomplete understanding of tropospheric chemical processes, the *indirect GWP* of methane has not been quantified reliably at the time of this report, although improvements and quantifications of uncertainties in the near future are highly likely. The signs of the net changes in radiative forcing from known indirect effects have been established for some of the trace gases: methane, carbon monoxide, and nonmethane hydrocarbons, which are all positive. The sign of the changes in radiative forcing due to the nitrogen oxides cannot currently be established. Furthermore, the basic concept of a GWP may indeed prove to be inapplicable for the very short-lived, inhomogeneously mixed gases, such as the nitrogen oxides and the nonmethane hydrocarbons. Hence, the IPCC (1990) *indirect* GWPs are not only uncertain, but many are also likely to be incorrect (e.g., for the nitrogen oxides).

Related Issues

- **Ultraviolet radiation.** Significant increases in ultraviolet radiation have been observed over Antarctica in conjunction with periods of intense ozone depletion. Under clear-sky conditions, these increases are consistent with theoretical predictions. Furthermore, a Erythemal Radiative Amplification Factor of 1.25 ± 0.20 has been deduced from simultaneous measurements of column ozone and surface ultraviolet radiation at a clean air site, which is in agreement with a model-calculated value of 1.1. Therefore, for the first time, the response of ground-level ultraviolet radiation to changes in column ozone has been observed and quantified.

- **Supersonic aircraft.** A previous, independent assessment of the impact of a projected fleet of supersonic aircraft on stratospheric ozone has reported the prediction that the ozone loss increases with the amount of nitrogen oxides emitted. These models used gas-phase chemistry and assessed ozone loss for the case of 500 aircraft flying at Mach 2.4 between 17 - 20 km with an annual fuel use of 7×10^{10} kg/yr. The annual-average loss of column ozone at middle latitudes in the northern hemisphere is predicted to be 2 - 6%. For a comparable fleet operated at Mach 3.2 between 21 - 24 km, the comparable column ozone losses are 7 - 12%. However, recent evidence has shown that reactions on sulfate aerosols can change the partitioning of nitrogen oxides. Two model studies incorporating this heterogeneous chemistry have recently reexamined the Mach 2.4 case and found substantially less ozone change (-0.5% to +0.5%). These implications are being examined as part of a separate assessment.

- **Shuttles and rockets.** The increase in the abundance of stratospheric chlorine from one projection of U. S. annual launches of nine Space Shuttles and six Titan rockets is calculated to be less than 0.25% of the annual stratospheric chlorine source from halocarbons in the present day atmosphere (with maximum increases of 0.01 ppbv in the

middle and upper stratosphere in the northern middle and high latitudes). The TOMS ozone record shows no detectable changes in column ozone immediately following each of several launches of the Space Shuttle.

- **Volcanoes, ozone loss, and climate perturbations.** Major volcanic eruptions, such as Mt. Pinatubo, substantially increase the stratospheric abundance of sulfate aerosols for a few years. Since laboratory and field data show that heterogeneous processes can lead to increased levels of reactive chlorine in the stratosphere, such injections have the potential to increase ozone losses temporarily. Furthermore, the increased levels of stratospheric sulfate aerosols are predicted to warm the lower stratosphere by about 4°C (which has been observed) and cool the Earth's surface by a much smaller amount.

- **Tropospheric sulfate aerosols and climate.** Fossil fuel emissions over the past century have increased the tropospheric sulfate aerosol concentrations. Their contribution to the direct radiative forcing of the clear-sky northern hemisphere is opposite to that due to the greenhouse gases and is estimated to be a substantial fraction of the trace gas forcing.

IMPLICATIONS FOR POLICY FORMULATIONS

The findings and conclusions of the research of the past few years have several major implications as input to policy decisions regarding human-influenced substances that lead to stratospheric ozone depletions and to changes in the radiative forcing of the climate system:

- **Continued global ozone losses:** Even if the control measures of the amended Montreal Protocol (London, 1990) were to be implemented by all nations, the current abundance of stratospheric chlorine (3.3 - 3.5 ppbv) is estimated to increase during the next several years, reaching a peak of about 4.1 ppbv around the turn of the century. With these increases, the additional middle-latitude ozone losses during the 1990s are expected to be comparable to those observed during the 1980s, and there is the possibility of incurring wide-spread losses in the Arctic. *Reducing these expected and possible ozone losses requires further limitations on the emissions of chlorine- and bromine-containing compounds.*

- **Approaches to lowering global risks:** Lowering the peak and hastening the subsequent decline of chlorine and bromine levels can be accomplished in a variety of ways, including an accelerated phase-out of controlled substances and limitations on currently uncontrolled halocarbons. Chlorine. A significant reduction in peak chlorine loading (a few tenths of a ppbv) can be achieved with accelerated phase-out schedules of CFCs, carbon tetrachloride, and methyl chloroform. Even stringent controls on HCFC-22 would not significantly reduce peak chlorine loading (at most 0.03 ppbv, especially when ODP weighted), but do hasten the decline of chlorine. Bromine. A 3-year acceleration of the phase-out schedule for the Halons would reduce peak bromine loading by about 1 pptv. If the anthropogenic sources of methyl bromide are significant and their emissions can be reduced, then *each* 10% reduction in methyl bromide would rapidly result in a decrease in stratospheric bromine of 1.5 pptv, which is equivalent to a reduction in stratospheric chlorine of 0.045 to 0.18 ppbv. This gain is comparable to that of a three-year acceleration of the scheduled phase-out of the CFCs.

- **Elimination of the Antarctic ozone hole:** The phase-out schedule of the amended Montreal Protocol, *if fully complied by all nations* and if there are no *continued* uses of HCFCs, affords the opportunity to return to stratospheric chlorine abundances of 2 ppbv sometime between the middle and the end of the next century. This is the level at which the

Antarctic ozone hole appeared in the late 1970s and hence is about the level that is thought to be necessary (other conditions assumed constant, including bromine loading) to eliminate the ozone hole. *Such levels could never have been reached under the provisions of the original Protocol (Montreal, 1987).*

- **Uncertain greenhouse role of CFCs:** The weight of evidence suggests that a large part of the observed lower stratospheric decrease in ozone is the result of CFC emissions. Furthermore, the radiative impact of this ozone decrease may have largely offset the predicted direct radiative perturbations, at middle to high latitudes, due to the CFCs increases over the last decade. *Hence, even the sign of the overall radiative effect of CFC increases on the climate system over the last decade is uncertain.*

- **Utility of GWPs:** The direct GWPs are a useful indicator of the relative radiative effects of long-lived, well-mixed, radiatively active trace species. However, GWPs may be inapplicable for comparing the direct radiative effects of a long-lived, well-mixed gas to the indirect effects of a short-lived gas (for example, carbon dioxide to the nitrogen oxides). *For the latter need, the application of new tools, such as three-dimensional, fully coupled coupled chemistry-climate models may be required.*

CHAPTER SUMMARIES

Chapter 1—Source Gases: Concentrations, Emissions, and Trends

The major anthropogenic source gases implicated directly in halogen induced stratospheric ozone loss, i.e., chlorofluorocarbons (CFCs), hydrochlorofluorocarbon-22 (HCFC-22), the halons, methyl chloroform and carbon tetrachloride, continue to grow in concentration in the background troposphere of both hemispheres. Total tropospheric chlorine is increasing by ≈0.1 parts per billion by volume (ppbv) per year. CFCs contribute approximately 75 percent to this increase, methyl chloroform 13 percent, and HCFC-22 ≈5 percent.

The 1989 global mean concentrations and trends of the various source gases that can directly or indirectly influence the global abundance of stratospheric and tropospheric ozone are given in Table 1-1. In general, the data are similar to those reported for 1987 in the previous assessment (WMO, 1990b), but there have also been some important new developments.

CFC-11 and CFC-12 trends have not changed significantly since the last assessment. The global CFC-113 trend in 1989 (≈5–6 parts per trillion by volume (pptv), 9 percent) is higher than observed in 1987 (≈4–5 pptv, 7 percent). Absolute calibration remains uncertain (±10 percent). The global average CCl_4 concentration for 1989 (≈107 pptv) is lower than that reported for 1987 in the last assessment (≈140 pptv), due essentially to a change in calibration based on a comparison of Atmospheric Lifetime Experiment–Global Atmospheric Gases Experiment (ALE–GAGE) data with data collected in several other programs. Absolute calibration remains uncertain (±10 percent).

The CH_3CCl_3 global trend in 1989 from the ALE–GAGE program (5.5 pptv, 3.7 percent) is lower than that reported for 1987 (6.0 pptv, 4.0 percent). Absolute calibration remains uncertain (±10 percent), and the ALE–GAGE calibration could be high by ≈15 percent, inferring a global mean 1989 concentration of 135 pptv rather than 150 pptv based on the current ALE–GAGE calibration scale. The oceans are a significant sink for CH_3CCl_3, implying that computed OH levels are 5–10 percent too high if this sink is ignored. These variations are well within the uncertainty of the rate of methyl chloroform-hydroxyl radical reaction (±40 percent). By analogy, HCFCs and HFCs may also have an oceanic sink although HCFCs and HFCs are more resistant to hydrolysis than CH_3CCl_3. Assuming that the ALE–GAGE calibration and industrial emissions are accurate, then the CH_3CCl_3 trend implies that the CH_3CCl_3 sink and hence global OH levels are increasing by 1.0±0.8 percent per year.

Spectroscopic and gas chromatographic measurements of HCFC-22 both show similar global increases of 6–7 pptv per year. The calibration uncertainty is ±10 percent.

Exponential increases in the bromine containing chemicals Halon-1211 and -1301 have been observed (≈15 percent and ≈20 percent per year respectively), although absolute calibration remains quite uncertain (±15 and ±40 percent respectively). Methyl bromide is the major source of stratospheric bromine. While the possibility of a trend in methyl bromide cannot be assessed due to lack of data, a large anthropogenic methyl bromide source has been previously suggested.

Nitrous oxide continues to increase globally about 0.8 ppbv per year. New global nitrous oxide sources have been proposed (adipic acid production, legume pastures), but the sum of all known sources is not sufficient to balance the calculated atmospheric sink.

The rate of increase of global tropospheric CH_4 continues to decline, with increases of 17–21 ppbv per year observed during 1978–1982 and 12–14 ppbv per year during 1988–1990, or even lower in the Southern Hemisphere. No satisfactory explanation of this phenomenon has been put forward. Ice core studies indicate that CH_4 growth rates have shown significant temporal variability over the past 100 years. The problem of reconciling atmospheric CH_4 observations with estimates of emission sources is severely limited by the lack of observations in major source regions. There is significant uncertainty in the direct estimates of CH_4 emissions from rice agriculture. Indian studies suggest that the global CH_4 source from rice agriculture may be significantly lower than 100 Tg (10^{12} g) per year. Recent methane isotopic studies suggest that approximately 20 percent of the total methane source (500 Tg per year) is fossil, and 10 percent is from biomass burning. The CH_4 sink due to OH oxidation may be increasing due to increasing levels of OH radical. Global levels of H_2 are increasing (0.5–0.7 percent per year), presumably partly in response to growing CH_4 levels.

Increasing CO concentrations of about 1 ppbv per year appear to be confined to the Northern Hemisphere. In the Southern Hemisphere there have been periods of CO growth (1986–1988) and decline (1983–1985), with no overall change from 1978 to 1990. Some CO sources are known to be increasing (CH_4) and others decreasing (fuel CO emissions from OECD* countries). The CO sink due to OH oxidation may also be increasing due to increasing levels of OH radical.

*Organization for Economic Cooperation and Development (OECD) countries include Australia, Austria, Belgium, Canada, Denmark, Finland, France, Germany, Greece, Iceland, Ireland, Italy, Japan, Luxembourg, Netherlands, New Zealand, Norway, Portugal, Spain, Sweden, Switzerland, Turkey, U.K., U.S., and Yugoslavia (Special Member).

Chapter 2—Ozone and Temperature Trends

Observational Record: Since the 1989 assessment, the observational record includes an additional 2.5 years of Dobson, Stratospheric Aerosol and Gas Experiment (SAGE) and Total Ozone Mapping Spectrometer (TOMS) data and a complete re-analysis of 29 ground-based M83/M124 stations in the former Soviet Union. This is complemented by a major new advance in the observational record of an internally-calibrated TOMS data set that is now independent of ground-based observations. Trend analyses of SAGE data have been extended to the lower stratosphere and the Umkehr data have been reanalyzed.

Antarctic Ozone: The Antarctic ozone hole in 1991 was as deep and as extensive in area as those of 1987, 1989, and 1990. The low value of total ozone measured in 1991 was 110 Dobson Units, a decrease of 60 percent compared with ozone levels prior to the mid-1970s. The previously noted quasi-biennial modulation of the severity of the ozone hole did not occur during the last 3 years. The area of the ozone hole was similar for these 4 years.

Trends in Total Ozone: Ground-based (Dobson and M83/M124) and satellite (TOMS) observations of total column ozone through March 1991 were analyzed, allowing for the influence of solar cycle and quasi-biennial oscillation (see table). They show that:

- The northern mid-latitude winter and summer decreases during the 1980s were larger than the average trend since 1970 by about 2 percent per decade. A significant longitudinal variance of the trend since 1979 is observed.
- For the first time there are statistically significant decreases in all seasons in both the Northern and Southern Hemispheres at mid- and high-latitudes during the 1980s; the northern mid-latitude long-term trends (1970 to 1991), while smaller, are also statistically significant in all seasons.

- There has been no statistically significant decrease in tropical latitudes from 25°N to 25°S.

Trends in the Vertical Distribution of Ozone: Balloonsonde, ground-based Umkehr, and satellite SAGE observations show that:

- Ozone is decreasing in the lower stratosphere, i.e., below 25 km, at about 10 percent per decade, consistent with the observed decrease in column ozone.
- Changes in the observed vertical distribution of ozone in the upper stratosphere near 40 km are qualitatively consistent with theoretical predictions, but are smaller in magnitude.
- Measurements indicate that ozone levels in the troposphere, over the few existing ozone sounding stations at northern mid-latitudes, have increased about 10 percent per decade over the past two decades.

Trends in Stratospheric Temperature: The temperature record indicates a small cooling (about 0.3°C per decade) of the lower stratosphere in the sense of that expected from the observed change in the stratospheric concentration of ozone.

Total Ozone Trends (% per decade with 95% confidence limits)

	TOMS: 1979-91			Ground-based: 26°N - 64°N	
Season	45°S	Equator	45°N	1979-1991	1970-1991
Dec-Mar	-5.2 ± 1.5	+0.3 ± 4.5	-5.6 ± 3.5	-4.7 ± 0.9	-2.7 ± 0.7
May-Aug	-6.2 ± 3.0	+0.1 ± 5.2	-2.9 ± 2.1	-3.3 ± 1.2	-1.3 ± 0.4
Sep-Nov	-4.4 ± 3.2	+0.3 ± 5.0	-1.7 ± 1.9	-1.2 ± 1.6	-1.2 ± 0.6

Chapter 3–Heterogeneous Processes: Laboratory, Field, and Modeling Studies

Since the previous assessment, there have been major advances in understanding the role of heterogeneous reactions on Polar Stratrospheric Clouds (PSCs) and stratospheric sulfate (H_2SO_4/H_2O) aerosols in increasing the abundance of active chlorine compounds in the lower stratosphere.

Reaction Efficiencies: Direct chlorine activation, e.g., via $ClONO_2(g) + HCl(s) \rightarrow Cl_2(g) + HNO_3(s)$ is very efficient on surfaces which mimic PSCs. Denoxification, e.g., $N_2O_5(g) + H_2O(s) \rightarrow 2\ HNO_3(s)$, is very efficient on H_2SO_4/H_2O surfaces typical of mid-latitude stratospheric aerosols and indirectly enhances active chlorine by inhibiting formation of the reservoir $ClONO_2$. Direct chlorine activation on sulfate aerosols may also occur under volcanic conditions or at very cold temperatures, the latter becoming more important with expected future increases in stratospheric H_2O vapor. Furthermore, there may be other important heterogeneous processes that have not yet been identified.

PSC Physical Characteristics: Additional laboratory studies have confirmed that HNO_3/H_2O clouds can form above the frost point. Significant HNO_3 supersaturation may be required for Type 1 PSC formation, implying that heterogeneous processing by sulfate aerosols may be more important at lower temperatures than previously thought. Type 1 PSCs may exist in two subclasses, which, in turn, may have different surface area characteristics and different heterogeneous processing efficiencies. HNO_3 has been shown to stick readily on pure ice and

retard its sublimation, supporting the idea that falling ice crystals are responsible for stratospheric denitrification.

SAM II PSC Climatology:

Antarctic: Average PSC sighting frequency peaks at about 60 percent near 18 km in August. Sighting frequency remains at 10 to 20 percent at lower altitudes—under dehydrated and denitrified conditions—well past the spring equinox. Individually or collectively, the high PSC frequency and persistence of the clouds into sunlit conditions provide firm evidence of a direct link between heterogeneous chlorine activation and South Polar ozone losses.

Arctic: Appreciable PSC sightings occur only from December through February, and the peak average sighting frequency is only about 10 percent. However, the limited spatial coverage of Stratospheric Aerosol Measurements (SAM) II likely yields an underestimate of cloud frequency in the polar region as a whole. More robust PSC statistics will be required before the relationship between lower stratospheric ozone losses in the Northern Hemisphere and heterogeneous chlorine activation on Arctic PSCs can be quantified.

Stratospheric Sulfate Aerosols: Long-term observational records all show a 40 to 50 percent increase in loading over the decade from 1979 to 1989. The effective aerosol surface area available for heterogeneous chemical processing most likely increased by a comparable amount on a global scale during the same period. Additional loading from the June 1991 Mt. Pinatubo eruption will most likely be the greatest of the century to date (exceeding that of El Chichón) and is expected to persist for several years.

Heterogeneous processes must be included in stratospheric chemistry models. Measurements of ClO and HNO_3 are better explained by model calculations that include heterogeneous processing on PSCs and sulfate aerosols. Since there have been more extensive measurements of chemical changes in the polar regions, the picture of heterogeneous processing on PSCs is clearer. Direct heterogeneous chlorine activation in these clouds appears to be rapid and may not be dependent on detailed particle characteristics. Experimental opportunities provided by the Mt. Pinatubo injection should yield the data required to examine this issue more fully with regard to sulfate aerosols.

Chapter 4—Stratospheric Processes: Observations and Interpretation

The primary cause of the Antarctic ozone hole is firmly established to be halogen chemistry. Increased confidence in this mechanism results from analyses using reevaluated field measurements, new laboratory data, and modeling studies.

The year-to-year fluctuation in the area and depth of the ozone hole over the last decade, which has been attributed to dynamical effects, is not fully explained. The apparent lack of variability in recent years—extensive ozone holes have been observed in four of the last five years—may imply that halogen chemistry is becoming dominant over dynamically-induced fluctuations in Antarctic ozone depletion.

High concentrations of ClO between 16 and 20 km have been observed in wintertime in the Arctic lower stratosphere. These observations have been incorporated into diagnostic models that have calculated localized ozone depletions of about 10 percent at these altitudes over a period of about 1 month, which are consistent with concurrent ozone measurements.

Should an unusually cold and long winter occur in the Arctic polar vortex, the appearance of clearly detectable ozone depletions there will be more likely.

Limited observations suggest that the abundance of ClO in the lower stratosphere at mid-latitudes is greater than that predicted by current models containing only gas phase chemistry, and the observed seasonal and latitudinal dependences are opposite to those predicted. Some new studies that incorporate currently known heterogeneous processes provide an improved simulation for some observed gases, such as ClO and nitric acid.

There is not a full accounting of the observed downward trend in global ozone. Plausible mechanisms include heterogeneous chemistry on sulfate aerosols and the transport of chemically perturbed polar air to middle latitudes. Although other mechanisms cannot be ruled out, those involving catalytic destruction of ozone by chlorine and bromine appear to be largely responsible for the ozone loss and are the only ones for which direct evidence exists.

The potential importance of ozone loss in the lower stratosphere due to bromine, through bromine-chlorine interaction, is significantly increased by the widespread enhanced ClO abundances.

Because heterogeneous processes are important and the levels of chlorine in the stratosphere are increasing, volcanic injections into the stratosphere could have a substantial effect on global ozone.

Increasing levels of atmospheric chlorine and bromine are expected to lead to significantly more ozone depletion.

Chapter 5—Tropospheric Processes: Observations and Interpretation

- **Calculated O_3 changes:** Models predict increasing tropospheric ozone in the Northern Hemisphere in response to increasing emissions of NO_x, CO, CH_4, and NMHC that vary markedly with latitude, altitude, and season. These variations have to be taken into account if indirect climate effects are to be estimated.
  Model differences in the calculated ozone increase from NO_x emissions are large (~factor of 3). In addition the spatial and temporal variations are particularly large, and the model results are highly sensitive to the adopted background concentrations. All this precludes a quantitative assessment at the present time. NO_x emitted from aircrafts produces ozone much more efficiently than ground-based emission (by > a factor 10).
  Model differences and spatial variations in the O_3 increase in response to CH_4 emissions are moderate (both within 50 percent). The sensitivity to background assumptions is also moderate. Calculations of ozone changes can be done with reasonable accuracy.

- **Calculated OH changes:** Increases in CH_4, CO and HC emissions lead to reduced OH values, while increased NO_x emissions lead to enhanced OH levels. As a result of these opposing effects the sign of future OH changes cannot be predicted. The indirect effect of CH_4 emission on the CH_4 distribution, through its effect on OH, is estimated to be ~35 percent.

- **Indirect effects on global warming potential (GWP):** The indirect effects from CH_4 emissions on O_3 and CH_4 concentrations can be estimated with moderate accuracy. At present no estimates can be made of the indirect effects of NO_x surface emissions, as uncertainties in

the calculations are too large. Furthermore, the impact on O3 and CH_4 from NO_x emissions is in opposing directions.

- **Tropospheric chemistry of hydrochlorofluorocarbons (HCFCs) and hydrofluorocarbons (HFCs):** Experimental studies show that the breakdown of the HCFCs and HFCs is generally as expected from analogy with the C_1 haloalkanes, and alkanes. However, several of the intermediate oxidation products (COFCl, COF_2, CF_3COF, CCl_3COF, and the halogenated peroxyacyl nitrates) may have long lifetimes in the upper troposphere, and transport to the stratosphere could occur. This could influence the stratospheric ozone chemistry and radiation. Although future changes in OH, which cannot yet be estimated, will affect the breakdown of HCFCs and HFCs, these compounds will not have an effect on OH and the tropospheric O3 chemistry.

Impact of increased emission on climate gases (+ gives increases in global averages, – gives decreases):

Incr. emission	OH	O3	t (CH_4, HCFC, HCF)
CH_4	–	+	+
NO_x	+	+	–
CO	–	+	+
HC	–	+	+

Chapter 6—Ozone Depletion and Chlorine Loading Potentials

The recognition of the roles of chlorine and bromine compounds in ozone depletion has led to the regulation of their source gases. Some source gases are expected to be more damaging to the ozone layer than others, so that scientific guidance regarding their relative impacts is needed for regulatory purposes. Parameters used for this purpose include the steady-state and time-dependent chlorine loading potential (CLP) and the ozone depletion potential (ODP). Chlorine loading potentials depend upon the estimated value and accuracy of atmospheric lifetimes and are subject to significant (~20–50 percent) uncertainties for many gases. Ozone depletion potentials depend on the same factors, as well as the evaluation of the release of reactive chlorine and bromine from each source gas and corresponding ozone destruction within the stratosphere.

ODPs have generally been calculated with two-dimensional numerical models, which have limitations in the treatments of atmospheric transport and chemistry required for evaluation of ozone losses. In particular, such models do not fully represent the transport processes of the lower stratosphere (so that the calculated release of reactive chlorine from the source gases there is subject to uncertainties) nor do they reproduce in detail the large observed ozone losses in the lower stratosphere, especially in polar regions. The sensitivity of modeled ODPs to these problems is reduced by virtue of the fact that the ODP is a relative parameter, but is not completely eliminated, so that the more conservative assessment parameter represented by the CLP has also been considered. In this assessment, ODPs are estimated both from models and with a new semi-empirical approach that uses measurements and/or deduced correlations between source gases (to evaluate reactive chlorine release) together with observations of ozone losses. A critical assumption in the semi-empirical approach is that observed lower stratospheric ozone losses are due to halogen chemistry. This assumption is well justified in polar regions and likely to be largely true at mid-latitudes. Therefore, the semi-empirical ODPs are expected to be more realistic than those derived from current models, at least in polar regions.

Modeled steady-state ODPs and CLPs have been evaluated using improved kinetic schemes. Further, some preliminary model results include a treatment of known heterogeneous chemistry on mid-latitude sulfate aerosols. The numerical values of these modeled ODPs are close to those of previous assessments.

Semi-empirical steady-state ODPs are given for the polar lower stratosphere and, in a few cases, for the global average. The semi-empirical ODPs are generally larger than the modeled values for chlorocarbons whose stratospheric loss rates are slower than that of CFC-11 and smaller for those whose loss rates are faster than that of CFC-11. For example, the semi-empirical ODP for HCFC-22 is between about 20 and 80 percent greater than the range of the model values. For some halons (brominated halocarbons), the semi-empirical ODPs for polar regions exceed some model estimates by as much as a factor of two. For all of the HCFCs considered here, the inferred ODP values are well below the CLPs and show that the upper limit to ozone loss represented by the CLP is not realized in the stratosphere for these species. This narrows significantly the uncertainties in the ODPs for HCFCs.

During the next decade, stratospheric chlorine abundances are expected to rise substantially. This increase in chlorine will likely lead to further global ozone loss including larger reductions in the Arctic and perhaps in northern mid-latitudes. In this near-term period, the HCFCs and many halons will have an impact that is considerably larger than their steady-state ODPs, in some cases and over some time horizons by as much as a factor of two to five.

Chapter 7—Radiative Forcing of Climate

Global Warming Potentials

Direct Effect. Direct global warming potentials (GWP) have been recalculated for tropospheric, well-mixed, radiatively active species (CH_4, N_2O and the halocarbons). We use updated lifetimes of these species and follow the same methodology as in the Intergovernmental Panel on Climate Change report (IPCC, 1990), for time horizons corresponding to 20, 50, 100, 200, and 500 years. The new GWP results include a correction in the values for methane arising due to a typographical error in the IPCC (1990) report, as well as changes in values for other species that are a manifestation of the updated lifetimes. However, there still exist uncertainties in these calculations due to uncertainties in the carbon cycle.

Indirect Effect. While chemical reactions involving the radiatively active atmospheric species can contribute to the GWPs, our ability to estimate them is restricted at present owing to complexities in the chemical processes and uncertainties in the temporal and spatial variations of various species. While the sign of the radiative forcing due to some of the indirect effects can be evaluated with a fair measure of confidence (Chapter 5), the quantitative aspects of the indirect effects are more difficult to ascertain than was anticipated earlier in IPCC (1990) and we do not recommend the use of those values.

Radiative forcing due to trace gases, including ozone (1979–1990)

Stratospheric Ozone. The observed global ozone losses in the lower stratosphere cause a significant forcing of the climate system. The physical effects due to this loss consist of an increase in the solar and a decrease in the longwave forcing of the surface-troposphere system, together with a tendency to cool the lower stratosphere. The latter effect amplifies the longwave influences and can thereby give rise to a significant net negative radiative forcing of the surface-troposphere system, but the magnitude of the induced forcing is very sensitive to the change in the lower

stratospheric temperatures. This tendency is opposite to the direct positive (greenhouse) forcing exerted by the well-mixed gases and is pronounced in the mid-to-high latitudes of both hemispheres, and during all seasons. In fact, if the tendency to cool the lower stratosphere is fully realized as equilibrium temperature change, the magnitude of the negative ozone radiative forcing in the mid-to-high latitudes can be larger than the decadal greenhouse forcing due to the CFCs over this period, and could also be a significant fraction of the total decadal greenhouse forcing due to the non-ozone gases.

Tropospheric Ozone. Ozone in the troposphere, although present in smaller amounts than that in the stratosphere, has a significant opacity and exerts a greenhouse effect (positive forcing), with the sensitivity being greatest for ozone changes in the upper troposphere. However, the databases for tropospheric ozone trends are sparse and therefore inadequate for quantifying the global radiative influences due to changes in tropospheric ozone.

Radiative forcing due to sulfate aerosols

Tropospheric Aerosols. Fossil fuel emissions over the past century have increased significantly the tropospheric sulfate aerosol concentrations. The contribution of this species to the direct clear-sky radiative forcing of the Northern Hemisphere is opposite to that due to the greenhouse gases and is estimated to be a significant fraction of the trace gas forcing. Although we are confident of the sign of the forcing, uncertainties exist owing to the spatial inhomogeneity of the aerosol distributions and a lack of understanding of the aerosol effects in cloudy regions.

Stratospheric Aerosols. With the eruption of Mt. Pinatubo in mid-1991, there is again a radiative forcing of the climate system due to increases in the concentrations of the stratospheric sulfate aerosols. These aerosols produce a net negative radiative forcing of the climate system which is comparable to the positive ones due to the greenhouse gases, but this forcing is short-lived. The presence of the aerosols in the stratosphere also contributes to a warming tendency in the lower stratosphere. Preliminary observations indicate about a 4 K warming of the tropical lower stratosphere two months following the Mt. Pinatubo eruption.

Chapter 8—Future Chlorine-Bromine Loading and Ozone Depletion

The atmospheric loading of chlorine and bromine compounds and corresponding predictions of current and future ozone changes are examined using global two-dimensional models of stratospheric chemistry and transport. There has been a major advance in the two-dimensional assessment models used here: most models now include currently-known heterogeneous chemical reactions on the stratospheric sulfate layer. Further, three models also incorporate a parametric formulation of the chemistry involving polar stratospheric clouds (PSCs), but PSC simulations remain incomplete. Results are shown from these three types of models, denoted GAS (gas phase chemistry only), HET (includes reactions of N_2O_5 and $ClONO_2$ on sulfate-layer aerosols), and PSC (includes parameterization of PSC-chemistry). The HET models predict a substantially different balance among the chlorine, bromine, odd-hydrogen, and odd-nitrogen cycles for ozone destruction in the lower, mid-latitude stratosphere than do the GAS models, with important implications for the ozone response to a variety of perturbations in trace gases (e.g., chlorofluorocarbons (CFCs), halons, methane, nitrous oxide, and nitric oxides from aircraft). The only forcing considered in the model scenarios is the evolving atmospheric composition, which over the past decade has been dominated by the increase in halocarbon chlorine loading from 2.5 to 3.6 ppbv.

GAS models predict integrated column depletions and vertical profiles of ozone loss from 1980 to 1990 that are much less than those observed at middle latitudes over all seasons in both hemispheres.

HET models simulate most of the observed column ozone loss from 1980 to 1990 for the northern middle latitudes in summer, but only about half of that in winter (see Table 8-A below). Unlike previous assessments, the predicted vertical profile of ozone loss from 1980 to 1990 has the same structure as observed, including substantial losses in the lower middle latitude stratosphere. Largest relative ozone losses at 45°N from 1980 to 1990 are predicted to range from 7 percent to 16 percent near 44-km altitude, and, compared with observations, are similar in shape (loss versus altitude) but greater in magnitude. The sensitivity of these results to substantial (factor of 4) changes in the sulfate layer area is small (about 1/2 percent change in column ozone over the past decade). Similar results hold for the Southern Hemisphere, except near 60°S in winter–spring, where observed losses greatly exceed those predicted.

PSC models are still under development; current versions predict greater ozone loss at northern middle latitudes in winter.

Table 8-A Approximate Ranges of Column Ozone Losses (%) for 1980–1990

	TOMS*		GAS		HET		PSC	
lat./months	JFM	JAS	JFM	JAS	JFM	JAS	JFM	JAS
60°N	6–8	3–4	1–2	1	3–4	3	5–7	3–4
30°N	4–5	1–2	1	< 1	2–3	1–2	2	1–2

*TOMS (Total Ozone Mapping Spectrometer) from Figure 2-11.

We expect that atmospheric loading of chlorine and bromine will peak in the late 1990s at levels of about 4.1 ppbv and 25 pptv, respectively. The HET models predict the maximum ozone loss circa 2000, with the additional losses for the period 1990–2000, will be equal to or slightly less than those for 1980–1990. Predictions for the year 2050 depend on many competing changes in Cl_y, Br_y, NO_y (through nitrous oxide), CH_4, and stratospheric temperatures (through CO_2 and O_3 changes), and thus the model predictions show large differences.

The peak chlorine loading in the late 1990s may vary over a range of 0.2 ppbv in response to a wide variety of options for halocarbon phaseouts and hydrochlorofluorocarbon (HCFC) substitution. A significant reduction in peak chlorine loading can be achieved with accelerated phase-out schedules of CFCs, carbon tetrachloride, and methyl chloroform. The times at which chlorine loading falls below 3 and 2 ppbv can be shifted by at most 10 years with such an acceleration of the phaseout. The integral of high chlorine levels (i.e., cumulative exposure to ozone loss and, hence, ultraviolet (UV) increases) is more sensitive to the differences between certain policy options: heavy substitution with HCFCs can increase this number by at most 20 percent, whereas accelerated phaseouts can reduce it by as much as 50 percent. Acceleration of the halon phaseout by 3 years would reduce peak bromine loading by 1 pptv (about 4 percent). Stringent controls on current use of HCFC-22, or on substitution with alternative HCFCs, would not significantly reduce peak chlorine, but would accelerate the decay in chlorine loading in the decades following the peak. Scenarios in Table 8-B show the sensitivity of tropospheric chlorine loading to a range of halocarbon phase-out schedules.

To represent the differences in effectiveness of halocarbons in destroying ozone, we define a new quantity: the stratospheric free halogen content (FH in ppbv), the weighted sum of the free chlorine (FC in ppbv), and free bromine (FB) in the stratosphere, which are measures of the Cl_y and Br_y, respectively, available in the stratosphere to contribute to ozone depletion (e.g., particularly in the lower, high-latitude stratosphere). The FC is calculated from the chlorine loading by weighting individual chlorocarbons by a factor proportional to their relative ozone depletion potentials (ODPs). All of the bromine in the halons and methyl bromide is assumed to be available in the stratosphere as Br_y, which is 30 to 120 times more effective per atom than Cl_y in catalyzing ozone loss (i.e., the scale factor to convert FB into the same units as FC and FH, effective ppbv of Cl_y). These preliminary calculations of FH demonstrate that a large proportion (0.8 to 2.8 ppbv) is due to bromine, predominantly methyl bromide. But, the Br_y/Cl_y scale factor is highly uncertain due to large uncertainties in the bromine chemistry and to differences in the model calculations of Br_y-catalyzed ozone destruction.

Chapter 9—Predicted Aircraft Effects on Stratospheric Ozone

Engine emissions from subsonic and supersonic aircraft include oxides of nitrogen (NO_x), water vapor, unburned hydrocarbons, carbon monoxide, carbon dioxide, and sulfur dioxide. Addition of NO_x to the atmosphere is expected to decrease ozone in the stratosphere and increase ozone in the troposphere. Resulting changes in ozone, water vapor, and aerosol loading in the altitudes around the tropopause may have a climatic impact since the response of radiative forcing to changes in concentrations is most sensitive here.

The first step in assessing these effects is to determine quantitatively the changes in background concentrations associated with emitted gases and aerosols. Most of the emissions from the projected supersonic fleet as well as one-quarter to one-half of the emissions from the subsonic fleet are deposited directly into the lower stratosphere, to be redistributed by large-scale transport. Current models cannot accurately simulate the accumulation of emitted materials in the stratosphere and their eventual removal, as much of the injection is close to the tropopause. Model predictions in this chapter are based on simulations from two-dimensional models that assume that the emitted material is zonally mixed. The impact of flight corridor effects on the predictions has not been assessed.

The current fleet of subsonic aircraft may be sufficiently large to have increased background concentrations of NO_x, ozone and the sulfate layer. Gas phase modeling studies predict that the current subsonic aircraft fleet (injection of 2 $Tg(NO_2)$/year) contributes to 5–10 percent of the total amount of ozone in the troposphere around 40°N. These models also predict a decrease in ozone in the lower stratosphere of less than 1 percent. Projected increases in the subsonic fleet could lead to further increases of tropospheric ozone with associated changes in OH and additional (although still small) reduction of ozone in the stratosphere. These estimates are subject to considerable uncertainties due to uncertainties in the magnitude and distribution of emissions and to differences among models. The role of heterogeneous chemical processes in the troposphere needs to be assessed.

The additional impact on ozone from projected fleets of supersonic aircraft [high-speed civil transports (HSCT)] operating in the year 2015 (cruise altitudes around 15, 19, and 22 km) has been examined by a model intercomparison exercise using gas phase models. With the operation of aircraft assumed to be concentrated in the Northern Hemisphere, the largest decrease in local ozone is found poleward of 30°N around the cruise altitude. There is very little increase in upper tropospheric ozone due to HSCT alone because of the reduced ozone flux from the stratosphere. For cruise altitudes below 28 km, the calculated decrease in column abundance of ozone is larger

for higher cruise altitudes and larger NO_2 emission indices. The calculated decrease in the Southern Hemisphere is typically a factor of 2 to 3 smaller than that in the Northern Hemisphere. In one of the cases (a fleet of aircraft flying Mach 3.2 between 21 and 24 km with NO_2 emission index of 15 and annual fuel use of 70 Tg per year), the calculated decrease in ozone column abundance at northern mid-latitudes ranges from 7 percent to 12 percent. This spread in model results increases with decreasing cruise altitude and reflects differences in transport and photochemical balance in the various models. In the Mach 2.4 case (cruise altitude of 17-20 km), the range of model-calculated decreases in column abundance in the same region is 2 to 6 percent.

Heterogeneous reactions occurring on polar stratospheric clouds (PSCs) or the global sulfate aerosol layer have a large impact on the ozone chemistry in the lower stratosphere, and hence, the predicted response to supersonic aircraft. If N_2O_5 is converted to HNO_3 via known heterogeneous reactions on the global sulfate layer, the column changes for the Mach 2.4 case from two of the models are calculated to be small (–0.5 to +0.5 percent). At the same time, there is an increase in upper tropospheric ozone of about 5 percent due to HSCT alone. Nevertheless, there could be large and unpredictable changes in ozone if emissions from the aircraft cause enhanced formation of PSCs or increases in the sulfate aerosol loading, leading to repartitioning of the chlorine species and higher concentrations of ClO.

Chapter 10—Predicted Rocket and Shuttle Effects on Stratospheric Ozone

The exhaust products of rockets contain many substances capable of destroying ozone. Although there are over a hundred rocket launches per year worldwide, studies so far have only considered the effects of the less frequent launches of the largest rockets. Most attention has focused on the potential reductions in ozone produced by chlorine compounds from solid fuel rockets. Rockets that release or are expected to release relatively large amounts of chlorine per launch into the stratosphere include NASA's Space Shuttle (68 tons) and Titan IV (32 tons) rockets, and European Space Agency's (ESA's) Ariane–5 (57 tons).

Within a few kilometers of the exhaust trail of these rockets, local ozone may be reduced by as much as 80 percent at some heights for up to 3 hours. Since the rocket trajectory is slanted, the corresponding column ozone loss is computed to be reduced over an area of order of a few hundred square kilometers, but the depletion nowhere exceeds 10 percent. A satellite study of column ozone loss associated with several NASA Space Shuttle launches failed to detect any depletion. Local effects of similar magnitude may also be produced by the NOx emitted by the Soviet Energy rocket. Recovery of the ozone in the wake is computed to be rapid in all cases. All but a fraction of a percent is predicted to be restored within 24 hours.

The stratospheric chlorine input from a NASA launch rate scenario of nine Space Shuttles and six Titan IV rockets per year is computed to be less than 0.25 percent of the annual stratospheric chlorine source from halocarbons in the present-day atmosphere. If the annual background source from halocarbons is reduced and/or the launch rate increases, the fractional contribution will become larger.

Steady-state model computations using the NASA scenario show increases in the middle to upper stratospheric chlorine amounts by a maximum of about 10 pptv (about 0.3 percent of a 3.3 to 3.5 ppbv background) in the northern middle and high latitudes. Independent steady-state model computations of the effect of 10 ESA Ariane–5 launches per year yield comparable maximum values, but at all latitudes. For both scenarios, corresponding decreases in ozone are computed to be less than 0.2 percent locally in the region of maximum chlorine increase, leading to changes in column ozone of much less than 0.1 percent.

It is not yet possible to quantify with confidence the effects of particulates from the exhausts, principally of Al_2O_3 from the solid-fueled rockets. However, simple steady-state estimates using the NASA scenario suggest increases of the chemically active area of stratospheric aerosols of less than 0.1 percent, so the long-term global impact is likely to be negligible.

Chapter 11—Ultraviolet Radiation Changes

A major consequence of ozone depletion is an increase in solar ultraviolet (UV) radiation received at the Earth's surface. This chapter discusses advances that have been made since the previous assessment (WMO, 1990) to our understanding of UV radiation. The impacts of these changes in UV on the biosphere are not included, because they are discussed in the effects assessment (UNEP, 1991). The major conclusions and recommendations are:

- Significant improvements in the UV data base have occurred since the last assessment. Spectral measurements are becoming available, but, to determine trends, long-term accurate measurements of UV are required at unpolluted sites.
- Biologically damaging UV has been observed to more than double during episodes of ozone depletion in Antarctica. Smaller episodic enhancements have been measured in Australia. The observed enhancements are consistent with the results of radiative transfer calculations for clear sky conditions.
- An erythemal Radiative Amplification Factor (RAF) of 1.25 ± 0.20 has been deduced from measurements of ozone and UV at a clean air site. This is in agreement with the RAF derived from model calculations (RAF = 1.1 at 30° N).
- There is an apparent discrepancy between observed UV trends from the Robertson-Berger (RB) network and those calculated from TOMS ozone data. Cloud variability, increases in tropospheric ozone and aerosol extinctions may have masked the UV increase due to ozone depletion. In addition, the data record available for comparison is short, and the instrument calibration (which is critical) is still in question. However, at a high-altitude European observatory, the observed positive trends in UV appear to be larger than expected. Further studies of the effects of cloud and aerosol on UV are required.
- Clear-sky radiative transfer calculations using ozone fields measured by the TOMS instrument show that during the 1980s erythemally active UV has increased significantly at latitudes poleward of 30°, with larger increases in the Southern Hemisphere, particularly at high latitudes.
- Significant increases in UV effects are most likely to appear first in the Southern Hemisphere where in the summer, historical ozone levels are lower and the Earth-Sun separation is a minimum. Further, in the Southern Hemisphere, stratospheric ozone losses are more severe, tropospheric ozone has not increased, and aerosol concentrations are lower.
- Existing chemical models underestimate the changes in the observed ozone fields. Therefore, they cannot be used to accurately predict future changes in UV fields.

SECTION C

METHYL BROMIDE AND THE OZONE LAYER: A SUMMARY OF CURRENT UNDERSTANDING

EXECUTIVE SUMMARY

General

- This report is an interim summary of the current understanding of the relationship of methyl bromide (CH_3Br) to the ozone layer and was requested by UNEP on behalf of the Parties to the Montreal Protocol. It builds upon the relevant parts of the recent Scientific Assessment of Ozone Depletion: 1991 (WMO, 1992) and utilizes new information presented and discussed at the international Methyl Bromide Science Workshop held in Washington, DC on June 2-3, 1992.

- The conclusions from this assessment support and expand those contained in WMO (1992) and confirm the need to focus attention on CH_3Br.

- The current state of scientific knowledge concerning bromine compounds in the atmosphere is considerably less developed than the corresponding understanding of chlorine compounds.

To what extent do anthropogenic emissions of methyl bromide contribute to the global stratospheric abundance of bromine?

- Based on an emerging body of observational data, the current best estimate for the global abundance of CH_3Br in the troposphere is about 9-13 pptv (1 pptv = 1 part in 10^{12}), which is equivalent to a total global burden of 150-220 thousand tonnes (1 tonne = 10^3 kg).

- The observational data from several independent investigations demonstrate that the atmospheric abundance of CH_3Br is a factor of 1.30 ± 0.15 greater in the Northern Hemisphere than in the Southern Hemisphere, probably indicating an excess source in the Northern Hemisphere.

- Combining the CH_3Br use-pattern data with the currently estimated fraction that escapes to the atmosphere indicates that about half of the production (exclusive of that used for chemical intermediates) is emitted into the atmosphere; this implies an anthropogenic emission from fumigation applications of about 30 thousand tonnes in 1990.

- The current best estimate is that the total anthropogenic emissions of CH_3Br from fumigation applications (30 thousand tonnes per year, primarily in the Northern Hemisphere) represent $25 \pm 10\%$ of the total emissions, which is consistent with the observed interhemispheric gradient.

- There are major uncertainties in the budget of CH_3Br, including: (i) the absolute calibration for CH_3Br measurements and the quantification of: (ii) natural sources; (iii) the fraction that escapes to the atmosphere when used as a fumigant, especially when used in pre-planting applications; and (iv) possible oceanic and terrestrial surface removal processes. The

current best estimate of 25±10% for the anthropogenic contribution to the observed atmospheric abundance of CH_3Br would be lower if there were to be major surface removal processes or if the fraction of anthropogenic production that is released to the atmosphere were to be smaller than presently estimated. On the other hand, the anthropogenic contribution would be larger if there were to be unaccounted-for industrial production and release of CH_3Br, or, of course, if the fraction that is released to the atmosphere from agricultural application were to be larger than presently estimated.

How well is the role of bromine in ozone destruction quantified?

- Overall, the current understanding of most of the atmospherically important bromine reactions appears to be in reasonably good shape, with the exception of the quantification of possible reaction channels that produce the relatively unreactive form of bromine, HBr.

- The observed polar and mid-latitude abundances of BrO in the lower stratosphere, the key ozone-depleting bromine species, are broadly consistent with those predicted by photochemical models that incorporate known gas phase and heterogeneous reactions and adopt an atmospheric abundance of bromine of between 15 and 20 pptv, in the form of observed abundances of CH_3Br and halons.

- The two models used in recent sensitivity studies show an enhancement in ozone loss of about a factor of 1.3 over the time period 1990 to 2000 for a 10 pptv increase in the abundance of bromine. These model results suggest that anthropogenic emissions of CH_3Br could have accounted for about one-twentieth to one-tenth of the current observed global ozone loss of 4-6%, and could grow to about one-sixth of the predicted ozone loss by the year 2000 if emissions continue to increase at the present rate of about 5-6% per year.

- Models and interpretations of observations show that ozone removal by bromine is far more efficient on a per molecule basis than by chlorine (by a factor of 20 to 100 in the lower stratosphere, with a current best estimate of about 40). Therefore, 1 pptv of bromine is equivalent to 0.04 (0.02-0.10) ppbv of stratospheric chlorine.

- The current best estimate of the steady state value of the ODP for CH_3Br is 0.7. Because of the short atmospheric lifetime of CH_3Br, its relative impact on ozone is expected to be much greater over the next decade (when chlorine abundances and ozone losses are predicted to reach their maximum) than is indicated by its steady-state ODP. For example, the estimated ODP over the next 20 years is about a factor of four larger than the steady-state ODP. Evaluation of the importance of reducing CH_3Br concentrations over the next decade can be carried out either with a time-horizon ODP (which yields the integrated ozone destruction over particular times) or via prediction of the chlorine and bromine loading in the stratosphere (which provides a measure of the contribution of the gas to the ozone loss at any specific time).

- A major remaining uncertainty in the calculation of bromine-related ozone loss and ODPs is associated with quantification of the rate of formation of HBr in the stratosphere. Further study of the stratospheric reactions that can produce HBr and direct measurements of bromine reservoir species would better constrain the model-calculated partitioning of the brominated species. If the rate of HBr formation were to be greater than currently estimated, then the calculated ODP and BrO (hence ozone loss) would be lower. Although the upper range of the observed BrO would appear to be in conflict with a significant HBr source, the lack of definitive data for HBr and the large scatter in observed BrO make it difficult to rule out this possibility. In addition, the value of the ODP would be lower if there were to be significant removal of CH_3Br by terrestrial or oceanic surfaces.

Alternatively, if recent laboratory measurements indicating a faster rate of formation of HOBr (via $BrO + HO_2$) were to be correct, then the ODP would be larger.

Implications for Policy Formulation

- The anthropogenic contribution to the current atmospheric abundance of methyl bromide from fumigation applications is about 3 pptv, which is equivalent to about 0.09-0.18 ppbv of stratospheric chlorine. An advance of the CFC and CCl_4 phaseout schedule by three years reduces the peak chlorine loading by 0.18 ppbv. Therefore, elimination of anthropogenic methyl bromide would provide an ozone-layer protection comparable to that of an advance of the CFC and CCl_4 phaseout schedule by about 1.5-3 years.

SECTION D

CONCENTRATIONS, LIFETIMES, AND TRENDS OF CHLOROFLUOROCARBONS (CFCs), HALONS, AND RELATED MOLECULES IN THE ATMOSPHERE

EXECUTIVE SUMMARY

The atmospheric lifetimes of molecules containing chlorine and bromine are the dominant parameters influencing their ability to promote enhanced ozone destruction in the stratosphere. The purpose of this report is to assess the present state of our knowledge of the lifetimes of halocarbons using two complementary approaches. First, a time series of measurements of gas concentrations is used together with information on their emissions histories and a computational model of atmospheric circulation and chemistry to infer lifetimes through a mass balance approach. Second, an atmospheric chemical-dynamical model is used with detailed information on the chemistry and spectroscopy of the molecules of interest to calculate lifetimes. The lifetimes determined by these two methods are then compared.

In this report, attention will be focused most closely on fully halogenated chlorine- and bromine-containing molecules, primarily the chlorofluorocarbons, and the halons, because of their ability to deliver chlorine and bromine to the stratosphere. Some attention will be given to those molecules containing hydrogen, such as methyl chloroform, hydrochlorofluorocarbons (HCFCs), methyl chloride, and methyl bromide. These molecules are subject to removal in the troposphere primarily by reaction with OH and by other processes. This summary very briefly enumerates the main conclusions from present understanding of the behavior of halogen-containing source gases. A fuller description of the contents of the report, including a summary representation of measurements and models included, may be found in the report overview which follows this summary.

CFC Abundances

Tropospheric Measurements

- The Atmospheric Lifetime Experiment/Global Atmospheric Gases Experiment (ALE/GAGE) network has provided an extensive set of measurements for CFC-11 (CCl_3F), CFC-12 (CCl_2F_2), CFC-113 ($CF_2ClCFCl_2$), methyl chloroform (CH_3CCl_3) and carbon tetrachloride (CCl_4) at 4 or 5 surface sites from 41°S to 52°N for more than a decade (for all but CFC-113), from which long-term trends can be derived.
- Concentrations of these and related species are measured by additional networks at surface level which have different temporal and/or spatial coverage than ALE/GAGE as well as smaller sampling frequency. Comparison of these alternative data with those obtained from ALE/GAGE allows for improved determination of measurement accuracy.
- Recent data from the middle to high Northern Hemisphere from several different measurement programs show that the growth rates of CFC-11 and CFC-12 have started to level off, presumably in response to reduced emissions.
- A significant new Northern Hemispheric data set on tropospheric HCFC-22 ($CHClF_2$) based on infrared absorption shows some difference from previous measurements made using *in-situ* techniques.

PRECEDING PAGE BLANK NOT FILMED

- There is a serious lack of data on the global distributions and trends of other important chlorine- and bromine-containing species, most notably methyl bromide (CH_3Br) and methyl chloride (CH_3Cl), along with several other organobromine species.

Calibrations

- Calibration issues continue to limit our understanding of the global atmospheric distributions and trends of these species. In the case of CFC-11 and CFC-12 the calibration uncertainty range between various laboratories is currently less than 5%, whereas for CFC-113 and CCl_4 it is greater than 20%. For CH_3CCl_3 and HCFC-22, the uncertainty range is on the order of 30%.

Stratospheric Measurements

- Simultaneous measurements have been made in the stratosphere for most of the substances controlled under the Montreal Protocol, along with several others. The individual profiles for many molecules removed by photolysis in the stratosphere correlate well with respect to scale height and allow a check on the lifetimes calculated with atmospheric chemistry models.
- Most data have been collected in balloon flights at mid latitudes in the Northern Hemisphere. Some data are available from polar regions and the tropics, but these are limited. The observed fall-offs show the expected variation with latitude.
- The existing database of stratospheric profiles from space-based measurements is very limited, but will improve in the future due to data from the Upper Atmosphere Research Satellite (UARS) and the Atmospheric Trace Molecule Spectroscopy (ATMOS) instrument.

Production and Emission

- Production of CFC-11 and CFC-12 peaked in 1987 and their estimated emissions have decreased substantially since 1988.
- The major uncertainties in the calculations of current global emissions for CFC-11 and CFC-12 are the lack of data from companies not reporting to industry panels and estimates of banking times for long-term uses.
- For CFC-11, CFC-12 and CFC-113, reporting companies are estimated to account for 85-90% of total production; higher percentages are believed for most other CFCs and methyl chloroform. At least 95% of the CFC production and emission is believed to take place in the Northern Hemisphere.
- The proportion of emissions of CFC-11 and CFC-12 from non-reporting companies is projected to increase as production is phased out under the Montreal Protocol. In addition, the fraction of total emissions arising from the service bank of CFCs will also increase as new production decreases. Emission levels are therefore likely to fall off less rapidly than production, and the uncertainty in emission relative to production will grow.
- Methyl chloroform emissions increased during the 1980s, partly due to its substitution for restricted substances, including CFC-113 and other volatile organic compounds. There are no industrial estimates for current production of carbon tetrachloride produced for dispersive uses. Somewhat imprecise production and emission data are available for methylene chloride (CH_2Cl_2), trichloroethylene ($CHClCCl_2$) and perchloroethylene (CCl_2CCl_2), which are short-lived compounds whose study may help shed light on global average distributions of tropospheric OH.
- HCFC-22 emissions have increased at approximately 8.5% per year since 1980. This increase is due in part to substitution for restricted CFCs. There are no industrial estimates

for other HCFCs since their emissions are significantly lower and presently do not have any agreed-upon criteria for industry reporting.

- Some proportion of methyl chloride emissions may be due to anthropogenic sources (15-30%), probably almost all from biomass burning. The rest of the emissions are from natural sources, primarily the oceans.
- Methyl bromide emissions to the atmosphere have a number of sources. These include a significant natural component, most likely from the oceans, and various anthropogenic sources, such as fumigant use. There is considerable uncertainty about both the anthropogenic and natural emissions of methyl bromide.

Inferred Lifetimes

- The length of the atmospheric measurement record for various halocarbons is as yet short by comparison with their atmospheric lifetimes. The only molecules for which the record can be used with some confidence for determining their lifetimes are CFC-11 and methyl chloroform..
- Using the ALE/GAGE data, an optimal inversion analysis, and a two-dimensional model with parameterized transport, the steady state atmospheric lifetime of CFC-11 is estimated to be 42 years (+7,-5, 68% confidence limits)
- Inference of CFC-11 lifetimes using the ALE/GAGE data with three-dimensional models and differing statistical techniques yields contradictory results:

  + A 3-D model from the Max Planck Institut für Meteorologie yields a lifetime of 55.61 years

  + A 3-D model from the Goddard Institute for Space Studies did not converge to a reasonable lifetime unless a systematic correction to CFC abundance was introduced (corresponding to a correction to the total CFC distribution in the model and/or errors in network calibration), in which case a 39 year (+4, -3, 95% confidence limits) lifetime was obtained.
- Using the ALE/GAGE data together with an optimal inversion analysis and a two-dimensional model with parameterized transport, the tropospheric lifetime of CH_3CCl_3 is estimated to be 5.7 years (+0.7,-0.6, 68% confidence limits). This analysis yields a percentage linear trend in inverse lifetime of 1.0 ± 0.6 % $year^{-1}$, which may correspond to a similar percentage increase in averaged tropospheric OH.
- Inference of CH_3CCl_3 lifetimes using the ALE/GAGE data with the GISS three-dimensional model yielded a lifetime of 5.7-5.9 years assuming an OH increase comparable to that suggested by the ALE/GAGE data. If the ALE/GAGE calibration factor were 0.70 (instead of 0.8 as currently believed), the best fit to the measurements obtained using the GISS model would yield a lifetime of approximately 5 years with no trend.
- The steady state atmospheric lifetime of CFC-12 is estimated to be 122 years (+91,-37, 68% confidence limits) using the ALE/GAGE data, an optimal inversion analysis and a two-dimensional model with parameterized transport. Currently available information does not support the inference of a lifetime for CFC-113, other than to say that it is in excess of 20 years.
- Differences in lifetimes inferred by the two methods (two-dimensional vs. three-dimensional models) reflect substantial differences in the models, including in the total burden and in the vertical distribution of the CFCs. These differences are much more important for the longer-lived CFC-11 than they are for the shorter-lived CH_3CCl_3.

Laboratory Studies of Halocarbon Loss Processes

- Improved laboratory data have been obtained from reactions of OH with 14 different halocarbons. The most significant changes were those in reactions with HCFC-141b (CH_3CFCl_2), HCFC-142b (CH_3CF_2Cl), HFC-125 (CHF_2CF_3) and HFC-143a (CH_3CF_3). The largest change in rate constant at atmospheric temperatures is a decrease of about 30% for HCFC-141b.
- New evaluations of reaction rates of $O(^1D)$ with 8 different halocarbons were obtained. Reaction rates of Cl (chlorine) with 18 different halocarbons were measured and the rates of reactions of NO_3 (nitrogen trioxide) with various halocarbons were found to be very slow.
- Absorption cross sections (including temperature dependence) were re-evaluated for CFC-11, CFC-12, CFC-113, CFC-114 ($CClF_2CClF_2$), CFC-115 ($CClF_2CF_3$) and the halons. Hydrolysis rates and Henry's Law constants for methyl chloroform and carbon tetrachloride have been reviewed in the context of recent data.

Model Calculation of Atmospheric Lifetimes

Species primarily removed in the Stratosphere

- Atmospheric lifetimes for the CFCs and halons have been calculated using several multi-dimensional atmospheric models simulating stratospheric photochemistry and transport.
- The calculated steady-state atmospheric lifetimes for CFC-11 are generally consistent with the lifetimes inferred from observations and emission rates based on 95% confidence intervals.
- Simultaneous measurements of the stratospheric concentrations of any two species can be used to estimate the ratio of their lifetimes if enough is known about their local removal processes and a sufficiently broad set of measurements is available. This does allow the determination of the ratio of lifetimes for longer-lived CFCs.

Species primarily removed in the Troposphere

- Lifetimes for HCFCs were obtained using model-calculated stratospheric loss and removal by tropospheric OH. Since calculations of troposheric OH in photochemical models are expected to have significant uncertainty, the tropospheric OH removal in the models is scaled to simulate distributions of methyl chloroform, using the tabulated emissions estimates, the estimated ocean removal rate, the model-calculated stratospheric removal, and knowledge of the OH-induced loss at mid-tropospheric temperatures.

Recommendations

- Long-term *in-situ* measurement networks need to be continued with increased speciation. HCFCs, CH_3Cl, CH_3Br and more reactive halocarbon measurements need to be added to existing CFC and halon measurements. Developments in analytical techniques are needed to facilitate these additional measurements.
- Increased attention needs to be given to calibration issues for *in-situ* measurements, especially for CH_3CCl_3, HCFC-22, and bromine-containing molecules.
- Increased use should be made of ground-based spectroscopic measurements, especially for HCFC-22. Laboratory work needed for improvement of accuracy of absorption cross-sections should be conducted.
- Additional balloon and aircraft flights for measurement of multiple species are needed for tropical, mid-latitude, and high-latitude conditions. Continuing flights of the ATMOS instrument are needed, with occultations being made at a variety of latitudes.

- Accurate production and emission information is needed for HCFCs and other CFC replacement compounds; complete worldwide geographic coverage is needed for the production and emission reports for these molecules as well as the CFCs.
- Both natural and anthropogenic components of the source distributions for methyl-halides need to be better understood, particularly for CH_3Br.
- Use of atmospheric chemistry/transport models to examine the consistency between emissions, concentrations, transport and loss processes should be continued. The results from different approaches need to be intercompared and the differences between model results, if any, need to be understood.
- Continuing measurements of ultraviolet absorption cross sections and reaction rates of OH with halocarbons are needed, with the aim of improving measurement accuracy. Particular attention needs to be paid to removing the effects of impurities.
- Continuing application of multidimensional photochemical models for studies of long-lived tracer distribution in the stratosphere is required. Improvements in tropospheric chemistry-transport models are also needed so that better distributions of global OH can be determined from distributions of short-lived halocarbons.

OVERVIEW

I. Atmospheric Lifetimes - Definition

In attempting to understand the effect of industrially produced halogenated hydrocarbon molecules on the Earth's atmosphere, one crucial quantity which must be known is the length of time over which these molecules will have a significant impact. This atmospheric residence time, commonly referred to as the lifetime, represents the average length of time a molecule will stay in the atmosphere from its release to its destruction. The lifetime may also be thought of as the ratio of the total atmospheric burden to its destruction rate or as the inverse of a linear loss coefficient, which to a high degree of approximation is independent of concentration. While in the atmosphere, halogenated hydrocarbons can destroy stratospheric ozone through their photochemical breakdown to chlorine and/or bromine atoms which lead to ozone destruction through catalytic cycles. They can also contribute to global warming through their absorption of infrared radiation (WMO, 1992; IPCC, 1992).

The differential equation for the total molecular burden, B(t) in the atmosphere is related to the lifetime, t(t), by the expression

$$\frac{dB(t)}{dt} = E(t) - \frac{B(t)}{t(t)} \qquad (1)$$

where E(t) is the emission rate for the molecule into the atmosphere from the Earth's surface.

At steady state $\frac{dB(t)}{dt} = 0$ and $t = \frac{B(t)}{E(t)}$ (2)

The lifetime is not a quantity which can be simply measured or calculated, however. In principle, the lifetime can be determined in one or two ways. First, it can be inferred in an inverse way using eq. (1) if an accurate series of measurements of B(t) and a record of the emission rates E(t) is available. This is far from trivial however, as eq. (1) is global. To solve the inverse problem one ideally needs to know the total global burden of molecular concentrations and of the emissions. Typically, concentrations are available at only a small number of surface sites and an even smaller number of points in the free troposphere and stratosphere, in which concentrations are also needed if an accurate global burden is to be calculated. In these inverse calculations, only surface observations are used in the comparison of data with models.

The alternative approach to obtaining lifetimes is to calculate them in a forward sense with a photochemical model. In the most straightforward way, a time-dependent photochemical model is used to simulate the evolution of the molecular distribution in the atmosphere by accounting for transport and chemical processes occurring there. The lifetime can be obtained by evaluating the global burdens and integrated global loss rate.

The purpose of this report is to assess how well we can determine the lifetimes of industrially-produced halogenated hydrocarbons. The two approaches described above, inference from concentration and emission data and calculation with atmospheric photochemical models, will be used. Particular attention will be paid to a detailed understanding of how well the components required for these analyses are understood: molecular concentrations and emission rates for the inference procedure; molecular spectroscopy, photochemistry, and atmospheric transport for the calculation procedure. The usefulness and accuracy of the atmospheric models used in the two approaches will also be examined. To help provide some information in this area, several different modeling approaches will be used in both procedures.

This report does not consider the fate of the halocarbon molecules following their breakdown, and does not consider their effectiveness in either the destruction of ozone or in contributing to global warming. For those questions, the reader should refer to other reports such as the assessment reports prepared for the United Nations Environment Programme (UNEP) and the Intergovernmental Panel on Climate Change (IPCC). (See WMO/UNEP Ozone Assessments, 1986, 1989, 1990, 1991; UNEP/IPCC 1990, 1992; and UNEP/WMO, 1992.)

The range of molecules to be treated in this respect spans the full range of halogenated hydrocarbons, including the fully halogenated molecules, chlorofluorocarbons (CFCs), carbon tetrachloride (CCl_4), and carbon tetrafluoride (CF_4), bromofluorocarbons (halons), hydrogen-containing CFCs (HCFCs) and molecules containing hydrogen, carbon and one type of halogen atom, for example the hydrogenated fluorocarbons (HFCs) and molecules such as methyl chloroform (CH_3CCl_3). For comparison purposes, naturally produced molecules such as methyl chloride (CH_3Cl) and methyl bromide (CH_3Br) will also be included.

In order to provide the most critical test of our current knowledge, effects on lifetime inference and calculation were focused on two molecules - trichlorofluoromethane ($CFCl_3$, or CFC-11) and 1,1,1 trichloroethane (CH_3CCl_3, usually referred to as methyl chloroform). First, these two molecules span a useful set of atmospheric behavior - CFC-11 is lost mainly by photodissociation in the stratosphere, while methyl chloroform is lost mainly by reaction with hydroxyl (OH) in the troposphere. These molecules can then serve as a surrogate for other molecules with similar atmospheric properties. Second, these molecules are particularly well-suited for this analysis in that the industrial production is thought to be especially well understood, there is a good long record of measurements, and the lifetime is believed to be sufficiently short (~50 years for CFC-11 and ~6 years for CH_3CCl_3) that one stands a reasonable chance of being able to infer an accurate lifetime from the available data.

This report is broken up into five sections (beyond this introduction). First, the set of available concentration data for the surface, free troposphere, and the stratosphere is reviewed. Second, estimates of production and emission for these molecules is presented. In both these chapters, data are presented in both tabular and graphical form. The extensive use of tabular data allows for use of these data in subsequent analysis. Third, the results of the inverse inference procedures are presented; methods involving both two-and-three dimensional models are employed. Fourth, data needed in the atmospheric photochemical models are presented. This includes spectroscopic parameters (temperature-dependent absorption cross-sections), chemical reaction rates with OH, $O(^1D)$, and Cl, and a few kinetic and thermodynamic quantities for processes occurring in aqueous solution. Finally, results of atmospheric photochemical model calculations of lifetimes are presented, and the results are intercompared to the inverse inference method to better understand the origin of some of the differences between the model results. A comprehensive summary of the data included in this report sorted by molecule is given in Table 1. The content for individual chapters is summarized below.

II. Summary of Scope of Report

The plan for this report and the material included were developed by an international group of scientists in the time period from 1991 to mid-1993 when the report was completed. The formal meetings which led up to this report included an organizational meeting in Alexandria, Virginia, USA in February 1991, a science results exchange/discussion meeting in Newport Beach, California, USA in July 1991, and a report preparation workshop in Blakeney, UK in January 1992. A follow-on meeting specifically related to lifetime inference (see Chapter 3) was held in Washington, DC, USA in June 1992. Additional meetings among scientists working on

Table 1: Summary of Molecular Information*

			Chapter 1: CONC DATA			Chapter 2: PROD/ EMIS	Chapter 3: INFER.		Chapter 4: CHEM DATA			Chapter 5: CALC LIFE/ EST. LIFE	
Class	Formula	Abbrev.	Sur	FT	Strat	P/E	I2	I3	S	K	A	Calc.	Est.
CFCs	CCl_3F	CFC-11	x	x	x	x	x	x	x	x		x	
	CCl_2F_2	CFC-12	x	x	x	x	x		x	x		x	
	$CClF_3$	CFC-13			x	x			x	x			
	CCl_2FCClF_2	CFC-113	x	x	x	x			x	x		x	
	$CClF_2CClF_2$	CFC-114		x	x	x			x	x		x	
	$CClF_2CF_3$	CFC-115		x	x	x			x	x		x	
	C_2F_6	CFC-116			x								
	CCl_4	--------	x	x	x					x	x	x	
	CF_4	--------			x								
	C_2Cl_4	--------	x			x							
CHCs	CH_3CCl_3		x	x	x	x	x	x		x	x	x	
	CH_3Cl		x		x							x	
	$CHCl_3$		x	x						x			
	CH_2Cl_2		x			x				x			
	$CHClCCl_2$		x			x							
	CH_3Br		x			x						x	
HCFCs	$CHFCl_2$	HCFC-21								x			
	$CHClF_2$	HCFC-22	x	x		x				x		x	x
	CH_2FCl	HCFC-31								x			
	$CHCl_2CF_3$	HCFC-123								x			x
	$CHFClCF_3$	HCFC-124								x			x
	CH_2ClCF_3	HCFC-133a								x			
	CH_3CFCl_2	HCFC-141b								x			x
	CH_3CF_2Cl	HCFC-142b								x			x
	$CF_3CF_2CHCl_2$	HCFC-225ca								x			x
	CF_2ClCF_2CHClF	HCFC-225cb								x			x
	$CH_3CF_2CFCl_2$	HCFC-243cc								x			
HFCs	CH_2F_2	HFC-32								x			
	CH_3F	HFC-41								x			
	CHF_2CF_3	HFC-125								x			x
	CHF_2CHF_2	HFC-134								x			
	CH_2FCF_3	HFC-134a								x			x
	CH_2FCHF_2	HFC-143								x			
	CH_3CF_3	HFC-143a								x			
	CH_2FCH_2F	HFC-152								x			
	CH_3CHF_2	HFC-152a								x			x
	CH_3CH_2F	HFC-161								x			
Halons	CBr_2F_2	H-1202							x				
	$CBrClF_2$	H-1211	x		x	x			x	x		x	
	$CBrF_3$	H-1301	x		x	x			x	x		x	
	$C_2F_4Br_2$	H-2402							x				

* Table notes only molecules for which tabular or graphical data are included in the indicated chapter.

Legend:
- Chapter 1: Sur: Surface Concentration Data; FT: Free Troposphere Data; Strat: Stratospheric Data
- Chapter 2: P/E: Production/Emission Data
- Chapter 3: I2: Lifetimes Inferred from 2D Model; I3: Lifetimes Inferred from 3D Model
- Chapter 4: S: Spectroscopic Data; K: Kinetic Data; A: Aqueous Phase Data
- Chapter 5: Calc. Life: Lifetime calculated with 2D Model; Est. Life: Estimated lifetime calculated with 2D Model.

Class:	CFCs:	Chlorofluorocarbons and fully chlorinated or fluorinated hydrocarbons
	CHCs:	Chlorinated Hydrocarbons
	HCFCs:	Hydrogenated Chlorofluorocarbons
	HFCs:	Hydrogenated Fluorinated Hydrocarbons
	Halons:	Fully Halogenated Hydrocarbons including Bromine

individual parts of the report occurred during this time period as part of the ongoing scientific process. Most of the material in this report is current as of the end of 1991, but modifications of the text of the chapters continued through 1992 and into mid-1993.

It is emphasized (see section IV. of this introduction, Future Studies) that much of the work covered in this report is rapidly evolving. In particular, continued investigations about calibrations of existing measurement networks are carried out, which could cause many of the concentration numbers in this report to be adjusted. Similarly, investigations in laboratory kinetics and spectroscopy, and developments in atmospheric modeling, could lead to changes in model calculated lifetimes (see Chapter 5). In using this report, the reader should be aware that more up-to-date information affecting some of the quantitative conclusions reached here may be found in the published literature. Readers are encouraged to examine the current literature and/or contact the appropriate investigators before quantitative conclusions from this report are used.

This section consists of a summary of the information contained in the report broken down by chapter.

1. Molecular Concentrations

Three types of data are included with this chapter: surface level concentrations measured from fixed locations or from aboard ships, free-tropospheric data measured *in situ* from aircraft, and stratospheric vertical profiles measured *in situ* from balloons or remotely from the space shuttle.

Surface data come from a variety of organized networks and more localized single stations. The mapping between measurement location and observing network or organization is given in Table 2; to provide some sense of geographical coverage, stations are arranged in order of decreasing latitude (north to south). The full names of the networks and organizations abbreviated in the text are given in an Appendix of this report.

The list of species measured by the various networks and stations for surface and free-tropospheric data are given in Table 3. This includes species for which graphical and/or tabular data are found in Chapter 1 (CCl_3F, CCl_2F_2, CCl_2FCClF_2, CCl_4, CH_3CCl_3, $CHCl_3$, and HCFC-22) and some additional species which are not dealt with in detail. Chapter 1 includes some discussion of additional species for which no data are presented in tables or figures (other than Table 1.1). These species are not included in Table 3.

A comprehensive list of relatively recent stratospheric profile data for the molecules under consideration is included in Chapter 1. Balloon-borne profiles cover the time period from 1985 to 1990, and were made at low latitudes, mid latitudes, and high latitudes in the Northern Hemisphere. There are also vertical profiles obtained from the Atmospheric Trace Molecule Spectroscopy (ATMOS) instrument at 30°N; these were obtained in April-May 1985 during the Spacelab-3 Space Shuttle mission at approximately 30°N latitude. The set of available stratospheric data is summarized in Table 4, the numbers in the table reflect the number and independent balloon-borne profiles for a given molecule in the indicated latitude region.

Table 2: Locations of Atmospheric Measurements Data

		NETWORKS									
Station	Latitude	ALE/GAGE	NOAA/ CMDL	UT	FIAER	OGIST	UCI	MRI	JPL	UE A	SIO
Alaska	71		x								
Ireland	52	x									
Oregon	45	x									
Colorado/PNW	40		x			x					
Hokkaido	40-45			x							
Table Mountain	34								x		
Kitt Peak	32								x		
Mauna Loa	19		x								
Barbados	13	x									
Samoa	-14	x	x								
Cape Point	-34	x				x					
Tasmania	-41				x						
Syowa	-69			x							
South Pole	-90		x			x					
Global Average		x	x	x		x	x				
Aircraft											
Europe/ Atlantic Ocean					x						
Japan								x			
Shipboard											
Various										x	x

Legend:

ALE/GAGE	Atmospheric Lifetime Experiment/ Global Atmospheric Gases Experiment
NOAA/CMDL	National Oceanic and Atmospheric Administration/ Climate Monitoring and Diagnostic Laboratory
UT	University of Tokyo, Japan
FIAER	Fraunhofer Institute for Atmospheric Research (Germany)
OGIST	Oregon Graduate Institute of Science and Technology
UCI	University of California, Irvine
MRI	Meteorological Research Institute (Japan)
JPL	Jet Propulsion Laboratory, Pasadena, California
UEA	University of East Anglia, Norwich, UK
SIO	Scripps Institution for Oceanography

Table 3: Summary of Measurement Networks

			MOLECULE						
Network	Altitude	Stations	CFC-11	CFC-12	CFC-113	CCl_4	CH_3CCl_3	$CHCl_3$	HCFC-22
ALE/GAGE	Surface	5	x	x	x	x	x	*	
NOAA/CMDL	Surface	4	x	x					
UT	Surface	2	x	x	x	x	x		x
UEA	Shipboard	-	x	x	x	x	x		
UCI	Surface	Averaged	x	x	x				
SIO	Shipboard	-	x	x					
FIAER-CSIR	Surface	1	x			x			
FIAER	Free Trop	-	x	x	x	x	x		
MRI	Free Trop		x	x					
OGIST	Surface	5					x	x	x
Kitt Peak	Ground Based Column								x
Table Mountain	Ground Based Column								x

*For Tasmania only. $CHCl_3$ not collected at other 4 stations in network.

Table 4: Summary of Stratospheric Data

	Number of Balloon Profiles			ATMOS
	Tropics	Mid Latitudes	High Latitudes	30°N
CFC-11		9	6	x
CFC-12	1	9	6	x
CFC-13	1	1		
CFC-14		3		x
CCl_4		9	4	
HCFC-22	1	1		x
CH_3Cl		8	4	x
CH_3CCl_3	1	9	4	
CFC-113	1	9	5	
CFC-114	1	1		
CFC-115	1	1		
CFC-116		3		
Halon-1301	1	1		
Halon-1211	1	1		

2. Emission Rates

In Chapter 2 of this report, estimates of the global emission rates of a variety of molecules are presented. Global emission rates are not measurable quantities, however; they need to be calculated based on a knowledge of molecular production, of their use, and of the characteristic times for molecular emission associated with a given use. Each of these issues is addressed in this chapter. The available data, including the time period of the emission estimates, are summarized in Table 5.

The process of estimating emissions has several steps. Molecular production levels are obtained from surveys carried out by the chemical industry and international organizations. Production from some countries was not included in the industry-sponsored surveys (non-reported emissions), and particular attention is given to assessing what the non-reported produced levels were likely to have been for these molecules. The industry-sponsored surveys also had information on end-use and geographical distribution of sales. Based on some experimental data and industrial experience, a correspondence between constituent end-use and characteristic emission time was derived. It is particularly important to differentiate between those uses of a molecule in which the emission rapidly follows its use, from those in which the molecule is retained for several years following its use. Molecules which are incorporated in various applications and which have not been released into the atmosphere constitute a "bank" from which they will slowly be released. As production of CFCs, halons, and related molecules is phased out due to international agreements such as the modified Montreal Protocol for Substances that Deplete the Ozone Layer, molecular emissions from this service bank will constitute an ever-increasing fraction of the global emissions.

Table 5: Summary of Production and Emission Data

	Production/Emission	Comment
CFC-11	1931-1991	
CFC-12	1931-1991	
CFC-113	1970-1991	
CFC-114	1934-1991	
CFC-115	1964-1991	
HCFC-22	1970-1991	
CH_3CCl_3	1971-1991	
H-1211	1963-1991	Emission data until 1990 only
H-1301	1963-1991	Emission data until 1990 only
CH_2Cl_2	1990	
C_2Cl_4	1987, 1990	Dispersive uses only
C_2HCl_3	1987, 1990	Dispersive uses only
CH_3Br	1984-1990	

3. Inference Procedures

The surface concentrations of CFC-11 and methyl chloroform measured with the ALE/GAGE Network are used in Chapter 3, together with the emission rates in the inference of molecular lifetimes. Two complementary modeling approaches are used. In one, carried out by the ALE/GAGE team, an ultra-low resolution two-dimensional (2-D) model (typically containing 12 grid boxes) with several adjustable dynamical parameters is used for the lifetime inference. In the other, three-dimensional (3-D) chemistry-transport models are used. Two of the latter models were used - in one study, carried out by Martin Heimann at the Max-Planck-Institut für Meteorologie in Hamburg, Germany, analyzed wind fields for the year 1987 are used in the transport model. In the other study, carried out by Michael Prather of the University of California at Irvine, winds from the general circulation model at NASA's Goddard Institute for Space Studies (GISS) were used in providing constituent transport. In the former model, there was no adjustment of dynamical parameters in fitting the data; in the latter a single parameter for horizontal diffusion was optimized to best fit the CFC-11 interhemispheric gradient in the early years of the ALE/GAGE data set. Differing statistical techniques were used with the different modeling approaches.

In carrying out this analysis, attention must be given to the uncertainties in the input parameters (concentration data, emission rates and global distribution) and to determining what effect these uncertainties have on the inferred lifetimes. The most critical parameter is the uncertainty in the absolute calibration of the ALE/GAGE data. The possibility of a systematic drift in the calibration must also be considered. Additional parameters for which uncertainties need to be considered include the assumed value of emissions related to unreported production, and the geographical distribution (especially the split between the Northern and Southern Hemisphere) of the surface emission. Attention must also be paid to the possibility of a systematic change in the lifetime of methyl chloroform as a result of changes in the global distribution and integrated concentration of the hydroxyl radicals that constitute its major sink.

4. Photochemical Data

In the atmospheric photochemical models, those processes responsible for the destruction of CFCs must be adequately represented. As was noted above, two types of destruction dominate - photodissociation in the stratosphere, and photochemical loss in the troposphere by reaction with hydroxyl. Calculation of stratospheric photodissociation rates requires accurate knowledge of molecular absorption cross-sections for the CFCs and molecular oxygen (O_2) and the CFCs' photolytic quantum yields, which are usually assumed to be unity. In this chapter, the absorption cross-sections are given as a function of wavelength and temperature for several fully halogenated hydrocarbons. The molecules covered are indicated in the appropriate column (Chapter 4-S) of Table 1.

Photochemical reactions which can destroy these molecules include those with OH, $O(^1D)$, and Cl. Reaction with OH is the dominant one for most of the hydrogen-containing halocarbons; the others are included mainly for completeness. For reactions with $O(^1D)$ there are two possible product channels - that leading to physical quenching of $O(^1D)$ to $O(^3P)$ without chemical reaction, and that leading to chemical reaction.

There is observational evidence that methyl chloroform and carbon tetrachloride. may be destroyed in the ocean by hydrolysis. For this reason, aqueous decomposition rates and Henry's Law coefficients for the two stated molecules in water are examined as a function of temperature.

Due to the salinity of the ocean, these quantities should be known as a function of ionic strength as well; to that end the salting-out coefficient of methyl chloroform was also examined.

5. Photochemical Model Calculation of Lifetimes

Lifetimes of the halogenated hydrocarbons were calculated by seven different modeling groups in Chapter 5. Six of these are two-dimensional models (in which only the dimensions of latitude and altitude are resolved; no variation is assumed in the longitudinal directions), and one is a low resolution three-dimensional model. Two types of lifetimes were calculated, steady-state lifetimes, in which fixed (time invariant) boundary conditions are assumed for all gases, and transient lifetimes, in which a time-dependent boundary condition is used to better simulate the actual evolution of CFCs in the atmosphere. The available lifetimes calculated for the different molecules by the modeling groups are given in Table 6; the symbol S is used for those constituents for which only steady-state lifetimes were calculated; T is used when both transient and steady-state lifetimes were calculated. The model-calculated lifetimes can be compared to the inferred ones for CFC-11 in Chapter 3. For CH_3CCl_3, the OH fields are not sufficiently accurate for trustworthy lifetimes to be determined, indeed the tropospheric OH levels in these models are typically adjusted in order to produce reasonable CH_3CCl_3 lifetimes.

Table 6: Summary of Model Calculations (Model 2D unless specified)

Molecule	AER	GSFC	LLNL	MIT (3D)	MPI	MRI	U. Wash.
CFC-11	T	T	S	T	S	T	T
CFC-12	T	T	S	T	S	T	T
CFC-113	T	T	S	T	S	T	T
CFC-114	S	S	S				
CFC-115	S	S	S				
CCl_4	T	T	S	T		T	T
N_2O	T	T	S	T	S	T	T
H-1211	T	T	S		S	T	
H-1301	T	T	S		S	T	
HCFC-22	T	T	S	S	S	T	
CH_3CCl_3	T	T	S	S	S	T	
CH_3Cl	S	S	S				
CH_3Br	S	S	S				

S: Steady State Lifetimes only calculated
T: Steady State and Transient Lifetimes calculated

Since the models obtain a range of lifetimes for CFC-11, some effort is placed on understanding the origin of the model differences. Both variations in model photochemistry and transport are considered. Photolysis rates of the CFCs and halons are compared to determine the likely magnitude of the differences between the models. Differences in transport are assessed by the use of simulated tracers in which their source distributions and/or emission rates and their destruction rates are very simply parameterized. Differences in the calculated distribution of these simulated tracers then points very clearly to the differences in particular aspects of the transport between the models.

Because of the critical role which transport plays in affecting the model-calculated distributions of CFCs and other halocarbons, model output can be analyzed in such a way that concentration profiles of constituents are considered not individually against altitude, but in pairs one against another. For molecules whose chemistry is governed by similar processes (*e.g.* slow photodissociation in the stratosphere), a good correlation is expected between their concentrations. Most typically, correlations of distributions of CFCs with those of N_2O are examined.

For HCFCs and HFCs, lifetimes are estimated using approximate tropospheric lifetimes (based on reaction rates with OH and the mean global OH distribution inferred from the CH_3CCl_3 lifetime data) and stratospheric lifetimes calculated with the AER 2-D model. The calculated tracer correlations are compared with those obtained in the stratospheric profiles presented in Chapter 1. Analytical models show that in such cases, accurate ratios of lifetimes should be obtained. The relative lifetime ratios suggested from the model calculations and the stratospheric vertical profiles can then be examined.

III. Summary of Results

In this section only those results most closely related to the inferred and calculated lifetimes of CFC-11 and methylchloroform will be presented. For additional results, the reader should consult the executive summary for the overall report and the summaries for each chapter.

The ALE/GAGE measurements provide a very useful data set for use in the procedure of inferring lifetimes. There is strong agreement among several measurement groups on the CFC-11 absolute calibrations, so the ALE/GAGE measurements should be usable in inference studies with some confidence. For methylchloroform, comparisons of data among several groups suggests that the absolute calibration is not yet completely fixed, and that the ALE/GAGE measurements need to be used with more attention paid to the effects of uncertainties in the calibration.

The CFC-11 lifetime inferred in Chapter 3 with the two-dimensional ALE/GAGE model and the three-dimensional MPI-Met are in reasonable agreement, with values in the 50-55 year range. These are consistent with the results calculated with the photochemical model (Chapter 5), which fall in the range 40 - 54 years (one model obtained a lifetime of approximately 60 years, but its transport differed markedly from that of the others). By consideration of the vertical profiles of N_2O and CFC-11 obtained from balloon flights and shuttle observations (See Chapter 1), the ratio of slopes suggests that the lifetime of CFC-11 is 53 years, assuming an N_2O lifetime of 110 years.

The GISS model used in Chapter 3 could only obtain an adequate fit to the data by assuming a calibration factor significantly different from that used by the ALE/GAGE Network. Fits of comparable quality can only be obtained by allowing for assumptions of a small calibration shift and a change in the magnitude of the unreported emissions; in such a case a smaller variation in the calibration adjustment would suffice.

There is clear evidence of a difference in the ALE/GAGE and GISS atmospheric models. Many of the differences in inferred lifetimes can be related to differences in the concentrations of CFCs in the two models; the connection between these quantities is very strong. The MPI-Met model may have a problem in its interhemispheric transport, as the optimally-determined interhemispheric mix of CFC-11 sources, puts an implausibly large (20%) fraction of the emission in the Southern Hemisphere.

For methyl chloroform, there is much better agreement between the ALE/GAGE and GISS models. A lifetime of the order of 6 years is computed by both assuming that the ALE/GAGE calibration factor is correct. If the actual calibration factor is appreciably lower, as was

suggested by studies at the University of Tokyo (UT), then an appreciably smaller (~4 year) lifetime is needed to best explain the data.

The result that the best fit to the methylchloroform data is obtained with increasing tropospheric OH levels, is very sensitive to the actual calibration factor. Were the network calibration value to be close to the UT-derived one, the best fit to the ALE/GAGE observations would require a slow decrease in the tropospheric OH amounts. The photochemical model calculations of CH_3CCl_3 lifetime carried out in Chapter 5 do not provide a truly independent value, as the models' tropospheric OH fields are typically adjusted to provide a reasonable lifetime for CH_3CCl_3 in the first place.

In the long term it seems clear that three-dimensional models would provide the most complete way of simulating station data and thus inferring lifetimes from measurements of trace gas concentrations and estimates of emissions. In the short term, however, there is no clear consensus about the optimal approach to use in inferring lifetimes. The current two- and three-dimensional models differ substantially from each other in their use of fitted parameters, methods for data comparisons, and use of atmospheric data as input parameters. The analysis of modeling approaches and also of statistical methods should remain an active area of research in coming years.

IV. Future Studies

This report represents a detailed look at the state of our knowledge of CFCs as of the early 1990s (data through 1990 are included in Chapter 1, for example, while production and emission data through 1991 are included). In the next few years, our ability to address several of the issues should improve. Particular areas in which improvement are likely include the following:

1. Improved knowledge of calibration

Recognition that the absolute calibrations for methylchloroform, carbon tetrachloride, and HCFC-22 are not fully established can be expected to lead measurement groups to refine their calibrations and determine more accurate values (both absolute and any concentration-dependence associated with detector non-linearity). Improved knowledge of HCFC-22 infrared spectroscopic parameters should also allow for more precise measurement of its atmospheric distribution as determined by ground-based column measurements.

2. Additional surface data

As the data record lengthens, it should become easier to do the inference process since it will correspond to a larger fraction of the lifetime. In the next few years it should be possible to detect a continuing decrease in the rate of growth of CFCs in the atmosphere as their use is phased out in response to international agreement. The behavior of the concentrations in response to this change may also shed valuable light on the relationship between production and emission. One drawback here is that unreported emissions may form a large component of the total.

3. Major additions to the database for vertical profiles of halocarbons

Several recent measurement programs will dramatically increase the availability of vertical profiles of CFCs and other halocarbons. These will typically include simultaneous measurements of several species, which allows for their use in studies of tracer correlations. Particular measurement programs include:

(i) The Second Airborne Arctic Stratospheric Expedition (AASE-2), in which the ER-2 was fitted with a new rapid-response instrument to measure CFC-11 and CFC-113 (which accompanies an existing N_2O-measuring instrument);

(ii) The European Arctic Stratospheric Ozone Expedition (EASOE), in which there were several balloon flights where the vertical profiles of several halocarbons were simultaneously measured;

(iii) Global distributions of CFC-11 and CFC-12 will become available from the Cryogenic Limb Array Etalon Spectrometer (CLAES) instrument onboard NASA's Upper Atmosphere Research Satellite (UARS). This instrument began operating shortly after the UARS launch in September 1991 and ceased operation in May 1993, when its supply of cryogen became depleted; and

(iv) Vertical profiles of CFC-11, CFC-12, CCl_4, HCFC-22, and CH_3Cl obtained with the ATMOS instrument which flew onboard NASA's Atmospheric Laboratory for Applications and Science (ATLAS) mission in March-April 1992 and April 1993. Some 90 profiles in the latitude range from 25°N - 55°S were obtained in the ATLAS-1 mission, while some 70 and 30, were obtained at high northern and mid-southern latitudes, respectively, during the ATLAS-2 mission.

4. Improvements in modeling capability

Improvements in general circulation models and availability of new sets of assimilated data should allow for better simulation of halocarbon distributions in the stratosphere. Results of ongoing model intercomparisons may provide improvements in model simulations of model transport, which are particularly important if the CFC distributions are to be accurately simulated. Advances in tropospheric chemical modeling should allow for improved calculation of OH fields; these could further enhance our capability to simulate the distribution of molecules which react with OH, such as CH_3CCl_3, this is a research activity which is to be strongly encouraged over the next 5-10 years.

Acknowledgments

We acknowledge the support of the Alternative Fluorocarbon Environmental Acceptability Study (AFEAS) which provided travel funds used to support the participation of most of the non-US scientists working on this report.

References

Intergovernmental Panel on Climate Change, *Climate Change, The IPCC Scientific Assessment*, WMO/UNEP, J. T. Houghton, G. J. Jenkins and J. J. Ephraums (Eds.), Cambridge University Press, Cambridge, UK, pp 365, 1990.

Intergovernmental Panel on Climate Change, *Climate Change 1992, The Supplementary Report to The IPCC Scientific Assessment Combined with Supporting Scientific Material*, WMO/UNEP, J. T. Houghton, B. A. Callander and S. K. Varney (Eds.), Cambridge University Press, Cambridge, UK, pp 200, 1992.

United Nations Environment Programme, Methyl bromide and the ozone layer: a summary of current understanding, Atmospheric Science Assessment in *Methyl Bromide: Its Atmospheric Science, Technology, and Economics, Montreal Protocol Assessment Supplement*, UNEP, D. L. Albritton and R. T. Watson, co-chairs of Science Assessment, 41 pp, 1992.

World Meteorological Organization, *Atmospheric Ozone 1985: Assessment of our Understanding of the Processes Controlling its Present Distribution and Change*, WMO Report No. 16, WMO Global Ozone Research and Monitoring Project, WMO/UNEP, R. T. Watson, Assessment Chair, (3 volumes) 1986.

World Meteorological Organization, *Report of the International Ozone Trends Panel 1988*, WMO Report No. 18, WMO Global Ozone Research and Monitoring Project, WMO/UNEP, R. T. Watson, Chair, (2 volumes) 1989.

World Meteorological Organization, *Scientific Assessment of Stratospheric Ozone: 1989*, WMO Report No. 20, WMO Global Ozone Research and Monitoring Project, WMO/UNEP, D. L. Albritton and R. T. Watson, co-chairs, (2 volumes) 1990.

World Meteorological Organization, *Scientific Assessment of Ozone Depletion: 1991*, WMO Report No. 25, .WMO Global Ozone Research and Monitoring Project, WMO/UNEP, D. L. Albritton and R. T. Watson, co-chairs, 1992.

CHAPTER SUMMARIES

Chapter 1—Measurements

Tropospheric Measurements

- Several extensive, global, long-term data sets, based on gas chromatographic techniques, are now available on surface measurements of CFC-12 (CCl_2F_2), -11 (CCl_3F), -113 (CCl_2FCClF_2), methyl chloroform (CH_3CCl_3) and carbon tetrachloride (CCl_4).

- A significant, new Northern Hemispheric data set on tropospheric HCFC-22 ($CHClF_2$), based on spectroscopic techniques, is available.

- There is a serious lack of data available on the global sources and distribution (and trends) of the important chlorine and bromine species, methyl chloride (CH_3Cl), the halons, and methyl bromide (CH_3Br), as well as several other organobromine species.

- Recent data from the mid-to-high latitudes of the Northern Hemisphere suggest that the growth rates of CFC-11 and -12 have started to decline, presumably in response to reduced emissions.

Stratospheric Measurements

- Simultaneous vertical profile measurements have been made in the stratosphere for most of the substances controlled under the Montreal Protocol and many others.

- Most data have been collected in balloon flights at mid latitudes in the Northern Hemisphere. Some data are available from polar regions and the tropics. Satellite instruments can provide global data, but they are very limited at the present time.

- Individual profiles for many molecules removed by photolysis in the stratosphere correlate well with each other confirming the good precision of the measurements.

- Profiles measured at tropical, mid- and high northern latitudes agree with model predictions as to the altitude at which photolysis begins to remove halocarbons.

- Observationally derived lifetimes can be compared with those obtained purely by calculation and serve to constrain uncertainties in the calculated values.

Calibration

- Calibration issues continue to limit our understanding of the global atmospheric distributions and trends of these species. Most activities undertaken to resolve this important issue are unsatisfactory at this stage.

- The calibration uncertainty range associated with measurements of CFC-11 and -12 by various laboratories appear to be currently less than 5%, whereas for CFC-113, CCl_4 and CH_3CCl_3 it is greater than 20%. This latter uncertainty must make a major contribution to the uncertainty of estimating atmospheric lifetimes of these species, and in the case of

CH_3CCl_3, in estimating global OH levels. There have been insufficient experiments to determine whether these calibration uncertainties may have changed with time. There are insufficient data to evaluate the uncertainty in the absolute calibration of HCFC-22.

Chapter 2—Production and Emission of CFCs, Halons, and Related Molecules

- Production of CFC-11 and CFC-12 peaked in 1987 and their estimated emissions have decreased substantially since 1988.

- The major uncertainties in the calculations of current, global emissions for CFC-11 and CFC-12 are the lack of data from companies not reporting to industry panels along with the estimation of banking times for long-term uses.

- For CFC-11, CFC-12 and CFC-113, reporting companies are estimated to account for 85-90% of total production; higher percentages are believed for most other CFCs and methyl chloroform. At least 95% of the CFC production and emission is believed to take place in the Northern Hemisphere.

- The proportion of emissions of CFC-11 and CFC-12 from non-reporting companies is projected to increase as production is phased out under the Montreal Protocol. In addition, the fraction of total emissions arising from the service bank of CFCs will also increase as new production decreases. Emission levels are therefore likely to fall off less rapidly than production, and the uncertainty in emission relative to production will grow.

- Methyl chloroform emissions increased during the 1980s, partly due to its substitution for restricted substances, including CFC-113 and other volatile organic compounds. There are no industrial estimates for current production of carbon tetrachloride produced for dispersive uses. Somewhat inprecise production and emission data are available for methylene chloride (CH_2Cl_2), trichloroethylene ($CHClCCl_2$) and perchloroethylene (CCl_2CCl_2), which are short-lived compounds whose study may help shed light on global average distributions of tropospheric OH.

- HCFC-22 emissions have increased at approximately 8.5% per year since 1980. This increase is due in part to substitution for restricted CFCs. There are no industrial estimates for other HCFCs since they are significantly lower and presently have not met the agreed-upon criteria for industry reporting.

- Some proportion of methyl chloride emissions, may be due to anthropogenic sources (15-30%), probably almost all from biomass burning. The rest of the emissions are from natural sources, primarily the oceans.

- Methyl bromide emissions to the atmosphere have a number of sources. These include a significant natural component, most likely from the oceans, and various anthropogenic sources, such as fumigant use. There is considerable uncertainty about both the anthropogenic and natural emissions of methyl bromide.

Chapter 3—Inferred Lifetimes

This chapter examines the empirical models used to derive the atmospheric residence lifetimes of the industrial halocarbons using four components: observed concentrations, history of emissions, a predictive atmospheric model, and an estimation procedure for describing an optimal model. The model describes both the mixing of the trace gas throughout the atmosphere and its chemical loss. The predictions of model plus emissions are compared with the observations. The estimation procedure is used to select a "best fit" for a range of chemical losses (and hence lifetimes), including uncertainties in emissions and observed concentrations.

We present here three efforts to infer the lifetime of $CFCl_3$ (CFC-11), two of which are also applied to CH_3CCl_3 (methyl chloroform). All studies used the same emissions (see Chapter 2) and observations (that is, monthly means of unpolluted air from the five ALE/GAGE surface sites). "Optimal inversion" results are those obtained by the ALE/GAGE researchers using their published statistical method for empirical determination of the atmospheric residence time for industrial halocarbons, whereas "least squares" refers to results obtained in the course of preparation of this report using a GISS atmospheric model with least squares and related methods to determine the atmospheric residence time. In addition, the Hamburg 3-D model was used to infer a "best" lifetime or emission source for CFC-11.

These studies considered one or more of the following key quantities to be "uncertain" in terms of optimizing the model simulation of the reported observations:

- "lifetime", the atmospheric lifetime of a gas. (Although the chemical loss of either $CFCl_3$ or CH_3CCl_3 is a complex pattern in space and time, only a uniform scaling of the loss frequencies was considered here.)
- "pseudo-calibration", an adjustment factor applied to the observed concentrations to give the best fit to the modeled concentrations. (This quantity effectively includes absolute errors in the calibrations and systematic offsets in the model predictions of surface concentrations.) If allowed to change with time, it can include drifts in the calibration as well.
- "estimated emissions", the emissions of $CFCl_3$ estimated from the non-reporting segment of global production. (See Chapter 2.)

The following quantities were not considered as formal uncertainties in these studies:

- the atmospheric circulation or parameterized mixing
- the location of chemical losses
- the emissions from reporting companies.

The different approaches used here have reported formal confidence intervals in various units. Scientific credibility is normally tied to 95% confidence intervals as reported in this chapter for the "least squares" approach; but the "optimal inversion" results here are available only as 1-σ uncertainties. In this summary alone, we compare the 1-σ range with 68% confidence intervals. Those associated with "optimal inversion" estimates reflect measurement error, natural variability, and emissions uncertainty; "least squares" intervals do not allow for emissions uncertainty.

CFC-11 Lifetime

For the case of fixed emissions (as tabulated in Chapter 2) and no pseudo-calibration we infer a lifetime of

50 (+24, -13)yr for "optimal inversion",
100 yr for "least squares" (fit is too poor, no statistical uncertainty).

When the methods allow the pseudo-calibration to be determined by the optimization procedures, the lifetimes become

40 (+10, -7) yr for "optimal inversion"

39 (+4, -3) yr for "least squares" (the pseudo-calibration factor (PCF) is 0.88, equivalent to reducing the absolute calibration by 12% from 0.948 to 0.839).

When the pseudo-calibration is allowed to drift by +2% per decade (to 0.88 in 1990, interpreted as either calibration drift or calibration nonlinearity) and the non-reporting emissions are halved, the lifetime is

56 (+5 -3) yr for "least squares"

The range in pseudo-calibration factors chosen by some of the optimization procedures is outside the expected uncertainty in the laboratory calibration. The PCF may also account for inaccuracies in the atmospheric model which is discussed below. If we accept the emissions history, then the preferred fit from the "least squares" is 39 years with a 95% confidence range of 34 - 47 yr.

Methyl Chloroform Lifetime

For the case of fixed emissions ("optimal inversion" assumes slightly different emissions from those derived from industry survey in Chapter 2) and adopting current ALE/GAGE calibration, the inferred lifetime is

6.1 (+1.4, -1.0) yr by "optimal inversion",

6.4 (+0.2, -0.2) yr by "least squares".

When the pseudo-calibration is determined separately at each station (which, for example, may also be considered as a systematic error in the atmospheric model's ability to predict concentrations at a given site) the lifetime is inferred to be

4.8 (+0.6, -0.7) yr by "optimal inversion" with average,

4.2 yr by "least squares" with average.

If the pseudo-calibration is fixed and the atmospheric loss frequency (L) is allowed to change linearly over the period, then the inferred lifetime is

5.7 - 5.9 yr with L = +1 (+0.6, -0.6) %/yr for pseudo-calibration = 1.00 from both methods,

4.9 yr with L = +0.5 %/yr for pseudo-calibration = 0.875,

4.3 yr with L = -0.3 %/yr for pseudo-calibration = 0.75.

The possible identification of a trend in tropospheric chemistry (for example, OH) will depend on the determination of the CH_3CCl_3 absolute calibration.

Atmospheric Models

Much of the difference between the optimal inversion-ALE/GAGE results and the least squares-GISS results can be attributed to the atmospheric models. The distribution of trace gases in the atmosphere relative to the surface sites (where comparisons are made with observations) can be equated to a shift in the pseudo-calibration factor. The differences between estimates obtained from different atmospheric models (1-box global mean, ALE/GAGE 12-box, GISS 3-D/8000-box) are not trivial, when no adjustment of calibration is allowed. In the case of CFC-11, the differences between the ALE/GAGE and GISS atmospheric models account for most of the differences in lifetimes (50 versus 100 yr) with the standard calibration. Likewise, both models give similar lifetimes in fitting the trend (40 versus 39 yr) but with substantially different pseudo-calibration factors. The lifetime inferred for more short-lived gases such as CH_3CCl_3 is much less sensitive to the atmospheric model.

Chapter 4—Laboratory Studies of Halocarbon Loss Processes

- Improved laboratory data have been obtained from reactions of OH with 14 different halocarbons. The most significant changes were those in reactions with HCFC-141b (CH_3CFCl_2), HCFC-142b (CH_3CF_2Cl), HFC-125 (CHF_2CF_3) and HFC-143a (CH_3CF_3). The largest change in rate constant at atmospheric temperatures is a decrease of about 30% for HCFC-141b.

- New evaluations of reaction rates of $O(^1D)$ with 8 different halocarbons were obtained. The branching ratios for the quenching of $O(^1D)$ to $O(^3P)$ were also obtained. In addition reaction rates of Cl (chlorine) with 18 different halocarbons were measured and the rates of reactions of NO_3 (nitrogen trioxide) with various halocarbons were found to be very slow (room temperature rates slower than 3×10^{-18} cm^3 $molec^{-1}$ sec^{-1}).

- Absorption cross sections (including temperature dependence) were re-evaluated for CFC-11, CFC-12, CFC-113, CFC-114 ($CClF_2CClF_2$), CFC-115 ($CClF_2CF_3$) and the halons. Hydrolysis rates and Henry's Law constants for methyl chloroform and carbon tetrachloride have been reviewed in the context of recent data.

Chapter 5—Model Calculations of Atmospheric Lifetime

- This chapter examines the model-calculated lifetimes of the species discussed in this report. The atmospheric lifetime is defined as the atmospheric burden divided by the atmospheric removal rate. By simulating explicit mechanisms that are responsible for the removal of the trace gases, model calculations can predict how the lifetimes of the species may change as the atmospheric compositions change. They also allow the calculation of lifetimes for species that are not yet emitted to the atmosphere.

- The species discussed in this report can be separated into two groups: those that are removed mainly by UV photolysis in the stratosphere and those that are removed mainly by reaction with OH in the troposphere. Species in each group require different observations for validation of the mechanisms for atmospheric removal.

For species that are mainly removed in the stratosphere by photolysis

- Photochemical removal processes and atmospheric transport are both important and each contribute to the variances in computed lifetimes among the models.

- Differences in computed photolysis loss frequencies for the numerical models are significant and further work is required to totally understand model differences.

- The effects of differences in atmospheric transport on atmospheric lifetimes among the numerical models are at least 30%. There are insufficient observations to allow one to decide whether the 2-D models are correctly simulating the bulk transport of the trace gases in the lower stratosphere. Due to the natural variabilities in the atmosphere, it would be difficult to use stratospheric observations to constrain the lifetimes of these species to better than 30%.

- Current model simulations indicate that the calculated transient lifetimes for the CFCs could be about 10% larger than the calculated steady-state lifetime through the 1980s.
- The calculated atmospheric lifetimes for CFC-11 ($CFCl_3$) are consistent with the values derived in Chapter 3.
- Simultaneous measurements of the stratospheric concentrations of two species can be used to estimate the ratio of their lifetimes if enough is known about their local removal processes and their emission histories.

For species that are removed mainly by reaction with OH in the troposphere

- We determine lifetimes for the HCFCs and HFCs using model calculated stratospheric loss and tropospheric OH loss. The tropospheric OH removal is adjusted using the tropospheric removal rate of methyl chloroform (CH_3CCl_3) derived from the atmospheric lifetime of CH_3CCl_3 from Chapter 3, the estimated ocean removal rate, and the model calculated stratospheric removal.
- Using the methyl chloroform data as a proxy of OH is complicated by uncertainties associated with the statistical methods and with the uncertain role of the ocean sink, not to mention the calibration problems identified in Chapter 1. Thus, it is difficult to be confident about the lifetimes of these species to better than a factor of 1.5.

The following modelling groups provided model results that are used in this chapter.

Table 5.1 Modelling groups that provided results for this report

Atmospheric and Environmental Research, Inc.	Malcolm Ko and Debra Weisenstein	AER
NASA/Goddard Space Flight Center	Charles Jackman and Anne Douglass	GSFC
Lawrence Livermore National Laboratory	Don Wuebbles and Peter Connell	LLNL
Max Planck Institute for Chemistry	Christoph Bruehl	MPI
Meteorological Research Institute, Japan	Toru Sasaki	MRI
University of Washington	Ka Kit Tung, Hu Yang, and Eduardo Olaguer	WASH
Massachusetts Institute of Technology*	Amram Golombek and Ronald Prinn	MIT

*3-D model

SECTION E

THE ATMOSPHERIC EFFECTS OF STRATOSPHERIC AIRCRAFT: INTERIM ASSESSMENT REPORT OF THE NASA HIGH-SPEED RESEARCH PROGRAM

EXECUTIVE SUMMARY

This report provides an interim assessment of the impact of proposed high-speed, i.e. supersonic, civil transport aircraft on the ozone layer. The degree to which the major scientific questions can be answered at this time is summarized as follows.

What emissions could occur from high-speed civil transport (HSCT) aircraft?

A key requirement in the assessment of the potential impact of such aircraft is to quantify their emissions and to evaluate whether these emissions are significantly transformed by homogeneous and heterogeneous processes in the exhaust plume or wake dispersion region.

- Predicted airframe and exhaust emissions from fleets of HSCTs show the possibility of significant increases in the stratospheric concentrations of nitrogen oxides, water vapor, sulfur oxides, and soot.

- Emissions of oxides of nitrogen (NO_x), carbon monoxide (CO), hydrocarbons (HC), water vapor, carbon dioxide (CO_2), and sulfur oxides (SO_x) have been estimated for nine scenarios comprising the 1990 aircraft fleet and projected fleets of subsonic and supersonic aircraft (HSCTs) flying in 2015. Subsonic scenarios for 1990 and 2015 consider the effects of scheduled commercial passenger and cargo air traffic, including turboprop aircraft, along with military, charter, and nonscheduled aircraft traffic. HSCT fleets for a fixed passenger demand in 2015 were configured with a range of about 5000 nautical miles and capability for carrying 300 passengers flying at cruise speeds of either Mach 1.6, 2.0, or 2.4 under a range of NO_x emission indices (EI).

- Model calculations of exhaust plume chemistry and condensation processes indicate a fraction of the exhaust NO_x and SO_x will be converted to HNO_3 and to H_2SO_4, respectively. Wake-vortex models indicate a potential for extensive new particle production in the plume due to binary homogeneous nucleation of sulfuric acid vapor and water vapor. Whether or not these plume induced new particles have a significant effect on general stratospheric properties awaits further analysis.

- Model analyses of radiative cooling in the wake dispersion regime indicate that the aircraft effluents will probably subside 0.5 to 1.0 km or less and will thus be deposited near or slightly below flight altitudes.

- Model calculations have not yet identified any plume or wake phenomena that alter NO_y speciation enough to seriously impact the input assumptions used in current assessment calculations.

What ozone-related chemical processes are important in today's atmosphere and in a future atmosphere perturbed by HSCT emissions?

Ozone in the lower stratosphere is controlled by both chemical and transport processes. Ozone is chemically controlled by radicals in the hydrogen, nitrogen, and halogen families. Because these chemical families are highly coupled, an increase in either NO_x or H_2O concentrations that will result from HSCT emissions will affect the ability of not only NO_x and HO_x to control ozone, but also ClO_x and BrO_x.

- Both homogeneous (gas phase) and heterogeneous (gas/particle) reactions are important in partitioning nitrogen, hydrogen, and halogen species between stable and reactive forms. The abundance of the reactive forms determines the chemical loss of ozone. Although significant progress has been made in laboratory studies of both homogeneous and heterogeneous processes, the former are better understood.

- Data from independent laboratory studies of the rates of heterogeneous processes are in reasonable agreement. In the absence of polar stratospheric clouds (PSCs) (i.e., outside of the wintertime polar stratosphere), hydrolysis of N_2O_5 in supercooled liquid sulfate aerosols appears to be the most important heterogeneous process in controlling the partitioning between reactive and stable forms in all the families of species that affect mid- and high-latitude ozone in the lower stratosphere. This reaction directly reduces NO_x and indirectly increases ClO and HO_x and, furthermore, is only modestly dependent on temperature and H_2O vapor pressure, making it relatively straightforward to incorporate into assessment models. Consequently NO_x emissions from HSCTs are now calculated to be less effective in perturbing stratospheric ozone than predicted in pre-1991 assessments.

- Because the hydrolysis of N_2O_5 reduces the abundance of NO_x, HO_x chemistry largely controls the chemical loss of O_3 in the current lower stratosphere at middle latitudes. A key reaction is that of HO_2 with O_3. The rate coefficient for this reaction needs to be better defined.

- Laboratory studies have established that the direct conversion of chlorine from reservoir species (HCl and $ClONO_2$) to reactive forms can take place on frozen or dilute liquid (~55 wt.% H_2SO_4 or lower) sulfate aerosol as well as on frozen HNO_3 surfaces.

- Our current picture of heterogeneous processing appears to be consistent with basic physical chemistry. Even though all laboratory studies have been confined to idealized surfaces and the composition, surface morphology, and chemical processing efficiency of atmospheric sulfate aerosols and PSCs have not been directly established, most of the laboratory data seem applicable to the atmosphere.

How consistent are atmospheric observations with the current understanding of the HSCT-related chemistry?

Atmospheric observations test the current understanding of HSCT-related chemistry and the validity of the chemistry and transport schemes used in the model calculations of ozone perturbations by HSCT exhaust emissions.

- Observations of reactive nitrogen and chlorine are inconsistent with models that contain gas-phase chemistry only. The observations support an important role for the hydrolysis of N_2O_5 in the lower stratosphere.

- The eruption of Mt. Pinatubo in June 1991 provided an opportunity to study atmospheric chemistry over a large range in sulfate aerosol loading. Extensive, global observations show that the sulfate aerosol surface area increased by a factor of 20-30 over background conditions. In situ observations confirm chemical model predictions that NO_x is reduced relative to total reactive nitrogen in the presence of sulfate aerosols. Observations further show that the impact of aerosols saturates at high aerosol surface areas with no further reduction in NO_x, a result consistent with the $N_2O_5 + H_2O$ heterogeneous mechanism.

- The chemical evolution of the wintertime polar vortex is observed to be basically consistent with the understanding of the heterogeneous and gas-phase chemical processes. The heterogeneous reactions of HCl and $ClONO_2$ on PSCs appear to be the dominant mechanism for conversion of chlorine into its active form, ClO, in the vortex. ClO concentrations decline back to their prewinter values through the reaction of ClO with NO_2 to form $ClONO_2$. The influence of these polar processes on the chemistry at middle latitudes and the possible changes caused by HSCTs have not been quantified.

- Limited observations suggest that conversion of $ClONO_2$ to reactive forms may be occurring on sulfate aerosols at temperatures above the PSC formation temperature. The importance of volcanically enhanced aerosol surface area to the $ClONO_2$ conversion in the winter polar stratosphere is not yet established. In contrast, observations (NO_x, ClO, O_3), laboratory studies and model calculations all indicate that direct conversion of $ClONO_2$ is not important in the warmer middle latitudes.

- The relative contributions of N_2O_5 hydrolysis in liquid sulfate and direct conversion of chlorine reservoirs on frozen particles to the repartitioning of NO_x is not well defined because of uncertainty on when sulfate aerosols freeze or Type I PSCs (nitric acid trihydrate or NAT) form. Hence, it is difficult to quantify heterogeneous processing at cold high latitudes outside polar vortices.

What are the predicted atmospheric changes associated with HSCTs?

This assessment has used six two-dimensional photochemical models as the basic tool for simulating the distribution of ozone in today's atmosphere and the changes in the ozone distribution in a projected atmosphere perturbed by HSCT aircraft emissions. Potential climate effects of HSCTs have not yet been addressed.

- Each 2-D model includes the same parameterization of the heterogeneous reactions of N_2O_5 and $ClONO_2$ with H_2O on the surfaces of the sulfate aerosol particles. The models were used to calculate the steady-state percent changes in the ozone content in response to injections of NO_x, H_2O, CO and unburnt hydrocarbon (as CH_4) from operation of a fleet of HSCTs. The effects from the emitted SO_2 and soot are highly uncertain and are not considered. Table 1 lists the changes in total column ozone in the northern hemisphere for six scenarios. The calculated ozone changes are either more negative or less positive (with one exception) with increasing emission index and flight altitude. It is important to note that the variance among the model results is not necessarily an indication of uncertainty.

Table 1. Calculated Percent Change in the Annual Averaged Content of Ozone in the Northern Hemisphere

Scenarios Model	AER	GSFC	LLNL	OSLO	CAMED	NCAR
I: Mach 1.6, NO_x EI=5*	-0.04	-0.12	-0.18	0.02	0.63	-0.04
II: Mach 1.6, NO_x EI=15*	-0.02	-0.14	-0.48	0.10	0.63	-0.54
III: Mach 2.4, NO_x EI=5*	-0.42	-0.27	-0.50	-0.39	0.25	-0.25
IV: Mach 2.4, NO_x EI=15*	-1.0	-0.80	-1.8	-1.0	-0.26	-1.5
V: Mach 2.4, NO_x EI=15†	-1.7	-1.2	-2.3	-0.43	-0.80	-1.9
VI: Mach 2.4, NO_x EI=45*	-4.6	-3.6	-7.0	-3.1	-2.1	-5.1

* Relative to a background atmosphere with chlorine loading of 3.7 ppbv, corresponding to the year 2015.
† Relative to a background atmosphere with chlorine loading of 2.0 ppbv, corresponding to about 2060.

- CO and unburned hydrocarbons from HSCTs are calculated to have a negligible impact on ozone.

- The model-calculated ozone loss rate in the lower stratosphere is related to the increases in the concentrations of NO_x and H_2O (ΔNO_x and ΔH_2O). These are controlled by the amount of exhaust emitted and by the formulation of the model transport.

- The model-calculated ozone changes between 40°N and 50°N are typically about 15-30% greater than those averaged over the whole northern hemisphere.

- Because most of the HSCT flights will occur in the northern hemispere, the calculated ΔNO_x , ΔH_2O, and ΔO_3 are much smaller in the southern hemisphere.

- Simulations from the 3-D models suggest that stratosphere/troposphere exchange due to synoptic scale events at midlatitudes occurs more rapidly than predicted by the 2-D models. Thus 2-D models could overestimate ΔNO_x and ΔH_2O relative to a 3-D calculation.

- Inclusion of the hydrolysis of N_2O_5 in the models using currently accepted rates based on laboratory measurements decreases the importance of odd nitrogen to the lower stratosphere ozone loss rate, L. The changes in the chlorine and hydrogen radicals tend to compensate for the increases in the ozone removal rate from increases in NO_x. Thus, the fractional change in the loss rate ($\Delta L/L$) is significantly smaller than the fractional change in NO_x. The calculated change in column ozone is larger in an atmosphere with smaller chlorine concentration because the chlorine cycle plays a smaller role in the ozone budget, and the buffering of the chlorine cycle compensates for less of the increased O_3 loss from the nitrogen cycle.

- Because the photochemical lifetime for O_3 is comparable to the transport lifetime in the lower stratosphere, the calculated ozone change is always smaller than the calculated change in the loss rate.

- The results reported in Table 1 do not include the effect of PSC chemistry in the polar regions. How this omission may affect the calculated ozone depletion depends on whether the added NO_x and H_2O change the frequency of occurrence of PSCs. If there is no change in PSC incidence, HSCT emissions of NO_x would alleviate ozone depletion in polar regions by converting some of the ClO to $ClONO_2$. On the other hand, increases in

NO_x and H_2O may result in more frequent formation of PSCs, hence possibly increasing ozone depletion. It is difficult to quantify this effect until we gain a better understanding of the microphysics of cloud formation, how processes in the polar region affect O_3 at middle latitudes, and the importance of heterogeneous reactions involving chlorine species if nitric acid/water ice clouds occur in the stratosphere at middle and tropical latitudes.

What are the uncertainties in these perturbation predictions?

Uncertainties associated with 2-D model predictions of ozone changes cannot be quantified at this time, but can be evaluated qualitatively by comparing 2-D model simulations with observations and with 3-D tracer simulations.

- Two-dimensional models are the standard tool for assessing the impact of tropospherically emitted long-lived trace gases such as CFCs, methane, and N_2O. The 2-D assessment models credibly simulate the seasonal and latitudinal variation of total ozone, qualitatively represent the tight correlation among long-lived trace gases observed at middle latitudes, and are able to simulate, with some notable exceptions, our current understanding of the basic photochemistry, including reaction of N_2O_5 on sulfate aerosols.

- Simulation of the Atmospheric Trace Molecule Spectroscopy Experiment (ATMOS) observations of partitioning in the NO_y and Cl_y families (NO, NO_2, HNO_3, HO_2NO_2, N_2O_5, $ClONO_2$, HCl) at 30°N over a wide range of altitudes from 50 to 20 km support the adequacy of the assessment models' chemical schemes.

- Global distributions of long-lived gases (N_2O, CH_4, NO_y, and O_3 in the lower stratosphere) are determined by a combination of chemistry and transport. Two-dimensional model predictions of these constituents agree reasonably with measurements in the middle stratosphere away from winter poles, but are less satisfactory in the lower stratosphere, and seriously underestimate the degree of descent at high latitudes, particularly in the lower stratosphere. The slope of the CH_4-N_2O relationship observed by aircraft, ATMOS, balloons, and the Stratospheric and Mesospheric Sounder (SAMS) is correctly simulated by many models, lending confidence to the modeled chemical cycles involving OH (CH_4 loss) relative to photodissociation (N_2O loss).

- Current assessment models do not include the variation of sulfate aerosol composition as a function of T and water vapor concentration, effects of temperature fluctuations, incorporation into the aerosols of other species (e.g., HCl, nitrosyl sulfuric acid formaldehyde), or PSC processing. In addition, enhanced sulfate and nitric acid/water ice cloud formation due to higher water vapor concentration, NO_x, and (possibly) higher sulfur from HSCT injections need to be assessed. For these reasons, further work is required to define the role of sulfate aerosol and PSC heterogeneous processing in assessing the impact of HSCTs.

- Microphysical models that calculate particle concentrations and composition are not included in the current global assessment models. Modeling the liquid-phase sulfate layer in a 2-D formulation may prove possible because the layer is typically long-lived and zonally uniform; however, the process of new particle formation and the potential perturbations by HSCTs may require treatment of non-zonal processes. Accurate simulation of the concentration of H_2O the possible perturbation by HSCTs in the lower stratosphere is hampered by limited observations and needs a physical model of sources and sinks involving microphysical processes near the tropopause.

- The quality of both the observations and modeling capability of water must be improved. Water is important to both the chemical and radiative balance of the lower stratosphere and upper troposphere, and the impact of water from aircraft is expected to be large. Currently water in this altitude range has not been effectively addressed by either stratospheric or tropospheric models.

- Predicted ozone changes in the troposphere are not reliable since these models have not been evaluated in terms of tropospheric transport and chemistry. Because the concentrations of O_3 in the troposphere are low, this uncertainty has a small impact on column O_3 except when subsonic NO_x emissions change substantially. Consequently, the climatic impact of ozone redistribution, which is sensitive to changes just above and below the tropopause, cannot be evaluated here.

- HSCTs emit exhaust directly in the lower stratosphere in longitudinally asymmetric patterns. Two-dimensional models have not been specifically formulated or designed to address this emission pattern. Therefore, 2-D models cannot simulate the high concentrations of exhaust emissions that might occur regionally and will not correctly represent transport out of the stratosphere into the troposphere because transport by synoptic scales is not included (2-D models appear to underestimate dispersion of injected chemicals and transport into the upper troposphere relative to 3-D models).

- A limited number of 3-D models have been used to evaluate the quality of the transport in 2-D simulations. The 3-D simulations indicate a potential for regional accumulation of material especially in middle latitudes in summer and in the tropics and subtropics, and hence, the possibility of threshold chemical processes that might be significantly increased by HSCT. The 3-D models emphasize that the boundaries between tropical, middle latitude, and polar zones and synoptic eddy activity are not independent processes; hence, any 2-D developments that address these dynamical issues must be formulated in a self-consistent pattern.

  - For zonal mean emissions on seasonal time scales, these 3-D models tend to disperse the tracer faster vertically than 2-D models, but have a similar latitudinal spread.

  - Three-dimensional models produce a more credible simulation than 2-D models of the observed tropical middle latitude separation, and the separation of the wintertime polar vortex from middle latitudes.

- Three-dimensional transport and chemistry models need to be used to evaluate the mixing of effluent calculated in 2-D models, to provide guidance for improvement of 2-D parameterizations, and to focus 2-D models on transport-related sensitivities. Three-dimensional models will not be able to provide full chemical assessments in the HSRP time frame; hence, 2-D simulations must be made as robust as possible.

INTRODUCTION

Consideration of the possible effects of stratospheric aircraft on the atmosphere was begun in the early 1970s under the Climatic Impact Assessment Program (CIAP) which carried out a thorough assessment based on the then current knowledge. CIAP and the High Altitude Pollution Program (HAPP) which followed considered the impact of numerous possible effluents from the aircraft including: nitrogen oxides (NO_x), water vapor (H_2O), sulfur, soot, hydrocarbons, carbon monoxide (CO), carbon dioxide (CO_2), and metals. It was concluded that the primary concern was the potential depletion of stratospheric ozone by NO_x.

The fundamental problem with stratospheric flight is that pollutant residence times are long because the stratosphere is a region of permanent temperature inversion with stable stratification. Nitrogen oxides are particularly important pollutants because of their ability to catalytically destroy ozone (Crutzen, 1970, 1971; Johnston, 1971). Water vapor reacts with excited atomic oxygen and produces HO_x radicals which catalytically destroy ozone and also interact with the nitrogen and chlorine cycles to modify their effect on ozone. Sulfur and soot are of potential importance because of the possibility of increasing the particulate surface area available for heterogeneous reactions. Hydrocarbons, CO, and CO_2 from aircraft exhaust appear to have only a minor impact because the perturbations are small compared with natural background concentrations. No important impacts of metals have been identified. Estimates of expected perturbations resulting from a fleet of stratospheric aircraft on stratospheric composition are compared with the observed background concentrations in Table 1.

Table 1. Estimates of Stratospheric Perturbations Due to Aircraft Effluents of a Fleet of Approximately 500 Mach 2.4 HSCTs (NO_x EI=15) Relative to Background Concentrations (Perturbations are Estimated for a Broad Corridor at Northern Midlatitudes) (expanded from Douglass et al., 1991)

Species	Perturbation	Background
NO_x	3-5 ppbv	2-16 ppbv
H_2O	0.2-0.8 ppmv	2-6 ppmv
SO_x	10-20 pptv	50-100 pptv
H_2SO_4	350-700 pptm	350-700 pptm
Soot	~7 pptm	~7 pptm
Hydrocarbons	2 ppbv (NMHC)	1600 ppbv (CH_4)
CO	~2 ppbv	10-50 ppbv
CO_2	~1 ppbv	350 ppmv

Since the mid-1970s the focus of stratospheric research has been on the effects of chlorine from chlorofluorocarbons on ozone which has led to a greatly increased knowledge of the

mechanisms controlling the abundance of stratospheric ozone. Numerous assessments of the impact of chlorofluorocarbons on the stratosphere have been carried out since the mid 1970s with little emphasis on the potential impact of stratospheric aircraft on the atmosphere. However, the Livermore model has updated both calculations in their model as new information has become available (Johnston et al., 1989). They have shown that the evaluation of the impact of aircraft has fluctuated with each introduction of new chemical or physical information.

The present assessment has been conducted in parallel with preparation of the Third Program Report of the Atmospheric Effects of Stratospheric Aircraft (AESA) element of the NASA High-Speed Research Program (HSRP). The assessment is an attempt to concisely summarize the status of our knowledge concerning the possible impacts of stratospheric aircraft on the atmosphere. The Third Program Report of AESA contains a description of the AESA program strategy and several extensive chapters that give background and details supporting the conclusions of the Assessment Report. These reports are being prepared for review by a panel of the Committee on Atmospheric Chemistry of the National Research Council.

The First AESA Program Report (Prather et al., 1992) contained a baseline assessment of stratospheric aircraft, using two-dimensional gas-phase photochemical models of the stratosphere. This assessment focused on the impact of NO_x and H_2O on the atmospheric ozone content, but also considered hydrocarbons, CO, and CO_2. Nitrogen oxides were identified as the main concern and the effects of hydrocarbons, CO, and CO_2 were shown to be small. The 1991 WMO/UNEP Assessment Report (WMO, 1992) contained a chapter on the impacts of stratospheric aircraft. This assessment, along with the Second Program Report of AESA (Stolarski and Wesoky, eds, 1993), contained an evaluation based on two-dimensional models which included a parameterization of the effects of heterogeneous reactions on the surfaces of sulfate aerosols. The result of these calculations is a much smaller predicted impact of injected NO_x on ozone. The photochemical balance of the lower stratosphere in a model with sulfate surface chemistry indicates a more prominent role for hydrogen oxide catalysis of ozone depletion. For small emission indices near 5 g/kg, the predicted impact of the hydrogen and nitrogen oxides now appear to be of comparable magnitude.

This assessment report considers the possible impact of the entire range of effluents from the aircraft using improve assessment models and detailed fleet emission scenarios. The emphasis is on the effects of NO_x and H_2O on the atmospheric ozone content. The realization of the importance of heterogeneous chemistry on sulfate aerosols emphasizes the importance of the question of increases in particle surface area which might be caused by the effluents of aircraft. Increased concentrations of H_2O and HNO_3 in aircraft corridors can raise the temperature at which nitric acid trihydrate (NAT) clouds can form at midlatitudes leading to an increase in their occurrence. This could enhance the ozone depletion due to the chlorine that is activated on NAT surfaces. Increased water vapor might also enhance the reactivity of sulfate aerosols which could lead to changes in the sensitivity of ozone to pollutants. The potential effects of changing particle surface areas are not yet completely understood. The assessment models do not include these effects, but the chapters on limitations of the predictions contain discussions of their potential influence and the associated uncertainties. The emerging understanding of these processes should lead to a significantly improved assessment in the near future.

Chapter 3 reviews and evaluates what we know about emissions from existing engines and prototype combustors. It also contains a summary of planned wake-vortex interaction studies using computational models of aircraft wakes to test for possible nonlinear processing effects.

The development of fleet emissions scenarios on a three-dimensional grid (i.e., altitude, latitude, and longitude), including an estimate for the 1990 scheduled and chartered airlines and military aviation, is reported in Chapter 4. Projections are made for a 2015 fleet scenario including

both subsonic aircraft and HSCTs. The emissions database includes the complete flight cycle (i.e., takeoff, climb, cruise, descent, and landing).

Addressed in Chapter 5 is the question of whether the representation of homogeneous and heterogeneous chemical reactions in models is adequate given our understanding of rate coefficients and product distributions. The chapter reviews laboratory observations, and evaluates the adequacy of model representations. Emphasis is placed on our understanding of heterogeneous chemistry and how the models can be improved to provide a better assessment of their role.

Chapter 6 considers how the atmospheric observations that have been made on several ER-2 and DC-8 missions have redefined our understanding of the processes controlling lower stratospheric ozone. This chapter reviews what was learned from the second Airborne Arctic Stratospheric Expedition (AASE-II) as it applies to the problem of emissions from stratospheric aircraft. It also reviews the data from the test flights for the current Stratospheric Photochemistry, Aerosols and Dynamics Expedition (SPADE). A description of the plans for SPADE and for the 1994 Measurements for the Assessment of the Effects of Stratospheric Aircraft (MAESA) expedition are contained in the program report.

Two-dimensional model calculations for the newly improved emissions scenarios and some 3-D analyses are discussed in Chapter 7. Calculations are made for NO_x emission indices typical of current combustor technology, as well as the HSRP goal level; and at least two HSCT cruise Mach numbers and altitudes are considered. These results are compared to previous analyses which used idealized fleet scenarios. Model calculations are tested for sensitivity to the level of chlorine in the atmosphere. Existing models, as improved by recent model/measurement intercomparisons, have been used. Emphasis has been placed on intercomparing the models on realistic scenarios. Sensitivity of the results to input assumptions has yet to be carried out.

Chapter 8 draws together the evidence regarding current understanding of the quality of the models. It reviews the lessons learned from the Models and Measurements Workshop (Prather and Remsberg, 1993). The chapter also examines the mean global transport, and focuses on the problem of near-tropopause transport and how it effects the buildup of pollutants. Possible future improvements in the 2-D assessment models and application of 3-D simulations are considered as well as uncertainties and robustness. The chapter touches on climatic effects which the AESA program has chosen to de-emphasize until clearer answers are obtained on the ozone issue.

References

Crutzen, P. J., The influence of nitrogen oxide on the atmospheric ozone content, *Quart. J. Roy. Met. Soc., 96*, 320, 1970.

Crutzen, P. J., Ozone production rates in an oxygen-hydrogen-nitrogen oxide atmosphere, *J. Geophys. Res., 76*, 7311, 1971.

Johnston, H., Reduction of stratospheric ozone by nitrogen oxide catalysts from supersonic transport exhaust, *Science, 173*, 517, 1971.

Johnston, J. S., D. E. Kinnison, and D. J. Wuebbles, Nitrogen oxides from hgih altitude aircraft: An update of potential effects on ozone, *J. Geophys. Res., 94*, 16351-16353, 1989.

Prather, M. J. et al., *The Atmospheric Effects of Stratospheric Aircraft: A First Program Report*, NASA Reference Publication 1272, NASA, Washington, D.C., 1992

Prather, M. J., and E. E. Remsberg, (eds), *The Atmospheric Effects of Stratospheric Aircraft: Report of the 1992 Models and Measurements Workshop*, NASA Reference Publication 1292, Washington, D.C., 1993.

Stolarski, R. S., and H. L. Wesoky, (eds), *The Atmospheric Effects of Stratospheric Aircraft: A Second Program Report*, NASA Reference Publication 1293, NASA, Washington, D.C., 1993.

WMO, (World Meteorological Organization), *Scientific Assessment of Ozone Depletion: 1991*, Global Ozone Research and Monitoring Project, Report No. 25, WMO, Geneva, Switzerland, 1992.

CHAPTER SUMMARIES

Chapter 3 - Emissions Characterization and Plume/Wake Vortex Interactions

- Assessments of predicted high-speed civil transport (HSCT) airframe and exhaust emissions show that the exhaust emissions are expected to produce major increases in the stratospheric concentrations of NO_y, H_2O, SO_x, and soot.

- No experimental emissions data from actual HSCT combustors, engines, or airframe components currently exist. Data from combustor rigs representing advanced low NO_x combustor concepts will be available in the near future.

- Model calculations of exhaust plume chemistry indicate that ~5% of exhaust NO_x will be converted to HNO_3 and ~10% of exhaust SO_x will be converted to H_2SO_4, with potentially significant implications for plume and wake microphysics.

- Model calculations of exhaust plume condensation processes indicate extensive new particle production in the plume due to binary homogeneous nucleation of sulfuric acid vapor and water vapor. Whether or not these plume induced new particles have a significant effect on general stratospheric properties awaits analysis of their subsequent evaporation and/or agglomeration kinetics and the development of a more definitive model of baseline aerosol climatology.

- Model analyses of radiatively active gases in the wake dispersion regime indicate that water vapor enhancements and ozone depletion will support measurable differential radiative cooling of up to 3 K/day leading to subsidence velocities up to 0.3 km/day. However, total subsidence will probably be limited to 0.5 to 1.0 km and will not significantly affect exhaust deposition altitudes.

- Model calculations have not yet identified any plume or wake phenomena that alter NO_y speciation or deposition altitude enough to seriously impact the input assumptions used in current assessment calculations.

- No measurements of stratospheric exhaust plume, vortex wake, or wake dispersion regime properties for supersonic transports are available to test model predictions.

Chapter 4 - Fleet Operational Scenarios

- The amount of fuel burned and the emissions of nitrogen oxides (NO_x), carbon monoxide (CO), and hydrocarbons were determined for nine scenarios comprising the 1990 aircraft fleet and projected fleets of subsonic and supersonic aircraft (high-speed civil transports, HSCTs) flying in 2015. From fuel burned, emissions of water vapor, carbon dioxide, and sulfur can also be evaluated. Boeing and McDonnell Douglas used their detailed scenario modeling capabilities to develop annually averaged, three-dimensional data sets onto a 1 degree longitude $\times$ 1 degree latitude $\times$ 1 kilometer altitude global atmospheric grid. The emissions data sets determined for these operational scenarios are the most realistic and most comprehensive ever developed.

- Subsonic scenarios for 1990 and 2015 consider the effects of scheduled commercial passenger and cargo air traffic, including turboprop aircraft, along with military, charter, and nonscheduled (mostly former Soviet Union, China, and Eastern Europe) aircraft traffic. HSCT fleets for 2015 were configured with a range of about 5000 nautical miles and capability for

carrying 300 passengers flying at cruise speeds of either Mach 1.6, 2.0, or 2.4 under a range of NO_x emission indices. Flight frequencies and the HSCT city-pairs network (consisting of 199 city-pairs) were generated based on a fixed passenger demand corresponding to 500 Mach 2.4 HSCTs. Actual flight paths between city-pairs were used to distribute emissions during take-off, climb, cruise, and descent.

- The individual component data sets were combined to produce the complete scenarios, which were then projected onto the two-dimensional and three-dimensional grids required by the atmospheric models employed in the assessment. Evaluated fuel burned for the 1990 aircraft accounted for 76% of the reported global consumption; operations near airports (e.g., ground operations and delays, air traffic control) and, to a lesser extent, the idealized flight patterns assumed in the scenario development likely account for the difference.

Chapter 5 - Chemical Processing: Homogeneous and Heterogeneous Reactions

- Both homogeneous and heterogeneous reactions are important in partitioning nitrogen, hydrogen, and halogen species between stable and reactive forms. The reactive forms determine the chemical loss of ozone. While significant progress has been made in laboratory studies of heterogeneous processes important for HSCT assessments, they are not as well understood as the homogeneous processes.

- Data from independent laboratory studies of the rates of heterogeneous processes are in reasonable agreement. Hydrolysis of N_2O_5 in supercooled liquid sulfate aerosols is largely independent of temperature and water vapor pressure, $P(H_2O)$. Therefore, it has been easy to incorporate into assessment models. It appears to be the most important heterogeneous process that control partitioning between reactive and nonreactive forms in all the families of species that affect mid and high-latitude ozone in the lower stratosphere. There is strong field evidence to show that this reaction does take place.

- Because N_2O_5 is hydrolyzed by sulfate aerosols, HO_x chemistry largely overshadows NO_x chemistry in controlling the chemical loss of O_3 in the lower stratosphere. A key reaction in this process is that of HO_2 with O_3. The rate coefficient for this reaction needs to be better defined to evaluate the effects of HSCT.

- For frozen sulfate aerosols and Type I PSCs (nitric acid-water ice), N_2O_5 hydrolysis ceases to be important.

- Conversion of chlorine from reservoir to reactive forms can take place on frozen or dilute ($\approx$55 wt.% H_2SO_4 or lower) sulfate aerosol as well as Type I PSCs. Conversion on PSCs due to $ClONO_2$ + HCl reaction is reasonably well established in the polar regions.

- The transition from N_2O_5 hydrolysis in liquid sulfate to direct conversion of chlorine reservoirs on frozen particles is not well defined because of the lack of information on when sulfate aerosols freeze or Type I PSCs form. Hence, it is difficult to quantify heterogeneous processing at cold high latitudes outside polar vortices, the regions of considerable importance to HSCT assessment.

- Our current picture of heterogeneous processing appears to be consistent with basic physical chemistry. Even though all laboratory studies have been confined to idealized surfaces and the composition, surface morphology, and chemical processing efficiency of atmospheric sulfate aerosols and PSCs have not been directly established, most of the laboratory data seem applicable to the atmosphere.

- Current HSCT assessment models do not include the variation of sulfate aerosol composition as a function of T and $P(H_2O)$, effects of temperature fluctuations, incorporation into the aerosols of other species such as HCl and nitrosyl sulfuric acid, or PSC processing. In addition, enhanced sulfate and PSC formation due to higher $P(H_2O)$, NO_x, and (possibly) higher sulfur from HSCT injections need to be assessed. For these reasons, further work is required to definitively define the role of heterogeneous processing in assessing the impact of HSCT.

Chapter 6 - Atmospheric Observations

- Simple relationships between long-lived chemical species observed in the lower stratosphere at middle latitudes can be used to extend measurements from one region to a much larger scale, to test some chemical transformations, and to assimilate observations from different platforms into an integrated picture of stratospheric chemistry.

- Observations of reactive nitrogen and chlorine are inconsistent with models that contain only gas-phase chemistry. They support an important role for the heterogeneous reaction of N_2O_5 + H_2O (hydrolysis of N_2O_5). This reaction directly reduces NO_x and indirectly increases ClO. These changes reduce the role of NO_x in ozone destruction and cause the HOx catalytic cycle to become the dominant mechanism for removal of ozone in the lower stratosphere.

- The eruption of Mt. Pinatubo in June 1991 provided an opportunity to study atmospheric chemistry over a large range in sulfate aerosol loading. Extensive, global observations show that the peak global sulfate aerosol mass loading reached about 30 Mt in the stratosphere and that sulfate aerosol surface area increased by a factor of 20-30 over background conditions. This loading decreased to about half this level by the end of 1992.

- In situ observations confirm that the reduction of NO_x relative to total reactive nitrogen that resulted from the N_2O_5 + H_2O heterogeneous reaction was less than proportional to the large increases in the aerosol surface area in the Mt. Pinatubo cloud. The agreement between the limited observations of this response and model results suggests that this heterogeneous mechanism has been correctly incorporated into the models.

- Limited observations suggest that the conversion of $ClONO_2$ to reactive forms on sulfate aerosols may be occurring in the cold polar vortex. Observations and model calculations indicate that direct conversion of $ClONO_2$ is not important in the warmer middle latitudes.

- Observed decreases in the column abundance of O_3 following the eruption of Mt. Pinatubo were as large as 6% in the tropics and high middle latitudes in 1991. Tropical changes may be due primarily to radiative and dynamical effects. The 1992 global average column abundance of ozone was 2% to 3% lower than in any other year since 1979. The cause of this decrease is not yet known.

- Isolated air parcels with enhanced ClO amounts have been observed in the northern middle latitudes in the winter. The occurrences of these enhancements, which may result from rapid heterogeneous chemistry on either sulfate aerosol or polar stratospheric clouds (PSCs), could be affected by effluents from HSCTs and need to be investigated.

- The chemical evolution of the wintertime polar vortex is observed to be basically consistent with the understanding of the heterogeneous and gas-phase chemical processes. The heterogeneous reaction between HCl and $ClONO_2$ is the dominant conversion mechanism for chlorine in the vortex, and recovery occurs through the reaction of ClO with NO_2 to form

$ClONO_2$. Polar processes could result in considerable removal of trace species such as H_2O, NO_y, and aerosols from the stratosphere.

- The observed HCl abundance in the wintertime lower stratosphere at middle latitudes is less than calculated by photochemical models. If confirmed, this observation suggests that the understanding of the chemistry governing the partitioning of reactive and reservoir chlorine species in middle latitudes is either incomplete or incorrect.

- Latitudinal gradients in the distribution of the volcanic aerosol and the NO_y/O_3 ratio have been observed in the subtropics. Aerosol gradients appear to vary with season and phase of the Quasi-Biennial Oscillation and to be smaller below 23 km than above. These gradients may indicate regions of restricted exchange between the middle latitudes and upwelling region in the tropics.

Chapter 7 - Model Calculation of HSCT Effect

The assessment results presented in this chapter are from six two-dimensional models. Each model includes the same parameterization of the heterogeneous reactions of N_2O_5 and $ClNO_3$ with H_2O on the surfaces of the sulfate aerosol particles. The models were used to calculate the steady-state percent changes in the ozone content in response to injections of NO_x, H_2O, CO, and unburned hydrocarbon (as CH_4) from operation of a fleet of HSCT. The effects from the emitted SO_2 and soot are not considered. Table 4a and Table 4b list the changes in ozone content between 40°N and 50°N and in the northern hemisphere, respectively, for the six scenarios discussed in Chapter 4. It is important to note that the variance among the model results is not necessarily an indication of uncertainty.

- Among the emitted species considered, NO_x and H_2O have the largest impact on O_3. The emissions cause a significant change in the respective background concentrations. Radicals derived from these emitted species are important to O_3 loss in the lower stratosphere. The changes in CH_4 and CO do not contribute appreciably to the calculated ozone loss.

- The model-calculated ozone removal rate in the lower stratosphere is related to the magnitudes of ΔNO_x and ΔH_2O that are controlled by model transport.

- As most of the HSCT flights will occur in the northern hemisphere, the calculated ΔNO_x and ΔH_2O are smaller in the southern hemisphere. The calculated ozone change in the southern hemisphere is also smaller.

- Simulations from 3-D models suggest that stratosphere/troposphere (strat/trop) exchange due to synoptic scale events at midlatitudes produces a faster strat/trop exchange than the 2-D models. This implies that 2-D models could overestimate ΔNO_x and ΔH_2O relative to a 3-D calculation.

- The calculated ozone loss is larger for higher emission indices of NO_x and for higher cruise altitudes, because emitted material deposited at higher altitudes has a longer residence time in the stratosphere.

- Inclusion of the $N_2O_5 + H_2O$ reaction in the models using currently accepted rates based on laboratory measurements decreases the importance of odd nitrogen to the ozone removal rate (L) in the lower stratosphere. With the addition of HSCT emissions, the decreases in the chlorine and hydrogen radicals tend to compensate for increases in the ozone removal rate from

increases in NO_x. For example, the concentration of ClO and the contribution of chlorine to the total ozone loss rate are suppressed due to the enhanced formation of $ClNO_3$ from the NO_x increase. Similarly, the HO_2 decrease that results from the NO increase reduces the contribution of the odd hydrogen species. Thus, the fractional change in the loss rate ($\Delta L/L$) is significantly smaller than the fractional change in NO_x. The interdependence among the chlorine, hydrogen, and nitrogen ozone removal cycles can be verified indirectly by in situ measurements of the present day atmosphere.

- The calculated change in column ozone is larger in an atmosphere with smaller chlorine concentration, because the chlorine cycle plays a smaller role in the ozone budget and the buffering of the chlorine cycle compensates for less of the increase from the nitrogen cycle.

- Because the photochemical lifetime for O_3 is comparable to its transport lifetime in the lower stratosphere, the calculated change in the local concentration of ozone is smaller than that expected from the calculated change in the chemical loss rate.

- The results reported in Tables 4a and 4b do not include the effect of polar stratospheric cloud (PSC) chemistry in the polar regions. How this omission may affect the calculated ozone depletion depends on whether the added NO_x and H_2O change the occurrence of PSCs. If there is no change in PSC occurrence, operation of the HSCT fleet would alleviate the ozone depletion in the polar region as some of the ClO produced by heterogeneous reactions on PSC surfaces would combine with the added NO_x to form $ClNO_3$. On the other hand, increases in NO_x and H_2O may result in more frequent formation of PSCs and exacerbate the ozone depletion. It is difficult to estimate this effect until we gain a better understanding of the microphysics of cloud formation, how processes in the polar region affect O_3 at midlatitudes, and the importance of heterogeneous reactions involving chlorine species if nitric acid particles form at middle and tropical latitudes.

Chapter 8 - Credibility of Assessment Models

Global two-dimensional stratospheric models are the standard tool for assessing the impact of tropospherically emitted long-lived trace gases such as chlorofluorocarbons (CFCs), methane, and nitrous oxide. The 2-D assessment models credibly simulate the seasonal and latitudinal variation of total ozone, and they qualitatively represent the tight correlation between long-lived trace gases observed at middle latitudes (although a greater latitude- altitude domain must be spanned to obtain the same range of concentrations as observed). In general, they are able to simulate, with some notable exceptions, our current understanding of the basic photochemistry, including reaction of N_2O_5 on sulfate aerosols.

- Simulation of observations made by the Atmospheric Trace Molecule Spectroscopy Experiment (ATMOS) of partitioning in the NO_y and Cl_y families (NO, NO_2, HNO_3, HO_2NO_2, N_2O_5, $ClONO_2$, and HCl) at 30°N over a wide range of altitudes from 50 to 20 km support the adequacy of the assessment models' chemical schemes.

- Global distributions of long-lived gases (N_2O, CH_4, and NO_y and O_3 in the lower stratosphere) are determined by a combination of chemistry and transport. Two-dimensional model predictions of these constituents agree reasonably with measurements in the middle stratosphere away from winter poles, but are less satisfactory in the lower stratosphere. The slope of the CH_4-N_2O relationship observed by aircraft, ATMOS, balloons, and the Stratospheric and Mesospheric Sounder (SAMS) is correctly simulated by many models, lending confidence to the modeling of chemical cycles involving OH (CH_4 loss) relative to photodissociation (N_2O loss).

- Photodissociation rates (J) of stratospheric molecules are readily calculable from first principles given the adopted set of cross sections and solar radiation (see Chapter 5). Atmospheric measurements are not readily available to evaluate this aspect of model performance. Uncertainties remain in the calculation of Schumann-Runge transmission affecting J(NO) and for scattered light affecting $J(NO_2)$, $J(HNO_3)$, and $J(O_3)$.

Gas-particle reactions have only recently been included in stratospheric models, and the variety of such reactions observed in the laboratory have not yet been evaluated in global models. Heterogeneous hydrolysis of N_2O_5 on sulfuric acid aerosols is largely independent of temperature and composition and, hence, has been successfully incorporated, greatly improving the assessment models' simulations of O_3 loss and NO_y-Cl_y partitioning in the lower stratosphere.

- Hydrolysis of $ClONO_2$, plus reactions involving dissolved HCl, in liquid sulfate aerosols must be implemented with great caution in these models because their rates are sensitive to liquid water content, i.e., hydrolysis becomes extremely rapid at cold temperatures and high H_2O pressures. Thus, application of a zonal and temporal mean temperature as in 2-D models would underestimate the importance of these reactions.

- The composition and reactivity of these droplets may be altered by other compounds known to dissolve in sulfuric acid such as HCl, nitrosyl sulfuric acid, or formaldehyde.

- Repartitioning of the Cl_y family on nitric acid trihydrate (NAT) and other ices in polar stratospheric clouds (PSCs) also poses a difficult problem for the global 2-D models because of the non-zonal nature of Arctic PSCs. However, enhanced ClO resulting from PSC reactions clearly impacts the ozone budget of the lower stratosphere and would be buffered directly by HSCT injections of NO_x. NAT clouds can possibly occur outside of polar regions and will also be sensitive to non-zonal processes.

Microphysical models that calculate particle concentrations and composition are not included in the current global assessment models. Modeling the liquid-phase sulfate layer in a 2-D formalism may prove possible because the layer is typically long-lived and zonally uniform; however, the process of new particle formation and the potential perturbations by HSCTs may require treatment of non-zonal processes. Modeling frozen sulfuric acid, NAT, or other ices requires understanding of the thresholds for phase changes and may be beyond the capability of 2-D models. Accurate simulation of H_2O concentrations and its perturbations in the lower stratosphere is hampered by lack of observations and a model for sources and sinks, which appear to involve some microphysical processes near the tropopause.

Predicted ozone changes in the troposphere are not reliable since these models have not been evaluated in terms of tropospheric transport and chemistry. This uncertainty has little impact on column O_3 except when subsonic, tropospheric NO_x emissions change substantially. Consequently, the climatic impact of ozone redistribution, which is sensitive to changes just above and below the tropopause, cannot be evaluated here.

The quality of both the observations and modeling capability of water must be improved. Water is important to both the chemical and radiative balance of the lower stratosphere and upper troposphere, and the impact of water from aircraft is potentially significant to both ozone and climate. Currently water in this altitude range has not been effectively addressed by either stratospheric or tropospheric models.

HSCTs emit directly in the lower stratosphere in non-uniform patterns. Two-dimensional models have not been specifically formulated or designed to address such emission patterns that are not uniform in longitude and time. Therefore, 2-D models cannot simulate the high concentrations

of exhaust emissions that might occur regionally and will not correctly represent transport out of the stratosphere into the troposphere because transport by synoptic scales is not included.

- Zonally non-uniform emissions are inconsistent with the theoretical basis for parameterizing diffusion in current 2-D models.

- Two-dimensional models do not explicitly include transport by synoptic scales. Observations and 3-D models show that these scales are important for lower stratospheric transport and stratosphere-troposphere exchange. In middle latitudes 2-D models probably underestimate dispersion of injected tracers and transport into the upper troposphere.

Three-dimensional models have been used to evaluate the quality of the 2-D simulations for a number of case studies. The simulations indicate regional accumulation of material, and hence, the possibility of chemical processes that might be strongly perturbed by HSCT emissions. Three-dimensional models emphasize that the structure of the zonal mean circulation, with distinct edges between subtropical, mid-latitude, and wintertime polar zones and with important synoptic eddy effects, are not independent processes; hence, any 2-D developments that address these dynamical issues must be formulated in a self-consistent pattern.

- For zonal mean emissions on seasonal time scales, when compared with 2-D models, three-dimensional models disperse the tracer faster vertically and have similar latitudinal spread.

- Three-dimensional models show that in regions of low wind speed (subtropics, tropics, summer in middle latitudes, episodic times in other seasons) effluent accumulates with significant regional enhancements in continental-scale areas.

- Three-dimensional models produce a more credible simulation than 2-D models of the observed tropical / mid-latitude separation. Transport studies constrained to observations (data assimilation) show a strong sensitivity to the quasi-biennial oscillation (QBO) of effluent accumulation. Free-running GCMs have not simulated both of the phases of the QBO. Likewise the 2-D assessment models do not accurately simulate the QBO.

- Three-dimensional models produce a more credible simulation than 2-D models of the separation of the wintertime polar vortex from midlatitudes. New, more physically based 2-D parameterizations of planetary wave transport also simulate this separation. These models have yet to be used in assessments, and they require extension to the more general problems of the lower stratosphere.

- The effects of local and regional accumulation will be most profound if the chemical environment is changed enough to initiate threshold processes (e.g., particle formation).

Three-dimensional transport and chemistry models and observations must be used to evaluate the mixing of effluents calculated in 2-D models, to provide guidance for improvement of 2-D parameterizations, and to focus 2-D models on transport-related sensitivities. Three-dimensional models also require extensive verification with observations to evaluate their quality. Three-dimensional models will not be able to provide full chemical assessments in the HSRP time frame; hence, 2-D simulations must be made as robust as possible.

Formal uncertainty analysis with statistical error bounds is impossible for an HSCT assessment involving such a combination of predictive models. The best approach may be to categorize the uncertainties as:

- Type 1 parameters (e.g., kinetic rates, emissions) can be assigned a statistical range of values and be formally propagated through the assessment;

- Type 2 quantities (e.g., circulation, H_2O perturbations) can be readily identified, but may be included in the assessment only as upper/lower bounds;

- Type 3 unknowns are those "IF" processes, including systematic errors, that we cannot begin to model and can at best identify and highlight their potential importance to the assessment.

SECTION F

CHEMICAL KINETICS AND PHOTOCHEMICAL DATA FOR USE IN STRATOSPHERIC MODELING

1. INTRODUCTION

This compilation of kinetic and photochemical data represents the tenth evaluation prepared by the NASA Panel for Data Evaluation. The Panel was established in 1977 by the NASA Upper Atmosphere Research Program Office for the purpose of providing a critical tabulation of the latest kinetic and photochemical data for use by modelers in computer simulations of stratospheric chemistry.

2. BASIS OF THE RECOMMENDATIONS

The recommended rate data and cross sections are based on laboratory measurements. In order to provide recommendations that are as up-to-date as possible, preprints and written private communications are accepted, but only when it is expected that they will appear as published journal articles. In no cases are rate constants adjusted to fit observations of stratospheric concentrations. The Panel considers the question of consistency of data with expectations based on the theory of reaction kinetics, and when a discrepancy appears to exist this fact is pointed out in the accompanying note. The major use of theoretical extrapolation of data is in connection with three-body reactions, in which the required pressure or temperature dependence is sometimes unavailable from laboratory measurements, and can be estimated by use of appropriate theoretical treatment. In the case of important rate constants for which no experimental data are available, the panel may provide estimates of rate constant parameters based on analogy to similar reactions for which data are available.

3. RECENT CHANGES AND CURRENT NEEDS OF LABORATORY KINETICS

In the present evaluation the numbers of new (80) and changed (42) recommendations are greater than those of the previous evaluation, reflecting the continuing high level of activity in laboratory studies of atmospheric chemistry. Reactions of singlet molecular oxygen are included for the first time. Another new addition is an appendix of model-generated concentration profiles and J-values for important species in the upper atmosphere. The appendix listing heats of formation of many atmospheric species has been updated and expanded.

Although the database for homogeneous reaction kinetics of the stratosphere is by now relatively mature, it is well to remember that no rate constant is known to better than 10%, and many have uncertainties of 20% or more. The rate constant for the important reaction, OH + CH_4, has been corrected in the present evaluation by approximately 20%. This change is typical of that for many OH abstraction reactions, for which early measurements have often been erroneously high. Such changes are important because oxidation by OH is the principal removal path for many trace species, including man-made compounds such as the HCFCs (hydrochlorofluorocarbons). For reactions of this type, including Cl abstraction reactions, there is often some difficulty in reconciling high temperature (above 298 K) and low temperature (below 298 K) rate constant data. Early problems in evaluating the rate constant for the important Cl + CH_4 reaction were related to

this situation. The frequent observation is that Arrhenius plots of the rate constant data show upward curvature at low temperatures which cannot be explained by tunneling or by expected departures from Arrhenius behavior. Some or perhaps all of these departures are due to secondary chemistry or reaction with walls and impurities. As a consequence, there is a continuing need for new techniques and approaches which minimize such errors.

As is now well-recognized, the role of heterogeneous processes is one of the most uncertain areas of atmospheric modeling. Efforts have continued in many laboratories to quantify these effects and to provide a basis for their incorporation into the models. Substantial difficulties and uncertainties remain, however. Our evaluation of laboratory data for heterogeneous chemistry, which began in the previous evaluation, now includes a recommendation of preferred values rather than just a compilation of reported data.

3.1 O_x Reactions

The kinetics of the O, O_2, and O_3 system are relatively well-established. However, the O + O_2 + M reaction remains of fundamental importance in atmospheric chemistry. This is because the extent of ozone destruction is determined by the relative rates of competing reactions such as O + O_3, O + NO_2, O + OH, and O + ClO. Additional studies of the ozone-forming reaction, or of its relative rate compared to the competing reactions, would be useful, especially at very low temperatures.

3.2 Reactions of Singlet Oxygen

3.2.1 $O(^1D)$ Reactions

The recommended rate coefficients for the $O(^1D)$ reactions correspond to the rate of removal of $O(^1D)$, which includes both chemical reactions and physical quenching of the excited O atoms. Details on the branching ratios are given in the notes.

The $O(^1D)$ reactions of 7 halocarbons have been added to this review. These compounds are generally long-lived trace species for which the reaction with $O(^1D)$ in the stratosphere may represent a significant destruction process. There are new measurements that improve our database for several of the hydrohalocarbons. Some of the latter seem to exhibit an unexpected efficiency for physical quenching of $O(^1D)$.

The kinetic energy or hot atom effects of photolytically generated $O(^1D)$ are probably not important in the atmosphere, although the literature is rich with studies of these processes and with studies of the dynamics of many $O(^1D)$ reactions. The important atmospheric reactions of $O(^1D)$ include: (1) deactivation by major gases, N_2 and O_2, which limit the $O(^1D)$ steady state concentrations; (2) reaction with trace gases, e.g., H_2O, CH_4, and N_2O, which generate radicals; and (3) reaction with long lived trace gases, e.g., HCN, which have relatively slow atmospheric degradation rates. There are no data for the $O(^1D)$ + HCN reaction.

3.2.2 O_2 ($^1\Delta$ and $^1\Sigma$)

Fourteen reactions of the ($a^1\Delta_g$) and ($b^1\Sigma^+_g$) excited states of molecular oxygen have been added to this evaluation. These states are populated via photochemical processes, mainly the UV photolysis of ozone and the reaction of $O(^1D)$ with O_2. Over the years they have been proposed as

contributors to various reaction schemes in the atmosphere, but as yet no significant role in the chemistry of the stratosphere has been demonstrated. The fate of most of these excited species is physical quenching by means of energy transfer processes. In the few cases where chemical reaction occurs, it is indicated in the corresponding note.

3.3 HO_x Reactions

There has been no change in the database for HO_x chemistry since the last evaluation. The $HO_2 + O_3$ reaction rate coefficient remains one of the most significant uncertainties in the HO_x system. High quality data at low temperatures are needed for this key reaction.

3.4 NO_x Reactions

The changes to the database on NO_x reactions are relatively minor. There are new entries for the reactions of OH + HONO, NH + NO, NH + NO_2, and H + NO_2. The latter is a reaction commonly used in laboratory preparations of the hydroxyl radical. There are minor changes to the recommendations for the reactions NO + HO_2, NO + NO_3, OH + NH_3 and NH_2 + O_2 due to recently published work.

3.5 Hydrocarbon Oxidation

The major change in the recommendations for the hydrocarbon oxidation chemistry since the last evaluation is the value for the rate coefficient for the reaction of OH with CH_4, which has been reduced by approximately 20%. Even though this is a rather small numerical change, it is quite significant in the atmospheric budget and chemistry calculations. A few reactions dealing with atmospheric chemistry of ethane, peroxyacetyl nitrate (PAN), and simple organic acids have been added. In addition, small changes have been made for many rate coefficients. The accuracies of many rate coefficients have improved, and are reflected in the revised rate constants.

There still remain some areas of large uncertainties. The major such area is the reactions of peroxy radical reactions. Further work is needed to clarify the rate coefficients for many peroxy radicals. Use of peroxy radical detection by methods other than UV absorption would be very beneficial. Also, controlling the chemistry in the experimental system to minimize secondary reactions would be beneficial. The reactions involving PAN, CH_3CN, and HCN also require some attention. PAN reactions may be important in the evaluation of the atmospheric acceptability of supersonic and subsonic aircraft and in estimating the long range transport of odd nitrogen in the upper troposphere.

3.6 Halogen Reactions

The kinetics database for homogeneous reactions of halogen species has been expanded since the previous evaluation. Rate coefficients for the reaction of OH with three propane-substituted HCFCs have been added, increasing to twenty-three the number of potential alternatives to the fully halogenated CFCs for which rate data for reaction with OH are now included. Rate coefficients for the reaction of chlorine atoms with eighteen of these species have also been added. Note that rate coefficient data for the reaction of these halocarbons with $O(^1D)$ are included in the $O(^1D)$ section of Table 1. Rate coefficients have also been added for the reaction of chlorine atoms with PAN ($CH_3CO_3NO_2$), for the reaction of OH with CHF_2Br (a proposed replacement for Halons), and for the reaction of OH with $ClNO_2$. There have been only minor changes in the

recommendations for reactions included in the previous evaluation, with the exception of the O + OClO reaction, for which the recommended bimolecular rate constant value has been significantly reduced and a termolecular reaction component forming ClO_3 has been included. With these additions and improvements, the kinetics database for homogeneous gas-phase reactions of halogen species appears to be well-established.

3.7 SO_x Reactions

The database on homogeneous sulfur chemistry has seen only minor changes in the recommendations for the reactions that were included in the previous evaluation. However, this section has undergone moderate expansion to include additional reactions of importance in the atmospheric oxidation of reduced sulfur compounds of natural and anthropogenic origin. These new entries include reactions involved in the oxidation of the radical products CH_3S, CH_3SS, and CH_3SSO. The database has also been expanded to include the reactions of SH with F_2, Cl_2, Br_2, and BrCl; the reactions of CS_2 and CH_3SH with Cl; as well as the reactions of H_2S with O_3, SO_3 with NH_3, and CH_3SCH_3 with N_2O_5.

3.8 Metal Chemistry

Sodium is deposited in the upper atmosphere by meteors along with larger amounts of silicon, magnesium, and iron; comparable amounts of aluminum, nickel, and calcium; and smaller amounts of potassium, chromium, manganese, and other elements. The interest is greatest in the alkali metals because they form the least stable oxides and thus free atoms can be regenerated through photolysis and reactions with O and O_3. The other meteoric elements are expected to form more stable oxides. A review by Plane (1991) describes many aspects of atmospheric metal chemistry.

The total flux of alkali metals through the atmosphere is relatively small, e.g., one or two orders of magnitude less than CFMs. Therefore extremely efficient catalytic cycles are required in order for Na to have a significant effect on stratospheric chemistry. There are no measurements of metals or metal compounds in the stratosphere which indicate a significant role.

It has been proposed that the highly polar metal compounds may polymerize to form clusters and that the stratospheric concentrations of free metal compounds are too small to play a significant role in the chemistry.

Some studies have shown that the polar species NaO and NaOH associate with abundant gases such as O_2 and CO_2 with very fast rates in the atmosphere. It has been proposed that reactions of this type will lead to the production of clusters with many molecules attached to the sodium compounds. In most cases thermal dissociation is slow, and photolysis competes with the association reactions and limits the cluster concentrations in daylight. If atmospheric sodium does form large clusters, it is unlikely that Na species can have a significant role in stratospheric ozone chemistry. In order to assess the importance of these processes, data are needed on the association rates and the photolysis rates involving the cluster species.

3.9 Photochemical Data

In order to reduce an important source of uncertainty in atmospheric modeling calculations, high resolution measurements around 300 nm (i.e. in the Huggins bands) should be carried out for

ozone absorption cross sections, quantum yields for O^1D production and their temperature dependency.

For Cl_2O_2, the small absorption cross sections beyond 320 nm are potentially very important for photodissociation in the polar stratosphere, and need to be further studied. In addition, the temperature dependence of the absorption cross sections in the 300 nm region may be very important for HNO_3, as well as for HO_2NO_2.

In the case of HCFCs, there are discrepancies among the available sets of UV absorption data on the magnitude of the temperature effect; further work in this area is still needed.

3.10 Heterogeneous Chemistry

There is no longer any question that heterogeneous processes on the surfaces of polar stratospheric cloud particles play a critical role in the chemistry of the winter and spring polar stratospheres. Furthermore, there is increasing observational and modeling evidence that heterogeneous reactions on background sulfuric acid aerosols may play a very important role in stratospheric processes at mid-latitudes, particularly when stratospheric sulfate levels are elevated by major volcanic eruptions.

Polar heterogeneous chemical processes identified to date have a tendency to enhance the destruction of stratospheric ozone, primarily by converting relatively inactive "reservoir" species HCl and $ClONO_2$ to more active Cl_2 and HOCl, which are easily photolyzed to Cl and ClO. In addition, interaction with PSC surfaces can remove N_2O_5 and HNO_3 vapor from the polar stratosphere, sequestering nitrogen oxides in the form of condensed phase nitric acid and, thus, reducing the normal mitigating effect gaseous NO_x can have on ClO_x-catalyzed ozone destruction. The net effect of these processes is a major buildup of ClO_x radicals in PSC-processed polar stratospheric air masses and, particularly over the Antarctic, a massive springtime destruction of stratospheric ozone.

Model calculations also suggest that the reaction of stratospheric N_2O_5 with liquid water in sulfuric acid aerosols to form HNO_3 can have a significant impact on NO_x/HNO_3 ratios in the lower mid-latitude stratosphere, bringing measured mid-latitude ozone losses into better agreement with observations. Models suggest that at current mid-latitude ratios of NO_x/ClO_x this process increases ozone loss by lowering NO_x levels and thus reducing the scavenging of ClO by $ClONO_2$ formation. However, at higher NO_x/ClO_x ratios, such as those projected for mid-latitude regions impacted by the exhaust from a future high altitude supersonic aircraft fleet, the projected additional ozone loss from homogenous NO_x catalyzed destruction is greatly reduced or eliminated.

The laboratory study of heterogeneous processes relevant to the stratosphere is an immature field in comparison to the measurement of gas phase kinetic and photodissociation parameters. Heterogeneous experimental techniques are not yet as well developed and the interpretation of experimental data is significantly more complex. Nonetheless, over the past several years, a number of experimental groups have made very significant progress and data from complementary techniques are increasingly available to help determine when the quantification of heterogeneous kinetic processes has been successfully distinguished from complicating mass transport and surface saturation processes.

However, it is well to remember that quantitative application of laboratory results on heterogeneous processes to the stratosphere is not straightforward. First, there is still a significant level of uncertainty in both the detailed chemical and physical characteristics of the droplet and particle surfaces present in the stratosphere and in how faithful the laboratory simulation of these

surfaces in various experimental configurations may be. Secondly, the proper incorporation of heterogeneous processes into models of stratospheric chemistry is very difficult and no current models incorporate formation of and reaction on droplet/particle surfaces in a fully coupled and self-consistent way. A great deal of effort will have to be expended before the modeling community is as adept at incorporating heterogeneous effects as they are in representing gas phase kinetic and photochemical processes.

4. RATE CONSTANT DATA

In Table 1 (Rate Constants for Second Order Reactions) the reactions are grouped into the classes O_x, $O(^1D)$, Singlet O_2, HO_x, NO_x, Hydrocarbon Reactions, ClO_x, BrO_x, FO_x, SO_x, and metal reactions. The data in Table 2 (Rate Constants for Three-Body Reactions), while not grouped by class, are presented in the same order as the bimolecular reactions. Further, the presentation of photochemical cross section data follows the same sequence.

4.1 Bimolecular Reactions

Some of the reactions in Table 1 are actually more complex than simple two-body reactions. To explain the pressure and temperature dependences occasionally seen in reactions of this type, it is necessary to consider the bimolecular class of reactions in terms of two subcategories, direct (concerted) and indirect (non-concerted) reactions.

A direct or concerted bimolecular reaction is one in which the reactants A and B proceed to products C and D without the intermediate formation of an AB adduct which has appreciable bonding, i.e., no stable A-B molecule exists, and there is no reaction intermediate other than the transition state of the reaction, $(AB)^{\neq}$.

$$A + B \rightarrow (AB)^{\neq} \rightarrow C + D$$

The reaction of OH with CH_4 forming H_2O and CH_3 is an example of a reaction of this class.

Very useful correlations between the expected structure of the transition state $[AB]^{\neq}$ and the A-Factor of the reaction rate constant can be made, especially in reactions which are constrained to follow a well-defined approach of the two reactants in order to minimize energy requirements in the making and breaking of bonds. The rate constants for these reactions are well represented by the Arrhenius expression $k = A \exp(-(E/R)/T)$ in the 200-300 K temperature range. These rate constants are not pressure dependent.

The indirect or non-concerted class of bimolecular reactions is characterized by a more complex reaction path involving a potential well between reactants and products, leading to a bound adduct (or reaction complex) formed between the reactants A and B:

$$A + B \leftrightarrow [AB]^* \rightarrow C + D$$

The intermediate $[AB]^*$ is different from the transition state $[AB]^{\neq}$, in that it is a bound molecule which can, in principle, be isolated. (Of course, transition states are involved in all of the above reactions, both forward and backward, but are not explicitly shown.) An example of this reaction type is ClO + NO, which normally produces Cl + NO_2. Reactions of the non-concerted type can have a more complex temperature dependence and can exhibit a pressure dependence if the lifetime of $[AB]^*$ is comparable to the rate of collisional deactivation of $[AB]^*$. This arises because the

relative rate at which [AB]* goes to products C + D vs. reactants A + B is a sensitive function of its excitation energy. Thus, in reactions of this type, the distinction between the bimolecular and termolecular classification becomes less meaningful, and it is especially necessary to study such reactions under the temperature and pressure conditions in which they are to be used in model calculation, or, alternatively, to develop a reliable theoretical basis for extrapolation of data.

The rate constant tabulation for second-order reactions (Table 1) is given in Arrhenius form: $k(T) = A \exp(-(E/R)/T)$ and contains the following information:

1. Reaction stoichiometry and products (if known). The pressure dependences are included, where appropriate.
2. Arrhenius A-factor.
3. Temperature dependence ("activation temperature") and associated uncertainty, $E/R \pm \Delta E/R$.
4. Rate constant at 298 K.
5. Uncertainty factor at 298 K.

4.2 Termolecular Reactions

Rate constants for third order reactions (Table 2) of the type $A + B \leftrightarrow [AB]^* \xrightarrow{M} AB$ are given in the form

$$k_0(T) = k_0^{300}(T/300)^{-n} \text{ cm}^6 \text{ molecule}^{-2} \text{ s}^{-1},$$

(where k_0^{300} has been adjusted for air as the third body), together with a recommended value of n. Where pressure fall-off corrections are necessary, an additional entry gives the limiting high pressure rate constant in a similar form:

$$k_\infty(T) = k_\infty^{300}(T/300)^{-m} \text{ cm}^3 \text{ molecule}^{-1} \text{ s}^{-1}.$$

To obtain the effective second-order rate constant for a given condition of temperature and pressure (altitude), the following formula is used:

$$k(Z) = k(M,T) = \left(\frac{k_0(T)[M]}{1 + (k_0(T)[M]/k_\infty(T))}\right) 0.6^{\{1 + [\log_{10}(k_0(T)[M]/k_\infty(T))]^2\}^{-1}}$$

The fixed value 0.6 which appears in this formula fits the data for all listed reactions adequately, although in principle this quantity may be different for each reaction, and also temperature dependent.

Thus, a compilation of rate constants of this type requires the stipulation of the four parameters, $k_0(300)$, n, $k_\infty(300)$, and m. These can be found in Table 2. The discussion that follows outlines the general methods we have used in establishing this table, and the notes to the table discuss specific data sources.

4.2.1 Low-Pressure Limiting Rate Constant [$k_0^x(T)$]

Troe (J. Chem. Phys. **66**, 4745 (1977)) has described a simple method for obtaining low-pressure limiting rate constants. In essence this method depends on the definition:

$$k_0^x(T) = \beta_x k_{0,sc}^x(T)$$

Here sc signifies "strong" collisions, x denotes the bath gas, and β_x is an efficiency parameter ($0 < \beta_x < 1$), which provides a measure of energy transfer.

The coefficient β_x is related to the average energy transferred in a collision with gas x, $\langle\Delta E\rangle_x$, via:

$$\frac{\beta_x}{1-\beta_x^{1/2}} = \frac{\langle\Delta E\rangle_x}{F_E kT}$$

Notice that $\langle\Delta E\rangle$ is quite sensitive to β. F_E is the correction factor of the energy dependence of the density of states (a quantity of the order of 1.1 for most species of stratospheric interest).

For many of the reactions of possible stratospheric interest reviewed here, there exist data in the low-pressure limit (or very close thereto), and this data has been evaluated and unified by calculating $k_{0,sc}^x(T)$ for the appropriate bath gas x and computing the value of β_x corresponding to the experimental value [Troe (1977)].

From the β_x values (most of which are for N_2, i.e., β_{N2}), we compute $\langle\Delta E\rangle_x$ according to the above equation. Values of $\langle\Delta E\rangle_{N2}$ of approximately 0.3-1 kcal $mole^{-1}$ are generally expected. If multiple data exist, we average the values of $\langle\Delta E\rangle_{N2}$ and recommend a rate constant corresponding to the β_{N2} computed in the equation above.

Where no data exist we have estimated the low-pressure rate constant by taking $\beta_{N2} = 0.3$ at T = 300 K, a value based on those cases where data exist.

4.2.2 Temperature Dependence of Low-Pressure Limiting Rate Constants: n

The value of n recommended here comes from measurements or, in some cases, a calculation of $\langle\Delta E\rangle_{N2}$ from the data at 300 K, and a computation of β_{N2} (200 K) assuming that $\langle\Delta E\rangle_{N2}$ is independent of temperature in this range. This β_{N2} (200 K) value is combined with the computed value of $k_{0,sc}$ (200 K) to give the expected value of the actual rate constant at 200 K. This latter in combination with the value at 300 K yields the value of n.

This procedure can be directly compared with measured values of k_0 (200 K) when those exist. Unfortunately, very few values at 200 K are available. There are often temperature-dependent studies, but some ambiguity exists when one attempts to extrapolate these down to 200 K. If data are to be extrapolated beyond the measured temperature range, a choice must be made as to the functional form of the temperature dependence. There are two general ways of expressing the temperature dependence of rate constants. Either the Arrhenius expression $k_0(T) = A\exp(-E/RT)$ or the form $k_0(T) = A' T^{-n}$ is employed. Since neither of these extrapolation techniques is soundly based, and since they often yield values that differ substantially, we have used the method explained earlier as the basis of our recommendations.

4.2.3 High-Pressure Limit Rate Constants [$k_\infty(T)$]

High-pressure rate constants can often be obtained experimentally, but those for the relatively small species of atmospheric importance usually reach the high-pressure limit at inaccessibly high pressures. This leaves two sources of these numbers, the first being guesses based upon some model, and the second being extrapolation of fall-off data up to higher pressures. Stratospheric conditions generally render reactions of interest much closer to the low-pressure limit, and thus are fairly insensitive to the high-pressure value. This means that while the extrapolation is long, and the value of $k_\infty(T)$ not very accurate, a "reasonable guess' of $k_\infty(T)$ will then suffice. In some cases we have declined to guess since the low-pressure limit is effective over the entire range of stratospheric conditions.

4.2.4 Temperature Dependence of High-Pressure Limit Rate Constants: m

There are very few data upon which to base a recommendation for values of m. Values in Table 2 are often estimated, based on models for the transition state of bond association reactions and whatever data are available.

4.3 Uncertainty Estimates

For second-order rate constants in Table 1, an estimate of the uncertainty at any given temperature may be obtained from the following expression:

$$f(T) = f(298) \exp \left| \frac{\Delta E}{R} \left(\frac{1}{T} - \frac{1}{298} \right) \right|$$

Note that the exponent is absolute value. An upper or lower bound (corresponding approximately to one standard deviation) of the rate constant at any temperature T can be obtained by multiplying or dividing the value of the rate constant at that temperature by the factor f(T). The quantities f(298) and $\Delta E/R$ are, respectively, the uncertainty in the rate constant at 298 K and in the Arrhenius temperature coefficient, as listed in Table 1. This approach is based on the fact that rate constants are almost always known with minimum uncertainty at room temperature. The overall uncertainty normally increases at other temperatures, because there are usually fewer data and it is almost always more difficult to make measurements at other temperatures. It is important to note that the uncertainty at a temperature T cannot be calculated from the expression $\exp(\Delta E/RT)$. The above expression for f(T) must be used to obtain the correct result.

The uncertainty represented by f(T) is normally symmetric; i.e., the rate constant may be greater than or less than the central value, k(T), by the factor f(T). In a few cases in Table 1 asymmetric uncertainties are given in the temperature coefficient. For these cases, the factors by which a rate constant are to be multiplied or divided to obtain, respectively, the upper and lower limits are not equal, except at 298 K where the factor is simply f(298 K). Explicit equations are given below for the case where the temperature dependence is (E/R +a, -b):

For T > 298 K, multiply by the factor

$$f(298\ K)e^{[a(1/298-1/T)]}$$

and divide by the factor

$$f(298\ K)e^{[b(1/298-1/T)]}$$

For $T < 298$ K, multiply by the factor

$$f(298\ K)e^{[b(1/T-1/298)]}$$

and divide by the factor

$$f(298\ K)e^{[a(1/T-1/298)]}$$

For three-body reactions (Table 2) a somewhat analogous procedure is used. Uncertainties expressed as increments to k_0 and k_∞ are given for these rate constants at room temperature. The additional uncertainty arising from the temperature extrapolation is expressed as an uncertainty in the temperature coefficients n and m.

The assigned uncertainties represent the subjective judgement of the Panel. They are not determined by a rigorous, statistical analysis of the database, which generally is too limited to permit such an analysis. Rather, the uncertainties are based on a knowledge of the techniques, the difficulties of the experiments, and the potential for systematic errors. There is obviously no way to quantify these "unknown" errors. The spread in results among different techniques for a given reaction may provide some basis for an uncertainty, but the possibility of the same, or compensating, systematic errors in all the studies must be recognized. Furthermore, the probability distribution may not follow the normal, Gaussian form. For measurements subject to large systematic errors, the true rate constant may be much further from the recommended value than would be expected based on a Gaussian distribution with the stated uncertainty. As an example, the recommended rate constants for the reactions $HO_2 + NO$ and $Cl + ClONO_2$ have changed by factors of 30-50, occurrences which could not have been allowed for with any reasonable values of σ in a Gaussian distribution.

4.4 Units

The rate constants are given in units of concentration expressed as molecules per cubic centimeter and time in seconds. Thus, for first-, second-, and third-order reactions the units of k are s^{-1}, cm^3 $molecule^{-1}$ s^{-1}, and cm^6 $molecule^{-2}$ s^{-1}, respectively. Cross sections are expressed as cm^2 $molecule^{-1}$, base e.

TABLE 1. RATE CONSTANTS FOR SECOND ORDER REACTIONS

Reaction	A-Factor[a]	E/R±(ΔE/R)	k(298 K)	f(298)[b]
	O_x Reactions			
$O + O_2 \xrightarrow{M} O_3$	(See Table 2)			
$O + O_3 \rightarrow O_2 + O_2$	8.0×10^{-12}	2060±250	8.0×10^{-15}	1.15
	$O(^1D)$ Reactions			
$O(^1D) + N_2O \rightarrow N_2 + O_2$	4.9×10^{-11}	0±100	4.9×10^{-11}	1.3
$\rightarrow$ NO + NO	6.7×10^{-11}	0±100	6.7×10^{-11}	1.3
$O(^1D) + H_2O \rightarrow OH + OH$	2.2×10^{-10}	0±100	2.2×10^{-10}	1.2
$O(^1D) + CH_4 \rightarrow OH + CH_3$	1.4×10^{-10}	0±100	1.4×10^{-10}	1.2
$\rightarrow H_2 + CH_2O$	1.4×10^{-11}	0±100	1.4×10^{-11}	1.2
$O(^1D) + H_2 \rightarrow OH + H$	1.0×10^{-10}	0±100	1.0×10^{-10}	1.2
$O(^1D) + N_2 \rightarrow O + N_2$	1.8×10^{-11}	-(110±100)	2.6×10^{-11}	1.2
$O(^1D) + N_2 \xrightarrow{M} N_2O$	(See Table 2)			
$O(^1D) + O_2 \rightarrow O + O_2$	3.2×10^{-11}	-(70±100)	4.0×10^{-11}	1.2
$O(^1D) + CO_2 \rightarrow O + CO_2$	7.4×10^{-11}	-(120±100)	1.1×10^{-10}	1.2
$O(^1D) + O_3 \rightarrow O_2 + O_2$	1.2×10^{-10}	0±100	1.2×10^{-10}	1.3
$\rightarrow O_2 + O + O$	1.2×10^{-10}	0±100	1.2×10^{-10}	1.3
$O(^1D) + HCl \rightarrow$ products	1.5×10^{-10}	0±100	1.5×10^{-10}	1.2
$O(^1D) + HF \rightarrow OH + F$	1.4×10^{-10}	0±100	1.4×10^{-10}	2.0
$O(^1D) + HBr \rightarrow$ products	1.5×10^{-10}	0±100	1.5×10^{-10}	2.0
$O(^1D) + Cl_2 \rightarrow$ products	2.8×10^{-10}	0±100	2.8×10^{-10}	2.0
$O(^1D) + CCl_4 \rightarrow$ products	3.3×10^{-10}	0±100	3.3×10^{-10}	1.2
$O(^1D) + CFCl_3 \rightarrow$ products	2.3×10^{-10}	0±100	2.3×10^{-10}	1.2
$O(^1D) + CF_2Cl_2 \rightarrow$ products	1.4×10^{-10}	0±100	1.4×10^{-10}	1.3

Table 1. (Continued)

Reaction	A-Factor[a]	E/R±(ΔE/R)	k(298 K)	f(298)[b]
$O(^1D) + CF_4 \rightarrow CF_4 + O$	-	-	2.0×10^{-14}	1.5
$O(^1D) + CCl_2O \rightarrow$ products	3.6×10^{-10}	0±100	3.6×10^{-10}	2.0
$O(^1D) + CFClO \rightarrow$ products	1.9×10^{-10}	0±100	1.9×10^{-10}	2.0
$O(^1D) + CF_2O \rightarrow$ products	7.4×10^{-11}	0±100	7.4×10^{-11}	2.0
$O(^1D) + NH_3 \rightarrow OH + NH_2$	2.5×10^{-10}	0±100	2.5×10^{-10}	1.3
$O(^1D) + CF_3Cl \rightarrow$ products	8.7×10^{-11}	0±100	8.7×10^{-11}	1.3
$O(^1D) + CF_2ClCFCl_2 \rightarrow$ products	2×10^{-10}	0±100	2×10^{-10}	2.0
$O(^1D) + CF_3CCl_3 \rightarrow$ products	2×10^{-10}	0±100	2×10^{-10}	2.0
$O(^1D) + CF_2ClCF_2Cl \rightarrow$ products	1.3×10^{-10}	0±100	1.3×10^{-10}	1.3
$O(^1D) + CF_3CFCl_2 \rightarrow$ products	1×10^{-10}	0±100	1×10^{-10}	2.0
$O(^1D) + CF_3CF_2Cl \rightarrow$ products	5×10^{-11}	0±100	5×10^{-11}	1.3
$O(^1D) + c\text{-}C_4F_8 \rightarrow$ products	-	-	8×10^{-13}	1.3
$O(^1D) + CHFCl_2 \rightarrow$ products	1.9×10^{-10}	0±100	1.9×10^{-10}	1.3
$O(^1D) + CHF_2Cl \rightarrow$ products	1.0×10^{-10}	0±100	1.0×10^{-10}	1.2
$O(^1D) + CHF_3 \rightarrow$ products	8.4×10^{-12}	0±100	8.4×10^{-12}	5.0
$O(^1D) + CH_2F_2 \rightarrow$ products	9.0×10^{-11}	0±100	9.0×10^{-11}	3.0
$O(^1D) + CH_3F \rightarrow$ products	1.4×10^{-10}	0±100	1.4×10^{-10}	2.0
$O(^1D) + CHCl_2CF_3 \rightarrow$ products	2.0×10^{-10}	0±100	2.0×10^{-10}	1.3
$O(^1D) + CHFClCF_3 \rightarrow$ products	8.6×10^{-11}	0±100	8.6×10^{-11}	1.3
$O(^1D) + CHF_2CF_3 \rightarrow$ products	1.2×10^{-10}	0±100	1.2×10^{-10}	2.0
$O(^1D) + CH_2ClCF_2Cl \rightarrow$ products	1.6×10^{-10}	0±100	1.6×10^{-10}	2.0
$O(^1D) + CH_2ClCF_3 \rightarrow$ products	1.2×10^{-10}	0±100	1.2×10^{-10}	1.3
$O(^1D) + CH_2FCF_3 \rightarrow$ products	4.9×10^{-11}	0±100	4.9×10^{-11}	1.3
$O(^1D) + CH_3CFCl_2 \rightarrow$ products	2.6×10^{-10}	0±100	2.6×10^{-10}	1.3

Table 1. (Continued)

Reaction	A-Factor[a]	E/R±(ΔE/R)	k(298 K)	f(298)[b]
$O(^1D) + CH_3CF_2Cl \rightarrow$ products	2.2×10^{-10}	0±100	2.2×10^{-10}	1.3
$O(^1D) + CH_3CF_3 \rightarrow$ products	1.0×10^{-10}	0±100	1.0×10^{-10}	3.0
$O(^1D) + CH_3CHF_2 \rightarrow$ products	2.0×10^{-10}	0±100	2.0×10^{-10}	1.3
$O(^1D) + C_2F_6 \rightarrow O + C_2F_6$	-	-	1.5×10^{-13}	1.5
$O(^1D) + SF_6 \rightarrow$ products	-	-	1.8×10^{-14}	1.5
	Singlet O_2 Reactions			
$O_2(^1\Delta) + O \rightarrow$ products	-	-	$<2\times10^{-16}$	-
$O_2(^1\Delta) + O_2 \rightarrow$ products	3.6×10^{-18}	220±100	1.7×10^{-18}	1.2
$O_2(^1\Delta) + O_3 \rightarrow O + 2O_2$	5.2×10^{-11}	2840±500	3.8×10^{-15}	1.2
$O_2(^1\Delta) + H_2O \rightarrow$ products	-	-	4.8×10^{-18}	1.5
$O_2(^1\Delta) + N \rightarrow NO + O$	-	-	$<9\times10^{-17}$	-
$O_2(^1\Delta) + N_2 \rightarrow$ products	-	-	$<10^{-20}$	-
$O_2(^1\Delta) + CO_2 \rightarrow$ products	-	-	$<2\times10^{-20}$	-
$O_2(^1\Sigma) + O \rightarrow$ products	-	-	8×10^{-14}	5.0
$O_2(^1\Sigma) + O_2 \rightarrow$ products	-	-	3.9×10^{-17}	1.5
$O_2(^1\Sigma) + O_3 \rightarrow$ products	2.2×10^{-11}	0±200	2.2×10^{-11}	1.2
$O_2(^1\Sigma) + H_2O \rightarrow$ products	-	-	5.4×10^{-12}	1.3
$O_2(^1\Sigma) + N \rightarrow$ products	-	-	$<10^{-13}$	-
$O_2(^1\Sigma) + N_2 \rightarrow$ products	2.1×10^{-15}	0±200	2.1×10^{-15}	1.2
$O_2(^1\Sigma) + CO_2 \rightarrow$ products	4.2×10^{-13}	0±200	4.2×10^{-13}	1.2
	HO_x Reactions			
$H + O_2 \xrightarrow{M} HO_2$	(See Table 2)			
$H + O_3 \rightarrow OH + O_2$	1.4×10^{-10}	470±200	2.9×10^{-11}	1.25

Table 1. (Continued)

Reaction	A-Factor[a]	E/R±(ΔE/R)	k(298 K)	f(298)[b]
$H + HO_2 \rightarrow$ products	$8.1x10^{-11}$	0±100	$8.1x10^{-11}$	1.3
$O + OH \rightarrow O_2 + H$	$2.2x10^{-11}$	-(120±100)	$3.3x10^{-11}$	1.2
$O + HO_2 \rightarrow OH + O_2$	$3.0x10^{-11}$	-(200±100)	$5.9x10^{-11}$	1.2
$O + H_2O_2 \rightarrow OH + HO_2$	$1.4x10^{-12}$	2000±1000	$1.7x10^{-15}$	2.0
$OH + HO_2 \rightarrow H_2O + O_2$	$4.8x10^{-11}$	-(250±200)	$1.1x10^{-10}$	1.3
$OH + O_3 \rightarrow HO_2 + O_2$	$1.6x10^{-12}$	940±300	$6.8x10^{-14}$	1.3
$OH + OH \rightarrow H_2O + O$	$4.2x10^{-12}$	240±240	$1.9x10^{-12}$	1.4
$\xrightarrow{M} H_2O_2$	(See Table 2)			
$OH + H_2O_2 \rightarrow H_2O + HO_2$	$2.9x10^{-12}$	160±100	$1.7x10^{-12}$	1.2
$OH + H_2 \rightarrow H_2O + H$	$5.5x10^{-12}$	2000±400	$6.7x10^{-15}$	1.2
$HO_2 + HO_2 \rightarrow H_2O_2 + O_2$	$2.3x10^{-13}$	-(600±200)	$1.7x10^{-12}$	1.3
$\xrightarrow{M} H_2O_2 + O_2$	$1.7x10^{-33}[M]$	-(1000±400)	$4.9x10^{-32}[M]$	1.3
$HO_2 + O_3 \rightarrow OH + 2O_2$	$1.1x10^{-14}$	$500\pm^{500}_{100}$	$2.0x10^{-15}$	1.3
	<u>NO_x Reactions</u>			
$N + O_2 \rightarrow NO + O$	$1.5x10^{-11}$	3600±400	$8.5x10^{-17}$	1.25
$N + O_3 \rightarrow NO + O_2$	-	-	$<2.0x10^{-16}$	-
$N + NO \rightarrow N_2 + O$	$3.4x10^{-11}$	0±100	$3.4x10^{-11}$	1.3
$N + NO_2 \rightarrow N_2O + O$	-	-	$3.0x10^{-12}$	3.0
$O + NO \xrightarrow{M} NO_2$	(See Table 2)			
$O + NO_2 \rightarrow NO + O_2$	$6.5x10^{-12}$	-(120±120)	$9.7x10^{-12}$	1.1
$O + NO_2 \xrightarrow{M} NO_3$	(See Table 2)			
$O + NO_3 \rightarrow O_2 + NO_2$	$1.0x10^{-11}$	0±150	$1.0x10^{-11}$	1.5
$O + N_2O_5 \rightarrow$ products	-	-	$<3.0x10^{-16}$	-
$O + HNO_3 \rightarrow OH + NO_3$	-	-	$<3.0x10^{-17}$	-

Table 1. (Continued)

Reaction	A-Factor[a]	E/R±(ΔE/R)	k(298 K)	f(298)[b]
$O + HO_2NO_2 \rightarrow$ products	7.8×10^{-11}	3400±750	8.6×10^{-16}	3.0
$H + NO_2 \rightarrow OH + NO$	4.0×10^{-10}	340±300	1.3×10^{-10}	1.3
$O_3 + NO \rightarrow NO_2 + O_2$	2.0×10^{-12}	1400±200	1.8×10^{-14}	1.2
$NO + HO_2 \rightarrow NO_2 + OH$	3.7×10^{-12}	-(250±80)	8.6×10^{-12}	1.2
$NO + NO_3 \rightarrow 2NO_2$	1.5×10^{-11}	-(170±100)	2.6×10^{-11}	1.3
$OH + NO \xrightarrow{M} HONO$	(See Table 2)			
$OH + NO_2 \xrightarrow{M} HNO_3$	(See Table 2)			
$OH + NO_3 \rightarrow$ products	-	-	2.3×10^{-11}	2.0
$OH + HONO \rightarrow H_2O + NO_2$	1.8×10^{-11}	$390\pm^{200}_{500}$	4.5×10^{-12}	1.5
$OH + HNO_3 \rightarrow H_2O + NO_3$	(See ≠ below)			1.3
$OH + HO_2NO_2 \rightarrow$ products	1.3×10^{-12}	$-(380\pm^{270}_{500})$	4.6×10^{-12}	1.5
$HO_2 + NO_2 \xrightarrow{M} HO_2NO_2$	(See Table 2)			
$HO_2 + NO_3 \rightarrow$ products	-	-	4.1×10^{-12}	2.0
$O_3 + NO_2 \rightarrow NO_3 + O_2$	1.2×10^{-13}	2450±150	3.2×10^{-17}	1.15
$O_3 + HNO_2 \rightarrow O_2 + HNO_3$	-	-	$<5.0\times10^{-19}$	-
$NO_2 + NO_3 \xrightarrow{M} N_2O_5$	(See Table 2)			
$NO_2 + NO_3 \rightarrow NO + NO_2 + O_2$	See Note in JPL 92-20			
$N_2O_5 + H_2O \rightarrow 2HNO_3$	-	-	$<2.0\times10^{-21}$	-

≠ $OH + HNO_3$ pressure and temperature dependence fit by

$$k(M,T) = k_o + \frac{k_3[M]}{1 + \frac{k_3[M]}{k_2}} \quad \text{with} \quad \begin{cases} k_0 = 7.2\times10^{-15} \exp(785/T) \\ k_2 = 4.1\times10^{-16} \exp(1440/T) \\ k_3 = 1.9\times10^{-33} \exp(725/T) \end{cases}$$

Table 1. (Continued)

Reaction	A-Factor[a]	E/R±(ΔE/R)	k(298 K)	f(298)[b]
$NH + NO \rightarrow$ products	4.9×10^{-11}	0±300	4.9×10^{-11}	1.5
$NH + NO_2 \rightarrow$ products	3.5×10^{-13}	-(1140±500)	1.6×10^{-11}	2.0
$OH + NH_3 \rightarrow H_2O + NH_2$	1.7×10^{-12}	710±200	1.6×10^{-13}	1.2
$NH_2 + HO_2 \rightarrow$ products	-	-	3.4×10^{-11}	2.0
$NH_2 + NO \rightarrow$ products	3.8×10^{-12}	-(450±150)	1.7×10^{-11}	2.0
$NH_2 + NO_2 \rightarrow$ products	2.1×10^{-12}	-(650±250)	1.9×10^{-11}	3.0
$NH_2 + O_2 \rightarrow$ products	-	-	$<6.0 \times 10^{-21}$	-
$NH_2 + O_3 \rightarrow$ products	4.3×10^{-12}	930±500	1.9×10^{-13}	3.0
	Hydrocarbon Reactions			
$OH + CO \rightarrow CO_2$	$1.5 \times 10^{-13}(1+0.6P_{atm})$	0±300	$1.5 \times 10^{-13}(1+0.6P_{atm})$	1.3
$OH + CH_4 \rightarrow CH_3 + H_2O$	2.9×10^{-12}	1820±200	6.5×10^{-15}	1.1
$OH + {}^{13}CH_4 \rightarrow {}^{13}CH_3 + H_2O$	See Note in JPL 92-20			
$OH + C_2H_6 \rightarrow H_2O + C_2H_5$	8.7×10^{-12}	1070±100	2.4×10^{-13}	1.1
$OH + C_3H_8 \rightarrow H_2O + C_3H_7$	1.1×10^{-11}	700±100	1.1×10^{-12}	1.2
$OH + C_2H_4 \rightarrow$ products	(See Table 2)			
$OH + C_2H_2 \rightarrow$ products	(See Table 2)			
$OH + H_2CO \rightarrow H_2O + HCO$	1.0×10^{-11}	0±200	1.0×10^{-11}	1.25
$OH + CH_3OH \rightarrow$ products	6.7×10^{-12}	600±300	8.9×10^{-13}	1.2
$OH + C_2H_5OH \rightarrow$ products	7.0×10^{-12}	235±100	3.2×10^{-12}	1.3
$OH + CH_3CHO \rightarrow CH_3CO + H_2O$	6.0×10^{-12}	-(250±200)	1.4×10^{-11}	1.4
$OH + CH_3OOH \rightarrow$ products	3.8×10^{-12}	-(200±200)	7.4×10^{-12}	1.5
$OH + HC(O)OH \rightarrow$ products	4.5×10^{-13}	0±200	4.5×10^{-13}	1.3
$OH + CH_3C(O)OH \rightarrow$ products	1.2×10^{-12}	170±150	6.8×10^{-13}	1.5
$OH + HCN \rightarrow$ products	1.2×10^{-13}	400±150	3.1×10^{-14}	3.0

Table 1. (Continued)

Reaction	A-Factor[a]	E/R±(ΔE/R)	k(298 K)	f(298)[b]
$OH + CH_3CN \rightarrow$ products	$7.8x10^{-13}$	1050±200	$2.3x10^{-14}$	1.5
$OH + CH_3C(O)O_2NO_2 \rightarrow$ products	$1.1x10^{-12}$	650±400	$1.2x10^{-13}$	3.0
$O_3 + C_2H_2 \rightarrow$ products	$1.0x10^{-14}$	4100±500	$1.0x10^{-20}$	3.0
$O_3 + C_2H_4 \rightarrow$ products	$1.2x10^{-14}$	2630±100	$1.7x10^{-18}$	1.25
$O_3 + C_3H_6 \rightarrow$ products	$6.5x10^{-15}$	1900±200	$1.1x10^{-17}$	1.2
$HO_2 + CH_2O \rightarrow$ adduct	$6.7x10^{-15}$	-(600±600)	$5.0x10^{-14}$	5.0
$O + HCN \rightarrow$ products	$1.0x10^{-11}$	4000±1000	$1.5x10^{-17}$	10.0
$O + C_2H_2 \rightarrow$ products	$3.0x10^{-11}$	1600±250	$1.4x10^{-13}$	1.3
$O + H_2CO \rightarrow$ products	$3.4x10^{-11}$	1600±250	$1.6x10^{-13}$	1.25
$O + CH_3CHO \rightarrow CH_3CO + OH$	$1.8x10^{-11}$	1100±200	$4.5x10^{-13}$	1.25
$O + CH_3 \rightarrow$ products	$1.1x10^{-10}$	0±250	$1.1x10^{-10}$	1.3
$CH_3 + O_2 \rightarrow$ products	-	-	$<3.0x10^{-16}$	-
$CH_3 + O_2 \xrightarrow{M} CH_3O_2$	(See Table 2)			
$C_2H_5 + O_2 \rightarrow C_2H_4 + HO_2$	-	-	$<2.0x10^{-15}$	-
$C_2H_5 + O_2 \xrightarrow{M} C_2H_5O_2$	(See Table 2)			
$CH_2OH + O_2 \rightarrow CH_2O + HO_2$			$9.1x10^{-12}$	1.3
$CH_3O + O_2 \rightarrow CH_2O + HO_2$	$3.9x10^{-14}$	900±300	$1.9x10^{-15}$	1.5
$C_2H_5O + O_2 \rightarrow CH_3CHO + HO_2$	$3.1x10^{-14}$	400±400	$8.1x10^{-15}$	2.0
$C_2H_5O + NO \rightarrow$ products	(See Table 2)			
$C_2H_5O + NO_2 \rightarrow$ products	(See Table 2)			
$HCO + O_2 \rightarrow CO + HO_2$	$3.5x10^{-12}$	-(140±140)	$5.5x10^{-12}$	1.3
$CH_3 + O_3 \rightarrow$ products	$5.4x10^{-12}$	220±150	$2.6x10^{-12}$	2.0
$CH_3O_2 + O_3 \rightarrow$ products	-	-	$<3.0x10^{-17}$	-
$CH_3O_2 + CH_3O_2 \rightarrow$ products	$2.5x10^{-13}$	-(190±190)	$4.7x10^{-13}$	1.5
$CH_3O_2 + NO \rightarrow CH_3O + NO_2$	$4.2x10^{-12}$	-(180±180)	$7.7x10^{-12}$	1.5

Table 1. (Continued)

Reaction	A-Factor[a]	E/R±(ΔE/R)	k(298 K)	f(298)[b]
$CH_3O_2 + NO_2 \xrightarrow{M} CH_3O_2NO_2$	(See Table 2)			
$CH_3O_2 + HO_2 \rightarrow$ products	3.8×10^{-13}	-(800±400)	5.6×10^{-12}	2.0
$CH_3O_2 + CH_3C(O)O_2 \rightarrow$ products	1.4×10^{-11}	0±400	1.4×10^{-11}	2.0
$C_2H_5O_2 + C_2H_5O_2 \rightarrow$ products	1.5×10^{-13}	270±270	6.1×10^{-14}	2.0
$C_2H_5O_2 + NO \rightarrow$ products	8.9×10^{-12}	0±300	8.9×10^{-12}	1.3
$C_2H_5O_2 + HO_2 \rightarrow$ products	6.5×10^{-13}	-(650±300)	5.8×10^{-12}	2.0
$CH_3C(O)O_2 + CH_3C(O)O_2 \rightarrow$ products	2.5×10^{-12}	-(550±250)	1.6×10^{-11}	2.0
$CH_3C(O)O_2 + NO \rightarrow$ products	2.4×10^{-11}	0±200	2.4×10^{-11}	2.0
$CH_3C(O)O_2 + NO_2 \rightarrow$ products	(See Table 2)			
$CH_3C(O)O_2 + HO_2 \rightarrow$ products	4.5×10^{-13}	-(1000±600)	1.3×10^{-11}	2.0
$NO_3 + CO \rightarrow$ products	-	-	$<4.0\times10^{-19}$	-
$NO_3 + CH_2O \rightarrow$ products	-	-	5.8×10^{-16}	1.3
$NO_3 + CH_3CHO \rightarrow$ products	1.4×10^{-12}	1900±300	2.4×10^{-15}	1.3
	<u>ClO_x Reactions</u>			
$Cl + O_3 \rightarrow ClO + O_2$	2.9×10^{-11}	260±100	1.2×10^{-11}	1.15
$Cl + H_2 \rightarrow HCl + H$	3.7×10^{-11}	2300±200	1.6×10^{-14}	1.25
$Cl + CH_4 \rightarrow HCl + CH_3$	1.1×10^{-11}	1400±150	1.0×10^{-13}	1.1
$Cl + C_2H_6 \rightarrow HCl + C_2H_5$	7.7×10^{-11}	90±90	5.7×10^{-11}	1.1
$Cl + C_3H_8 \rightarrow HCl + C_3H_7$	1.4×10^{-10}	-(40±250)	1.6×10^{-10}	1.5
$Cl + C_2H_2 \rightarrow$ products	(See Table 2)			
$Cl + CH_3OH \rightarrow CH_2OH + HCl$	5.7×10^{-11}	0±250	5.7×10^{-11}	1.5
$Cl + CH_3CN \rightarrow$ products	-	-	$<2.0\times10^{-15}$	-
$Cl + CH_3Cl \rightarrow CH_2Cl + HCl$	3.3×10^{-11}	1250±200	4.9×10^{-13}	1.2
$Cl + CH_2Cl_2 \rightarrow HCl + CHCl_2$	3.1×10^{-11}	1350±500	3.3×10^{-13}	2.0
$Cl + CHCl_3 \rightarrow HCl + CCl_3$	4.9×10^{-12}	1240±500	7.6×10^{-14}	3.0

Table 1. (Continued)

Reaction	A-Factor[a]	E/R±(ΔE/R)	k(298 K)	f(298)[b]
$Cl + CHFCl_2 \rightarrow HCl + CFCl_2$	-	-	$1.0x10^{-14}$	3.0
$Cl + CH_2FCl \rightarrow HCl + CHFCl$	$2.1x10^{-11}$	1390±500	$1.9x10^{-13}$	3.0
$Cl + CH_2F_2 \rightarrow HCl + CHF_2$	$1.7x10^{-11}$	1630±500	$7.1x10^{-14}$	3.0
$Cl + CH_3F \rightarrow HCl + CH_2F$	$4.8x10^{-12}$	770±500	$3.6x10^{-13}$	1.5
$Cl + CH_3CCl_3 \rightarrow CH_2CCl_3 + HCl$	-	-	$<4.0x10^{-14}$	-
$Cl + CHCl_2CF_3 \rightarrow HCl + CCl_2CF_3$	-	-	$1.2x10^{-14}$	1.5
$Cl + CHFClCF_3 \rightarrow HCl + CFClCF_3$	-	-	$2.7x10^{-15}$	2.0
$Cl + CH_2ClCF_3 \rightarrow HCl + CHClCF_3$	$1.8x10^{-12}$	1710±500	$5.9x10^{-15}$	3.0
$Cl + CHF_2CHF_2 \rightarrow HCl + CF_2CHF_2$	$8.2x10^{-12}$	2430±500	$2.4x10^{-15}$	3.0
$Cl + CH_2FCF_3 \rightarrow HCl + CHFCF_3$	-	-	$1.4x10^{-15}$	3.0
$Cl + CH_3CFCl_2 \rightarrow HCl + CH_2CFCl_2$	-	-	$2.2x10^{-15}$	1.5
$Cl + CH_3CF_2Cl \rightarrow HCl + CH_2CF_2Cl$	-	-	$3.9x10^{-16}$	3.0
$Cl + CH_2FCHF_2 \rightarrow HCl + CH_2FCF_2$	$5.5x10^{-12}$	1610±500	$2.5x10^{-14}$	3.0
$\rightarrow HCl + CHFCHF_2$	$7.7x10^{-12}$	1720±500	$2.4x10^{-14}$	3.0
$Cl + CH_3CF_3 \rightarrow HCl + CH_2CF_3$	$1.2x10^{-11}$	3880±500	$2.6x10^{-17}$	5.0
$Cl + CH_2FCH_2F \rightarrow HCl + CHFCH_2F$	$2.6x10^{-11}$	1060±500	$7.5x10^{-13}$	3.0
$Cl + CH_3CHF_2 \rightarrow HCl + CH_3CF_2$	$6.4x10^{-12}$	950±500	$2.6x10^{-13}$	1.5
$\rightarrow HCl + CH_2CHF_2$	$7.2x10^{-12}$	2390±500	$2.4x10^{-15}$	3.0
$Cl + CH_3CH_2F \rightarrow HCl + CH_3CHF$	$1.8x10^{-11}$	290±500	$6.8x10^{-12}$	3.0
$\rightarrow HCl + CH_2CH_2F$	$1.4x10^{-11}$	880±500	$7.3x10^{-13}$	3.0
$Cl + CH_3CO_3NO_2 \rightarrow$ products	-	-	$<1x10^{-14}$	
$Cl + H_2CO \rightarrow HCl + HCO$	$8.1x10^{-11}$	30±100	$7.3x10^{-11}$	1.15
$Cl + H_2O_2 \rightarrow HCl + HO_2$	$1.1x10^{-11}$	980±500	$4.1x10^{-13}$	1.5
$Cl + HOCl \rightarrow Cl_2 + OH$	$3.0x10^{-12}$	130±250	$1.9x10^{-12}$	2.0
$Cl + HNO_3 \rightarrow$ products	-	-	$<2.0x10^{-16}$	-

Table 1. (Continued)

Reaction	A-Factor[a]	E/R±(ΔE/R)	k(298 K)	f(298)[b]
$Cl + HO_2 \rightarrow HCl + O_2$	$1.8x10^{-11}$	-(170±200)	$3.2x10^{-11}$	1.5
$\rightarrow OH + ClO$	$4.1x10^{-11}$	450±200	$9.1x10^{-12}$	2.0
$Cl + Cl_2O \rightarrow Cl_2 + ClO$	$9.8x10^{-11}$	0±250	$9.8x10^{-11}$	1.2
$Cl + OClO \rightarrow ClO + ClO$	$3.4x10^{-11}$	-(160±200)	$5.8x10^{-11}$	1.25
$Cl + ClOO \rightarrow Cl_2 + O_2$	$2.3x10^{-10}$	0±250	$2.3x10^{-10}$	3.0
$\rightarrow ClO + ClO$	$1.2x10^{-11}$	0±250	$1.2x10^{-11}$	3.0
$Cl + Cl_2O_2 \rightarrow$ products	-	-	$1.0x10^{-10}$	2.0
$Cl + ClONO_2 \rightarrow$ products	$6.8x10^{-12}$	-(160±200)	$1.2x10^{-11}$	1.3
$Cl + NO \xrightarrow{M} NOCl$	(See Table 2)			
$Cl + NO_2 \xrightarrow{M} ClONO\ (ClNO_2)$	(See Table 2)			
$Cl + NO_3 \rightarrow ClO + NO_2$	$2.6x10^{-11}$	0±400	$2.6x10^{-11}$	2.0
$Cl + N_2O \rightarrow ClO + N_2$	See Note in JPL 92-20			
$Cl + ClNO \rightarrow NO + Cl_2$	$5.8x10^{-11}$	-(100±200)	$8.1x10^{-11}$	1.5
$Cl + O_2 \xrightarrow{M} ClOO$	(See Table 2)			
$Cl + CO \xrightarrow{M} ClCO$	(See Table 2)			
$ClO + O \rightarrow Cl + O_2$	$3.0x10^{-11}$	-(70±70)	$3.8x10^{-11}$	1.2
$ClO + NO \rightarrow NO_2 + Cl$	$6.4x10^{-12}$	-(290±100)	$1.7x10^{-11}$	1.15
$ClO + NO_2 \xrightarrow{M} ClONO_2$	(See Table 2)			
$ClO + NO_3 \rightarrow$ products	$4.0x10^{-13}$	0±400	$4.0x10^{-13}$	2.0
$ClO + HO_2 \rightarrow HOCl + O_2$	$4.8x10^{-13}$	$-(700\pm^{250}_{700})$	$5.0x10^{-12}$	1.4
$ClO + H_2CO \rightarrow$ products	$\sim 1.0x10^{-12}$	>2100	$<1.0x10^{-15}$	-
$ClO + OH \rightarrow$ products	$1.1x10^{-11}$	-(120±150)	$1.7x10^{-11}$	1.5
$ClO + CH_4 \rightarrow$ products	$\sim 1.0x10^{-12}$	>3700	$<4.0x10^{-18}$	-
$ClO + H_2 \rightarrow$ products	$\sim 1.0x10^{-12}$	>4800	$<1.0x10^{-19}$	-
$ClO + CO \rightarrow$ products	$\sim 1.0x10^{-12}$	>3700	$<4.0x10^{-18}$	-

Table 1. (Continued)

Reaction	A-Factor[a]	E/R±(ΔE/R)	k(298 K)	f(298)[b]
$ClO + N_2O \rightarrow$ products	$\sim 1.0 \times 10^{-12}$	>4300	$<6.0 \times 10^{-19}$	-
$ClO + ClO \rightarrow$ products	8.0×10^{-13}	1250±500	1.2×10^{-14}	2.0
$\xrightarrow{M} Cl_2O_2$	(See Table 2)			
$ClO + O_3 \rightarrow ClOO + O_2$			$<1.4 \times 10^{-17}$	-
$\rightarrow OClO + O_2$	1.0×10^{-12}	>4000	$<1.0 \times 10^{-18}$	-
$ClO + CH_3O_2 \rightarrow$ products	See Note in JPL 92-20			
$OH + Cl_2 \rightarrow HOCl + Cl$	1.4×10^{-12}	900±400	6.7×10^{-14}	1.2
$OH + HCl \rightarrow H_2O + Cl$	2.6×10^{-12}	350±100	8.0×10^{-13}	1.3
$OH + HOCl \rightarrow H_2O + ClO$	3.0×10^{-12}	500±500	5.0×10^{-13}	3.0
$OH + CH_3Cl \rightarrow CH_2Cl + H_2O$	2.1×10^{-12}	1150±200	4.4×10^{-14}	1.2
$OH + CH_2Cl_2 \rightarrow CHCl_2 + H_2O$	5.8×10^{-12}	1100±250	1.4×10^{-13}	1.2
$OH + CHCl_3 \rightarrow CCl_3 + H_2O$	4.3×10^{-12}	1100±200	1.1×10^{-13}	1.2
$OH + CCl_4 \rightarrow$ products	$\sim 1.0 \times 10^{-12}$	>2300	$<5.0 \times 10^{-16}$	-
$OH + CFCl_3 \rightarrow$ products	$\sim 1.0 \times 10^{-12}$	>3700	$<5.0 \times 10^{-18}$	-
$OH + CF_2Cl_2 \rightarrow$ products	$\sim 1.0 \times 10^{-12}$	>3600	$<6.0 \times 10^{-18}$	2.0
$OH + CHFCl_2 \rightarrow CFCl_2 + H_2O$	1.2×10^{-12}	1100±200	3.0×10^{-14}	1.2
$OH + CHF_2Cl \rightarrow CF_2Cl + H_2O$	1.2×10^{-12}	1650±300	4.7×10^{-15}	1.3
$OH + CH_2ClF \rightarrow CHClF + H_2O$	3.0×10^{-12}	1250±200	4.5×10^{-14}	1.2
$OH + CH_3CCl_3 \rightarrow CH_2CCl_3 + H_2O$	1.8×10^{-12}	1550±150	1.0×10^{-14}	1.1
$OH + CHCl_2CF_3 \rightarrow CCl_2CF_3 + H_2O$	7.7×10^{-13}	900±300	3.8×10^{-14}	1.3
$OH + CHFClCF_3 \rightarrow CFClCF_3 + H_2O$	6.6×10^{-13}	1250±300	1.0×10^{-14}	1.3
$OH + CH_2ClCF_2Cl \rightarrow CHClCF_2Cl + H_2O$	3.6×10^{-12}	1600±400	1.7×10^{-14}	2.0
$OH + CH_2ClCF_3 \rightarrow CHClCF_3 + H_2O$	5.2×10^{-13}	1100±300	1.3×10^{-14}	1.3
$OH + CH_3CFCl_2 \rightarrow CH_2CFCl_2 + H_2O$	1.3×10^{-12}	1600±300	6.0×10^{-15}	1.3
$OH + CH_3CF_2Cl \rightarrow CH_2CF_2Cl + H_2O$	1.4×10^{-12}	1800±200	3.3×10^{-15}	1.2

Table 1. (Continued)

Reaction	A-Factor[a]	E/R±(ΔE/R)	k(298 K)	f(298)[b]
$OH + CF_3CF_2CHCl_2 \rightarrow CF_3CF_2CCl_2 + H_2O$	1.5×10^{-12}	1250±200	2.3×10^{-14}	1.3
$OH + CF_2ClCF_2CHFCl \rightarrow CF_2ClCF_2CFCl + H_2O$	5.5×10^{-13}	1250±200	8.3×10^{-15}	1.3
$OH + CH_3CF_2CFCl_2 \rightarrow CH_2CF_2CFCl_2 + H_2O$	7.7×10^{-13}	1700±300	2.6×10^{-15}	2.0
$OH + C_2Cl_4 \rightarrow$ products	9.4×10^{-12}	1200±200	1.7×10^{-13}	1.25
$OH + C_2HCl_3 \rightarrow$ products	4.9×10^{-13}	-(450±200)	2.2×10^{-12}	1.25
$OH + ClNO_2 \rightarrow HOCl + NO_2$	-	-	3.5×10^{-14}	3.0
$OH + ClONO_2 \rightarrow$ products	1.2×10^{-12}	330±200	3.9×10^{-13}	1.5
$O + HCl \rightarrow OH + Cl$	1.0×10^{-11}	3300±350	1.5×10^{-16}	2.0
$O + HOCl \rightarrow OH + ClO$	1.0×10^{-11}	2200±1000	6.0×10^{-15}	10.0
$O + ClONO_2 \rightarrow$ products	2.9×10^{-12}	800±200	2.0×10^{-13}	1.5
$O + Cl_2O \rightarrow ClO + ClO$	2.9×10^{-11}	630±200	3.5×10^{-12}	1.4
$OClO + O \rightarrow ClO + O_2$	2.5×10^{-12}	950±300	1.0×10^{-13}	2.0
$OClO + O \xrightarrow{M} ClO_3$	(See Table 2)			
$OClO + O_3 \rightarrow$ products	2.1×10^{-12}	4700±1000	3.0×10^{-19}	2.5
$OClO + OH \rightarrow HOCl + O_2$	4.5×10^{-13}	-(800±200)	6.8×10^{-12}	2.0
$OClO + NO \rightarrow NO_2 + ClO$	2.5×10^{-12}	600±300	3.4×10^{-13}	2.0
$Cl_2O_2 + O_3 \rightarrow$ products	-	-	$<1.0\times10^{-19}$	-
$Cl_2O_2 + NO \rightarrow$ products	-	-	$<2.0\times10^{-14}$	-
$HCl + NO_3 \rightarrow HNO_3 + Cl$	-	-	$<5.0\times10^{-17}$	-
$HCl + ClONO_2 \rightarrow$ products	-	-	$<1.0\times10^{-20}$	-
$HCl + HO_2NO_2 \rightarrow$ products	-	-	$<1.0\times10^{-21}$	-
$H_2O + ClONO_2 \rightarrow$ products	-	-	$<2.0\times10^{-21}$	-
$CF_2ClO_2 + NO \rightarrow CF_2ClO + NO_2$	3.1×10^{-12}	-(500±200)	1.6×10^{-11}	1.3
$CFCl_2O_2 + NO \rightarrow CFCl_2O + NO_2$	3.5×10^{-12}	-(430±200)	1.5×10^{-11}	1.3

Table 1. (Continued)

Reaction	A-Factor[a]	E/R±(ΔE/R)	k(298 K)	f(298)[b]
$CCl_3O_2 + NO \rightarrow CCl_3O + NO_2$	5.7×10^{-12}	-(330±200)	1.7×10^{-11}	1.3
	<u>BrO_x Reactions</u>			
$Br + O_3 \rightarrow BrO + O_2$	1.7×10^{-11}	800±200	1.2×10^{-12}	1.2
$Br + H_2O_2 \rightarrow HBr + HO_2$	1.0×10^{-11}	>3000	$<5.0\times10^{-16}$	-
$Br + H_2CO \rightarrow HBr + HCO$	1.7×10^{-11}	800±200	1.1×10^{-12}	1.3
$Br + HO_2 \rightarrow HBr + O_2$	1.5×10^{-11}	600±600	2.0×10^{-12}	2.0
$Br + NO_2 \overset{M}{\rightarrow} BrNO_2$	(See Table 2)			
$Br + Cl_2O \rightarrow BrCl + ClO$	2.0×10^{-11}	500±300	3.8×10^{-12}	2.0
$Br + OClO \rightarrow BrO + ClO$	2.6×10^{-11}	1300±300	3.4×10^{-13}	2.0
$Br + Cl_2O_2 \rightarrow$ products	-	-	3.0×10^{-12}	2.0
$BrO + O \rightarrow Br + O_2$	3.0×10^{-11}	0±250	3.0×10^{-11}	3.0
$BrO + ClO \rightarrow Br + OClO$	1.6×10^{-12}	-(430±200)	6.8×10^{-12}	1.25
$\rightarrow Br + ClOO$	2.9×10^{-12}	-(220±200)	6.1×10^{-12}	1.25
$\rightarrow BrCl + O_2$	5.8×10^{-13}	-(170±200)	1.0×10^{-12}	1.25
$BrO + NO \rightarrow NO_2 + Br$	8.8×10^{-12}	-(260±130)	2.1×10^{-11}	1.15
$BrO + NO_2 \overset{M}{\rightarrow} BrONO_2$	(See Table 2)			
$BrO + BrO \rightarrow 2\,Br + O_2$	1.4×10^{-12}	-(150±150)	2.3×10^{-12}	1.25
$\rightarrow Br_2 + O_2$	6.0×10^{-14}	-(600±600)	4.4×10^{-13}	1.25
$BrO + O_3 \rightarrow Br + 2O_2$	$\sim1.0\times10^{-12}$	>1600	$<5.0\times10^{-15}$	-
$BrO + HO_2 \rightarrow$ products	6.2×10^{-12}	-(500±500)	3.3×10^{-11}	3.0
$BrO + OH \rightarrow$ products	-	-	1.0×10^{-11}	5.0
$OH + Br_2 \rightarrow HOBr + Br$	4.2×10^{-11}	0±600	4.2×10^{-11}	1.3
$OH + HBr \rightarrow H_2O + Br$	1.1×10^{-11}	0±250	1.1×10^{-11}	1.2
$OH + CH_3Br \rightarrow CH_2Br + H_2O$	3.6×10^{-12}	1430±150	3.0×10^{-14}	1.1
$OH + CHF_2Br \rightarrow CF_2Br + H_2O$	7.4×10^{-13}	1300±500	9.4×10^{-15}	3.0

Table 1. (Continued)

Reaction	A-Factor[a]	E/R±(ΔE/R)	k(298 K)	f(298)[b]
$OH + CF_2Br_2 \rightarrow$ products	-	-	$<5.0\times10^{-16}$	-
$OH + CF_2ClBr \rightarrow$ products	-	-	$<1.5\times10^{-16}$	-
$OH + CF_3Br \rightarrow$ products	-	-	$<1.2\times10^{-16}$	-
$OH + CF_2BrCF_2Br \rightarrow$ products	-	-	$<1.5\times10^{-16}$	-
$O + HBr \rightarrow OH + Br$	5.8×10^{-12}	1500±200	3.8×10^{-14}	1.3
$NO_3 + Br \rightarrow BrO + NO_2$	-	-	1.6×10^{-11}	2.0
$NO_3 + BrO \rightarrow$ products	-	-	1.0×10^{-12}	3.0
$NO_3 + HBr \rightarrow HNO_3 + Br$	-	-	$<1.0\times10^{-16}$	-
	<u>FO_x Reactions</u>			
$F + O_3 \rightarrow FO + O_2$	2.8×10^{-11}	230±200	1.3×10^{-11}	2.0
$F + H_2 \rightarrow HF + H$	1.4×10^{-10}	500±200	2.6×10^{-11}	1.2
$F + CH_4 \rightarrow HF + CH_3$	3.0×10^{-10}	400±300	8.0×10^{-11}	1.5
$F + H_2O \rightarrow HF + OH$	1.4×10^{-11}	0±200	1.4×10^{-11}	1.3
$F + O_2 \xrightarrow{M} FO_2$	(See Table 2)			
$F + NO \xrightarrow{M} FNO$	(See Table 2)			
$F + NO_2 \xrightarrow{M} FNO_2(FONO)$	(See Table 2)			
$F + HNO_3 \rightarrow HF + NO_3$	6.0×10^{-12}	-(400±200)	2.3×10^{-11}	1.3
$NO + FO \rightarrow NO_2 + F$	2.6×10^{-11}	0±250	2.6×10^{-11}	2.0
$FO + FO \rightarrow 2\,F + O_2$	1.5×10^{-11}	0±250	1.5×10^{-11}	3.0
$FO + O_3 \rightarrow F + 2\,O_2$	See Note in JPL 92-20			
$\rightarrow FO_2 + O_2$	See Note in JPL 92-20			
$FO + NO_2 \xrightarrow{M} FONO_2$	(See Table 2)			
$O + FO \rightarrow F + O_2$	5.0×10^{-11}	0±250	5.0×10^{-11}	3.0
$O + FO_2 \rightarrow FO + O_2$	5.0×10^{-11}	0±250	5.0×10^{-11}	5.0
$OH + CHF_3 \rightarrow CF_3 + H_2O$	1.5×10^{-12}	2650±500	2.1×10^{-16}	1.5

Table 1. (Continued)

Reaction	A-Factor[a]	E/R±(ΔE/R)	k(298 K)	f(298)[b]
$OH + CH_2F_2 \rightarrow CHF_2 + H_2O$	$1.9x10^{-12}$	1550±300	$1.0x10^{-14}$	1.3
$OH + CH_3F \rightarrow CH_2F + H_2O$	$5.4x10^{-12}$	1700±300	$1.8x10^{-14}$	1.2
$OH + CHF_2CF_3 \rightarrow CF_2CF_3 + H_2O$	$5.6x10^{-13}$	1700±300	$1.9x10^{-15}$	1.3
$OH + CHF_2CHF_2 \rightarrow CF_2CHF_2 + H_2O$	$8.7x10^{-13}$	1500±500	$5.7x10^{-15}$	2.0
$OH + CH_2FCF_3 \rightarrow CHFCF_3 + H_2O$	$1.7x10^{-12}$	1750±300	$4.8x10^{-15}$	1.3
$OH + CH_2FCHF_2 \rightarrow$ products	$2.8x10^{-12}$	1500±500	$1.8x10^{-14}$	2.0
$OH + CH_3CF_3 \rightarrow CH_2CF_3 + H_2O$	$1.6x10^{-12}$	2100±300	$1.4x10^{-15}$	1.3
$OH + CH_2FCH_2F \rightarrow CHFCH_2F + H_2O$	$1.7x10^{-11}$	1500±500	$1.1x10^{-13}$	2.0
$OH + CH_3CHF_2 \rightarrow$ products	$1.5x10^{-12}$	1100±200	$3.7x10^{-14}$	1.2
$OH + CH_3CH_2F \rightarrow$ products	$1.3x10^{-11}$	1200±300	$2.3x10^{-13}$	2.0
$CF_3O_2 + NO \rightarrow CF_3O + NO_2$	$3.9x10^{-12}$	-(400±200)	$1.5x10^{-11}$	1.3
	<u>SO_x Reactions</u>			
$OH + H_2S \rightarrow SH + H_2O$	$6.0x10^{-12}$	75±75	$4.7x10^{-12}$	1.2
$OH + OCS \rightarrow$ products	$1.1x10^{-13}$	1200±500	$1.9x10^{-15}$	2.0
$OH + CS_2 \rightarrow$ products	See Note in JPL 92-20	-	-	-
$OH + SO_2 \xrightarrow{M} HOSO_2$	(See Table 2)			
$O + H_2S \rightarrow OH + SH$	$9.2x10^{-12}$	1800±550	$2.2x10^{-14}$	1.7
$O + OCS \rightarrow CO + SO$	$2.1x10^{-11}$	2200±150	$1.3x10^{-14}$	1.2
$O + CS_2 \rightarrow CS + SO$	$3.2x10^{-11}$	650±150	$3.6x10^{-12}$	1.2
$O_3 + H_2S \rightarrow$ products	-	-	$<2.0x10^{-20}$	-
$S + O_2 \rightarrow SO + O$	$2.3x10^{-12}$	0±200)	$2.3x10^{-12}$	1.2
$S + O_3 \rightarrow SO + O_2$	-	-	$1.2x10^{-11}$	2.0
$S + OH \rightarrow SO + H$	-	-	$6.6x10^{-11}$	3.0
$SO + O_2 \rightarrow SO_2 + O$	$2.6x10^{-13}$	2400±500	$8.4x10^{-17}$	2.0
$SO + O_3 \rightarrow SO_2 + O_2$	$3.6x10^{-12}$	1100±200	$9.0x10^{-14}$	1.2

Table 1. (Continued)

Reaction	A-Factor[a]	E/R±(ΔE/R)	k(298 K)	f(298)[b]
$SO + OH \rightarrow SO_2 + H$	-	-	$8.6x10^{-11}$	2.0
$SO + NO_2 \rightarrow SO_2 + NO$	$1.4x10^{-11}$	0±50	$1.4x10^{-11}$	1.2
$SO + ClO \rightarrow SO_2 + Cl$	$2.8x10^{-11}$	0±50	$2.8x10^{-11}$	1.3
$SO + OClO \rightarrow SO_2 + ClO$	-	-	$1.9x10^{-12}$	3.0
$SO + BrO \rightarrow SO_2 + Br$	-	-	$5.7x10^{-11}$	1.4
$SO_2 + HO_2 \rightarrow$ products	-	-	$<1.0x10^{-18}$	-
$SO_2 + CH_3O_2 \rightarrow$ products	-	-	$<5.0x10^{-17}$	-
$SO_2 + NO_2 \rightarrow$ products	-	-	$<2.0x10^{-26}$	-
$SO_2 + NO_3 \rightarrow$ products	-	-	$<7.0x10^{-21}$	-
$SO_2 + O_3 \rightarrow SO_3 + O_2$	$3.0x10^{-12}$	>7000	$<2.0x10^{-22}$	-
$SO_3 + H_2O \rightarrow H_2SO_4$	-	-	$<6.0x10^{-15}$	-
$SO_3 + NO_2 \rightarrow$ products	-	-	$1.0x10^{-19}$	10.0
$SO_3 + NH_3 \rightarrow$ products	-	-	$6.9x10^{-11}$	3.0
$Cl + H_2S \rightarrow HCl + SH$	$5.7x10^{-11}$	0±50	$5.7x10^{-11}$	1.3
$Cl + OCS \rightarrow SCl + CO$	-	-	$<1.0x10^{-16}$	-
$Cl + CS_2 \rightarrow$ products	-	-	$<4.0x10^{-15}$	-
$Cl + CH_3SH \rightarrow CH_3S + HCl$	-	-	$1.4x10^{-10}$	1.4
$ClO + OCS \rightarrow$ products	-	-	$<2.0x10^{-16}$	-
$ClO + SO_2 \rightarrow Cl + SO_3$	-	-	$<4.0x10^{-18}$	-
$SH + H_2O_2 \rightarrow$ products	-	-	$<5.0x10^{-15}$	-
$SH + O \rightarrow H + SO$	-	-	$1.6x10^{-10}$	5.0
$SH + O_2 \rightarrow OH + SO$	-	-	$<4.0x10^{-19}$	-
$SH + O_3 \rightarrow HSO + O_2$	$9.0x10^{-12}$	280±200	$3.5x10^{-12}$	1.3
$SH + NO \xrightarrow{M} HSNO$	(See Table 2)			
$SH + NO_2 \rightarrow HSO + NO$	$2.9x10^{-11}$	-(240±100)	$6.5x10^{-11}$	1.3

Table 1. (Continued)

Reaction	A-Factor[a]	E/R±(ΔE/R)	k(298 K)	f(298)[b]
$SH + F_2 \rightarrow FSH + F$	$4.3x10^{-11}$	1390±200	$4.0x10^{-13}$	2.0
$SH + Cl_2 \rightarrow ClSH + Cl$	$1.7x10^{-11}$	690±200	$1.7x10^{-12}$	2.0
$SH + Br_2 \rightarrow BrSH + Br$	$6.0x10^{-11}$	-(160±160)	$1.0x10^{-10}$	2.0
$SH + BrCl \rightarrow$ products	$2.3x10^{-11}$	-(350±200)	$7.4x10^{-11}$	2.0
$HSO + O_2 \rightarrow$ products	-	-	$<2.0x10^{-17}$	-
$HSO + O_3 \rightarrow$ products	-	-	$1.0x10^{-13}$	1.3
$HSO + NO \rightarrow$ products	-	-	$<1.0x10^{-15}$	-
$HSO + NO_2 \rightarrow HSO_2 + NO$	-	-	$9.6x10^{-12}$	2.0
$HSO_2 + O_2 \rightarrow HO_2 + SO_2$	-	-	$3.0x10^{-13}$	3.0
$HOSO_2 + O_2 \rightarrow HO_2 + SO_3$	$1.3x10^{-12}$	330±200	$4.4x10^{-13}$	1.2
$CS + O_2 \rightarrow OCS + O$	-	-	$2.9x10^{-19}$	2.0
$CS + O_3 \rightarrow OCS + O_2$	-	-	$3.0x10^{-16}$	3.0
$CS + NO_2 \rightarrow OCS + NO$	-	-	$7.6x10^{-17}$	3.0
$OH + CH_3SH \rightarrow$ products	$9.9x10^{-12}$	-(360±100)	$3.3x10^{-11}$	1.2
$OH + CH_3SCH_3 \rightarrow H_2O + CH_2SCH_3$	$1.1x10^{-11}$	240±100	$4.9x10^{-12}$	1.2
$OH + CH_3SSCH_3 \rightarrow$ products	$5.7x10^{-11}$	-(380±300)	$2.0x10^{-10}$	1.3
$NO_3 + H_2S \rightarrow$ products	-	-	$<8.0x10^{-16}$	-
$NO_3 + OCS \rightarrow$ products	-	-	$<1.0x10^{-16}$	-
$NO_3 + CS_2 \rightarrow$ products	-	-	$<4.0x10^{-16}$	-
$NO_3 + CH_3SH \rightarrow$ products	$4.4x10^{-13}$	-(210±210)	$8.9x10^{-13}$	1.25
$NO_3 + CH_3SCH_3 \rightarrow$ products	$1.9x10^{-13}$	-(500±200)	$1.0x10^{-12}$	1.2
$NO_3 + CH_3SSCH_3 \rightarrow$ products	$1.3x10^{-12}$	270±270	$5.3x10^{-13}$	1.4
$N_2O_5 + CH_3SCH_3 \rightarrow$ products	-	-	$<1.0x10^{-17}$	-
$CH_3S + O_2 \rightarrow$ products	-	-	$<3.0x10^{-18}$	-

Table 1. (Continued)

Reaction	A-Factor[a]	E/R±(ΔE/R)	k(298 K)	f(298)[b]
$CH_3S + O_3 \rightarrow$ products	-	-	5.4×10^{-12}	1.3
$CH_3S + NO \rightarrow$ products	-	-	$<1.0 \times 10^{-13}$	-
$CH_3S + NO_2 \rightarrow CH_3SO + NO$	-	-	5.6×10^{-11}	1.3
$CH_3SO + O_3 \rightarrow$ products	-	-	6.0×10^{-13}	1.5
$CH_3SO + NO_2 \rightarrow CH_3SO_2 + NO$	-	-	1.2×10^{-11}	1.4
$CH_3SS + O_3 \rightarrow$ products	-	-	4.6×10^{-13}	2.0
$CH_3SS + NO_2 \rightarrow$ products	-	-	1.8×10^{-11}	2.0
$CH_3SSO + NO_2 \rightarrow$ products	-	-	4.5×10^{-12}	2.0
	Metal Reactions			
$Na + O_2 \xrightarrow{M} NaO_2$	(See Table 2)			
$Na + O_3 \rightarrow NaO + O_2$	7.3×10^{-10}	0±200	7.3×10^{-10}	1.2
$\rightarrow NaO_2 + O$	-	-	$<4.0 \times 10^{-11}$	-
$Na + N_2O \rightarrow NaO + N_2$	2.8×10^{-10}	1600±400	1.3×10^{-12}	1.2
$Na + Cl_2 \rightarrow NaCl + Cl$	7.3×10^{-10}	0±200	7.3×10^{-10}	1.3
$NaO + O \rightarrow Na + O_2$	3.7×10^{-10}	0±400	3.7×10^{-10}	3.0
$NaO + O_2 \xrightarrow{M} NaO_3$	(See Table 2)			
$NaO + O_3 \rightarrow NaO_2 + O_2$	1.6×10^{-10}	0±400	1.6×10^{-10}	2.0
$\rightarrow Na + 2O_2$	6.0×10^{-11}	0±800	6.0×10^{-11}	3.0
$NaO + H_2 \rightarrow NaOH + H$	2.6×10^{-11}	0±600	2.6×10^{-11}	2.0
$NaO + H_2O \rightarrow NaOH + OH$	2.2×10^{-10}	0±400	2.2×10^{-10}	2.0
$NaO + NO \rightarrow Na + NO_2$	1.5×10^{-10}	0±400	1.5×10^{-10}	4.0
$NaO + CO_2 \xrightarrow{M} NaCO_3$	(See Table 2)			
$NaO + HCl \rightarrow$ products	2.8×10^{-10}	0±400	2.8×10^{-10}	3.0
$NaO_2 + NO \rightarrow NaO + NO_2$	-	-	$<10^{-14}$	-

Table 1. (Continued)

Reaction	A-Factor[a]	E/R±(ΔE/R)	k(298 K)	f(298)[b]
$NaO_2 + HCl \rightarrow$ products	2.3×10^{-10}	0±400	2.3×10^{-10}	3.0
$NaOH + HCl \rightarrow NaCl + H_2O$	2.8×10^{-10}	0±400	2.8×10^{-10}	3.0
$NaOH + CO_2 \xrightarrow{M} NaHCO_3$	(See Table 2)			

a Units are cm^3/molecule-sec.

b f(298) is the uncertainty factor at 298 K. To calculate the uncertainty at other temperatures, use the expression:

$$f(T) = f(298) \exp \left| \frac{\Delta E}{R} \left(\frac{1}{T} - \frac{1}{298} \right) \right|$$

Note that the exponent is absolute value.

TABLE 2. RATE CONSTANTS FOR THREE-BODY REACTIONS

Reaction	Low Pressure Limit[a] $k_0(T) = k_0^{300}(T/300)^{-n}$		High Pressure Limit[b] $k_\infty(T) = k_\infty^{300}(T/300)^{-m}$	
	k_0^{300}	n	k_∞^{300}	m
$O + O_2 \xrightarrow{M} O_3$	(6.0±0.5) (-34)	2.3±0.5	-	-
$O(^1D) + N_2 \xrightarrow{M} N_2O$	(3.5±3.0) (-37)	$0.6\pm^{2.0}_{0.6}$	-	-
$H + O_2 \xrightarrow{M} HO_2$	(5.7±0.5) (-32)	1.6±0.5	(7.5±4.0) (-11)	0±1.0
$OH + OH \xrightarrow{M} H_2O_2$	(6.9±3.0) (-31)	$0.8\pm^{2.0}_{0.8}$	(1.5±0.5) (-11)	0±0.5
$O + NO \xrightarrow{M} NO_2$	(9.0±2.0) (-32)	1.5±0.3	(3.0±1.0) (-11)	0±1.0
$O + NO_2 \xrightarrow{M} NO_3$	(9.0±1.0) (-32)	2.0±1.0	(2.2±0.3) (-11)	0±1.0
$OH + NO \xrightarrow{M} HONO$	(7.0±2.0) (-31)	2.6±1.0	(1.5±1.0) (-11)	0.5±0.5
$OH + NO_2 \xrightarrow{M} HNO_3$	(2.6±0.3) (-30)	3.2±0.7	(2.4±1.2) (-11)	1.3±1.3
$HO_2 + NO_2 \xrightarrow{M} HO_2NO_2$	(1.8±0.3) (-31)	3.2±0.4	(4.7±1.0) (-12)	1.4±1.4
$NO_2 + NO_3 \xrightarrow{M} N_2O_5$	(2.2±0.5) (-30)	3.9±1.0	(1.5±0.8) (-12)	0.7±0.4
$Cl + NO \xrightarrow{M} ClNO$	(9.0±2.0) (-32)	1.6±0.5	-	-
$Cl + NO_2 \xrightarrow{M} ClONO$	(1.3±0.2) (-30)	2.0±1.0	(1.0±0.5) (-10)	1.0±1.0
$\xrightarrow{M} ClNO_2$	(1.8±0.3) (-31)	2.0±1.0	(1.0±0.5) (-10)	1.0±1.0
$Cl + O_2 \xrightarrow{M} ClOO$	(2.7±1.0) (-33)	1.5±0.5	-	-
$Cl + CO \xrightarrow{M} ClCO$	(1.3±0.5) (-33)	3.8±0.5	-	-
$Cl + C_2H_2 \xrightarrow{M} ClC_2H_2$	(8.0±1.0) (-30)	3.5±0.5	(1.0±0.5) (-10)	2.6±0.5
$ClO + ClO \xrightarrow{M} Cl_2O_2$	(1.9±0.5) (-32)	3.9±1.0	(7.0±1) (-12)	0±1.0
$ClO + NO_2 \xrightarrow{M} ClONO_2$	(1.8±0.3) (-31)	3.4±1.0	(1.5±0.7) (-11)	1.9±1.9
$O + OClO \xrightarrow{M} ClO_3$	(1.9±0.5) (-31)	1.1±1.0	(3.1±0.8) (-11)	0±1.0

Table 2. (Continued)

Reaction	Low Pressure Limit[a] $k_0(T) = k_0^{300}(T/300)^{-n}$		High Pressure Limit[b] $k_\infty(T) = k_\infty^{300}(T/300)^{-m}$	
	k_0^{300}	n	k_∞^{300}	m
$Br + NO_2 \xrightarrow{M} BrNO_2$	(4.2±0.8) (-31)	2.4±0.5	(2.7±0.5) (-11)	0±1.0
$BrO + NO_2 \xrightarrow{M} BrONO_2$	(5.2±0.5) (-31)	3.0±0.8	(9.0±1.0) (-12)	2.3±1.0
$F + O_2 \xrightarrow{M} FO_2$	(4.4±0.4) (-33)	1.2±0.5	-	-
$F + NO \xrightarrow{M} FNO$	(5.9±3.0) (-32)	1.7±1.7	-	-
$F + NO_2 \xrightarrow{M}$ products	(1.1±0.6) (-30)	2.0±2.0	(3.0±2.0) (-11)	1.0±1.0
$FO + NO_2 \xrightarrow{M} FONO_2$	(2.6±2.0) (-31)	1.3±1.3	(2.0±1.0) (-11)	1.5±1.5
$CH_3 + O_2 \xrightarrow{M} CH_3O_2$	(4.5±1.5) (-31)	3.0±1.0	(1.8±0.2) (-12)	1.7±1.7
$C_2H_5 + O_2 \xrightarrow{M} C_2H_5O_2$	(1.5±1.0) (-28)	3.0±1.0	(8.0±1.0) (-12)	0±1.0
$CH_3O + NO \xrightarrow{M} CH_3ONO$	(1.35±0.5) (-29)	3.8±1	(3.6±1.6) (-11)	0.6±1.0
$CH_3O + NO_2 \xrightarrow{M} CH_3ONO_2$	(2.8±0.6) (-29)	4.0±2.0	(2.0±0.4) (-11)	1.0±1.0
$C_2H_5O + NO \xrightarrow{M} C_2H_5ONO$	(2.0±1.0) (-27)	4.0±2.0	(4.4±0.4) (-11)	1.0±1.0
$C_2H_5O + NO_2 \xrightarrow{M} C_2H_5ONO_2$	(2.0±1.0) (-27)	4.0±2.0	(2.8±0.4) (-11)	1.0±1.0
$CH_3O_2 + NO_2 \xrightarrow{M} CH_3O_2NO_2$	(1.5±0.8) (-30)	4.0±2.0	(6.5±3.2) (-12)	2.0±2.0
$OH + SO_2 \xrightarrow{M} HOSO_2$	(3.0±1.0) (-31)	3.3±1.5	(1.5±10.5) (-12)	$0\pm^{0}_{2}$
$OH + C_2H_4 \xrightarrow{M} HOCH_2CH_2$	(1.0±0.6) (-28)	0.8±2.0	(8.8±0.9) (-12)	$0\pm^{0}_{2}$
$OH + C_2H_2 \xrightarrow{M} HOCHCH$	(5.5±2.0) (-30)	0.0±0.2	(8.3±1.0) (-13)	$-2\pm^{2}_{1}$
$CF_3 + O_2 \xrightarrow{M} CF_3O_2$	(1.5±0.3) (-29)	4.0±2.0	(8.5±1.0) (-12)	1.0±1.0
$CF_2Cl + O_2 \xrightarrow{M} CF_2ClO_2$	(3.0±1.5) (-30)	4.0±2.0	(3±2) (-12)	1.0±1.0
$CFCl_2 + O_2 \xrightarrow{M} CFCl_2O_2$	(5.0±0.8) (-30)	4.0±2.0	(6.0±1.0) (-12)	1.0±1.0

Table 2. (Continued)

Reaction	Low Pressure Limit[a] $k_0(T) = k_0^{300}(T/300)^{-n}$		High Pressure Limit[b] $k_\infty(T) = k_\infty^{300}(T/300)^{-m}$	
	k_0^{300}	n	k_∞^{300}	m
$CCl_3 + O_2 \xrightarrow{M} CCl_3O_2$	(1.0±0.7) (-30)	6.0±2.0	(2.5±2.0) (-12)	1.0±1.0
$CFCl_2O_2 + NO_2 \xrightarrow{M} CFCl_2O_2NO_2$	(3.5±0.5) (-29)	5.0±1.0	(6.0±1.0) (-12)	2.5±1.0
$CF_2ClO_2 + NO_2 \xrightarrow{M} CF_2ClO_2NO_2$	(3.5±1.8) (-29)	5.0±1.0	(5.2±1.0) (-12)	2.5±1.0
$CH_3C(O)O_2 + NO_2 \xrightarrow{M} CH_3C(O)O_2NO_2$	(8±4) (-29)	7.0±2.0	(12±2)(-12)	1.0±1.0
$CF_3O_2 + NO_2 \rightarrow CF_3O_2NO_2$	(2.2±0.5) (-29)	5.0±1.0	(6.0±1.0) (-12)	2.5±1.0
$CCl_3O_2 + NO_2 \rightarrow CCl_3O_2NO_2$	(5.0±1.0) (-29)	5.0±1.0	(6.0±1.0) (-12)	2.5±1
$HS + NO \xrightarrow{M} HSNO$	(2.4±0.4) (-31)	3.0±1.0	(2.7±0.5) (-11)	$0\pm^{0}_{2}$
$CH_3S + NO \xrightarrow{M} CH_3SNO$	(3.2±0.4) (-29)	4.0±1	(3.9±0.6) (-11)	2.7±1.0
$Na + O_2 \xrightarrow{M} NaO_2$	(2.4±0.5) (-30)	1.2±0.5	(4.0±2.0) (-10)	0±1.0
$NaO + O_2 \xrightarrow{M} NaO_3$	(3.5±0.7) (-30)	2.0±2.0	(5.7±3.0) (-10)	0±1.0
$NaO + CO_2 \xrightarrow{M} NaCO_3$	(8.7±2.6) (-28)	2.0±2.0	(6.5±3.0) (-10)	0±1.0
$NaOH + CO_2 \xrightarrow{M} NaHCO_3$	(1.3±0.3) (-28)	2.0±2.0	(6.8±4.0) (-10)	0±1.0

Note: $k(Z) = k(M,T) = \left(\frac{k_0(T)[M]}{1 + (k_0(T)[M]/k_\infty(T))}\right) 0.6^{\{1 + [\log_{10}(k_0(T)[M]/k_\infty(T))]^2\}^{-1}}$

The values quoted are suitable for air as the third body, M.

[a] Units are $cm^6/molecule^2$-sec.

[b] Units are $cm^3/molecule$-sec.

5. EQUILIBRIUM CONSTANTS

Some of the three-body reactions in Table 2 form products which are thermally unstable at atmospheric temperatures. In such cases the thermal decomposition reaction may compete with other loss processes, such as photodissociation or radical attack. Table 3 lists the equilibrium constants, K(T), for eleven reactions which may fall into this category. The table has three column entries, the first two being the parameters A and B which can be used to express K(T):

$$K(T)/cm^3\ molecule^{-1} = A \exp(B/T)\ (200 < T < 300\ K)$$

The third column entry in Table 3 is the calculated value of K at 298 K.

The data sources for K(T) are described in the individual notes to Table 3. When values of the heats of formation and entropies of all species are known at the temperature T, we note that:

$$\log[K(T)/cm^3\ molecule^{-1}] = \frac{\Delta S^o_T}{2.303R} - \frac{\Delta H^o_T}{2.303RT} + \log T - 21.87$$

Where the superscript "o" refers to a standard state of one atmosphere. In some cases K values were calculated from this equation, using thermochemical data. In other cases the K values were calculated directly from kinetic data for the forward and reverse reactions. When available, JANAF values were used for the equilibrium constants. The following equations were then used to calculate the parameters A and B:

$$B/^oK = 2.303 \left[\log \frac{K_{200}}{K_{300}}\right] \left(\frac{300 \times 200}{300 - 200}\right)$$

$$= 1382 \log(K_{200}/K_{300})$$

$$\log A = \log K(T) - B/2.303\ T$$

TABLE 3. EQUILIBRIUM CONSTANTS

Reaction	A/cm^3 molecule^{-1}	B±ΔB/°K	K_{eq}(298 K)	f(298 K)[a]
$HO_2 + NO_2 \rightarrow HO_2NO_2$	2.1×10^{-27}	10900±1000	1.6×10^{-11}	5
$NO + NO_2 \rightarrow N_2O_3$	3.0×10^{-27}	4700±100	2.1×10^{-20}	2
$NO_2 + NO_2 \rightarrow N_2O_4$	5.9×10^{-29}	6600±250	2.5×10^{-19}	2
$NO_2 + NO_3 \rightarrow N_2O_5$	4.0×10^{-27}	10930±500	3.4×10^{-11}	1.3
$CH_3O_2 + NO_2 \rightarrow CH_3O_2NO_2$	1.3×10^{-28}	11200±1000	2.7×10^{-12}	2
$Cl + O_2 \rightarrow ClOO$	5.7×10^{-25}	2500±750	2.5×10^{-21}	2
$ClO + O_2 \rightarrow ClO \cdot O_2$	2.9×10^{-26}	<3700	$<7.2 \times 10^{-21}$	-
$Cl + CO \rightarrow ClCO$	1.6×10^{-25}	4000±500	1.1×10^{-19}	5
$ClO + ClO \rightarrow Cl_2O_2$	3.0×10^{-27}	8450±850	6.2×10^{-15}	2
$ClO + OClO \rightarrow Cl_2O_3$	1.6×10^{-27}	7200±1400	5.0×10^{-17}	1 0
$F + O_2 \rightarrow FOO$	3.2×10^{-25}	6100±1200	2.5×10^{-16}	1 0
$OH + CS_2 \rightarrow CS_2OH$	4.5×10^{-25}	5140±500	1.4×10^{-17}	1.4

K/cm^3 molecule^{-1} = A exp (B/T) [200 < T/K < 300]

[a] f(298) is the uncertainty factor at 298 K. To calculate the uncertainty at other temperatures, use the expression:

$$f(T) = f(298\ K) \exp\left(\Delta B \left| \frac{1}{T} - \frac{1}{298} \right| \right).$$

6. PHOTOCHEMICAL DATA

6.1 Discussion of Format and Error Estimates

In Table 4 we present a list of photochemical reactions considered to be of stratospheric interest. The absorption cross sections of O_2 and O_3 largely determine the extent of penetration of solar radiation into the stratosphere and troposphere. Some comments and references to these cross sections are presented in the text, but only a sample of the data is listed here. (See, for example, WMO Report #11, 1982; WMO-NASA, 1985.) The photodissociation of NO in the O_2 Schumann-Runge band spectral range is another important process requiring special treatment and is not discussed in this evaluation (see, for example, Frederick and Hudson, 1979; Allen and Frederick, 1982; and WMO Report #11, 1982).

For some other species having highly structured spectra, such as CS_2 and SO_2, some comments are given in the text, but the photochemical data are not presented. The species CH_2O, NO_2, NO_3, ClO, BrO, and OClO also have complicated spectra, but in view of their importance for atmospheric chemistry a sample of the data is presented in the evaluation; for more detailed information on their high-resolution spectra and temperature dependence, the reader is referred to the original literature.

Table 5 gives recommended reliability factors for some of the more important photochemical reactions. These factors represent the combined uncertainty in cross sections and quantum yields, taking into consideration the atmospherically important wavelength regions, and they refer to the total dissociation rate regardless of product identity (except in the case of $O(^1D)$ production from photolysis of O_3).

The error estimates are not rigorous numbers resulting from a detailed error propagation analysis of statistical manipulations of the different sets of literature values; they merely represent a consensus among the panel members as to the reliability of the data for atmospheric photodissociation calculations, taking into account the difficulty of the measurements, the agreement among the results reported by various groups, etc.

The absorption cross sections are defined by the following expression of Beer's Law:

$$I = I_0 \exp(-\sigma n l),$$

where I_0 and I are the incident and transmitted light intensity, respectively; σ is the absorption cross section in cm^2 $molecule^{-1}$; n is the concentration in molecule cm^{-3}, and l is the pathlength in cm. The cross sections are room temperature values at the specific wavelengths listed in the table, and the expected photodissociation quantum yields are unity, unless otherwise stated.

TABLE 4. PHOTOCHEMICAL REACTIONS

$O_2 + h\nu \rightarrow O + O$	$CF_2ClCF_2Cl + h\nu \rightarrow$ products
$O_3 + h\nu \rightarrow O_2 + O$	$CF_3CF_2Cl + h\nu \rightarrow$ products
$O_3 + h\nu \rightarrow O_2 + O(^1D)$	$CH_3CF_2Cl + h\nu \rightarrow$ products
$HO_2 + h\nu \rightarrow$ products	$CF_3CHCl_2 + h\nu \rightarrow$ products
$H_2O + h\nu \rightarrow H + OH$	$CF_3CHFCl + h\nu \rightarrow$ products
$H_2O_2 + h\nu \rightarrow OH + OH$	$CH_3CFCl_2 + h\nu \rightarrow$ products
$NO + h\nu \rightarrow N + O$	$CH_3CCl_3 + h\nu \rightarrow$ products
$NO_2 + h\nu \rightarrow NO + O$	$CF_3CF_2CHCl_2 + h\nu \rightarrow$ products
$NO_3 + h\nu \rightarrow$ products	$CF_2ClCF_2CHFCl + h\nu \rightarrow$ products
$N_2O + h\nu \rightarrow N_2 + O(^1D)$	$CF_3Br + h\nu \rightarrow$ products
$N_2O_5 + h\nu \rightarrow$ products	$CF_2Br_2 + h\nu \rightarrow$ products
$NH_3 + h\nu \rightarrow NH_2 + H$	$CF_2ClBr + h\nu \rightarrow$ products
$HONO + h\nu \rightarrow OH + NO$	$CF_2BrCF_2Br + h\nu \rightarrow$ products
$HNO_3 + h\nu \rightarrow OH + NO_2$	$CH_3Br + h\nu \rightarrow$ products
$HO_2NO_2 + h\nu \rightarrow$ products	$CHBr_3 + h\nu \rightarrow$ products
$Cl_2 + h\nu \rightarrow Cl + Cl$	$CF_4 + h\nu \rightarrow$ products
$ClO + h\nu \rightarrow Cl + O$	$C_2F_6 + h\nu \rightarrow$ products
$ClOO + h\nu \rightarrow$ products	$SF_6 + h\nu \rightarrow$ products
$OClO + h\nu \rightarrow O + ClO$	$CCl_2O + h\nu \rightarrow$ products
$ClO_3 + h\nu \rightarrow$ products	$CClFO + h\nu \rightarrow$ products
$Cl_2O + h\nu \rightarrow$ products	$CF_2O + h\nu \rightarrow$ products
$Cl_2O_2 + h\nu \rightarrow$ products	$BrO + h\nu \rightarrow$ products
$Cl_2O_3 + h\nu \rightarrow$ products	$BrONO_2 + h\nu \rightarrow$ products
$Cl_2O_4 + h\nu \rightarrow$ products	$HF + h\nu \rightarrow H + F$
$Cl_2O_6 + h\nu \rightarrow$ products	$CO + h\nu \rightarrow C + O$ (1)
$HCl + + h\nu \rightarrow H + Cl$	$CO_2 + h\nu \rightarrow CO + O$ (1)
$HOCl + h\nu \rightarrow OH + Cl$	$CH_4 + h\nu \rightarrow$ products (2)
$ClNO + h\nu \rightarrow Cl + NO$	$CH_2O \rightarrow$ products
$ClNO_2 + h\nu \rightarrow$ products	$CH_3OOH + h\nu \rightarrow$ products
$ClONO + h\nu \rightarrow$ products	$HCN + h\nu \rightarrow$ products
$ClONO_2 + h\nu \rightarrow$ products	$CH_3CN + h\nu \rightarrow$ products
$CCl_4 + h\nu \rightarrow$ products	$SO_2 + h\nu \rightarrow SO + O$
$CCl_3F + h\nu \rightarrow$ products	$OCS + h\nu \rightarrow CO + S$
$CCl_2F_2 + h\nu \rightarrow$ products	$H_2S + h\nu \rightarrow HS + H$
$CHClF_2 + h\nu \rightarrow$ products	$CS_2 + h\nu \rightarrow$ products
$CH_3Cl + h\nu \rightarrow$ products	$NaCl + h\nu \rightarrow Na + Cl$
$CF_2ClCFCl_2 + h\nu \rightarrow$ products	$NaOH + h\nu \rightarrow Na + OH$

(1) Hudson, R. D. and L. J. Kieffer, 1975, "Absorption Cross Sections of Stratospheric Molecules," The Natural Stratosphere of 1974, CIAP Monograph 1, (5-156)-(5-194).
(2) Turco, R. P., Geophys. Surveys 2, 153-192 (1975).

TABLE 5. COMBINED UNCERTAINTIES FOR CROSS SECTIONS AND QUANTUM YIELDS

Species	Uncertainty
O_2 (Schumann-Runge bands)	1.2
O_2 (Continua)	1.2
O_3 (Cross Sections Only)	1.1
$O_3 \rightarrow O(^1D)$	1.2
NO_2	1.2
NO_3	2.0
N_2O	1.2
N_2O_5	2.0
H_2O_2	1.3
HNO_3	1.3
HO_2NO_2	2.0
CH_2O	1.4
HCl	1.1
HOCl	1.4
$ClONO_2$	1.3
CCl_4	1.1
CCl_3F	1.1
CCl_2F_2	1.1
CH_3Cl	1.1
CF_2O	2.0
CH_3OOH	1.5
$BrONO_2$	1.4
CF_3Br	1.3
CF_2ClBr	2.0
CF_2Br_2	2.0
$C_2F_4Br_2$	2.0

7. HETEROGENEOUS CHEMISTRY

We have evaluated and tabulated the currently available information on heterogeneous stratospheric processes. However, this is a relatively new and rapidly developing field and further results can be expected to change our quantitative, and even qualitative, understanding on a regular basis. The topic's complexity is compounded by the difficulty of characterizing the chemical and physical properties of stratospheric heterogeneous surfaces and then reproducing suitable simulations in the laboratory.

7.1 Surface Types

To a first approximation there are three major types of surfaces believed to be present at significant levels in the stratosphere. They are: 1) Type I - polar stratospheric clouds (PSCs) nominally composed of nitric acid trihydrate ($HNO_3 \cdot 3H_2O$); 2) crystals of relatively pure water ice, designated as Type II PSCs because they form at lower temperatures than Type I and are believed to be nucleated by Type I (similar surfaces may form as contrails behind high altitude aircraft under some stratospheric conditions); and 3) sulfuric acid aerosol, which is nominally a liquid phase surface generally composed of 60 - 80 weight percent H_2SO_4 and concomitantly, 40-20 weight percent H_2O. While PSCs, as their name suggests, are formed primarily in the cold winter stratosphere at high latitudes, sulfuric acid aerosol is present year round at all latitudes and may influence stratospheric chemistry on a global basis, particularly after large injections of volcanic sulfur periodically increase their abundance and surface area.

The detailed composition and morphology of each surface type are uncertain and probably subject to a significant range of natural variability. Certain chemical and physical properties of these surfaces, such as their ability to absorb and/or solvate HCl and HNO_3, are known to be strongly dependent on their detailed chemical composition. Moreover, most heterogeneous processes studied under laboratory conditions (and in some cases proceeding under stratospheric conditions) can change the chemical composition of the surface in ways which significantly affect the kinetic or thermodynamic processes of interest. Thus, a careful analysis of the time-dependent nature of the active surface is required in the evaluation of measured uptake kinetics experiments. Experimental techniques which allow the measurement of mass accommodation or surface reaction kinetics with high time resolution and/or with low trace gas fluxes are often more credible in establishing that measured kinetic parameters are not seriously compromised by surface saturation or changing surface chemical composition.

The measured kinetic uptake parameters, mass accommodation coefficients and surface reaction probabilities are separately documented for relevant atmospheric trace gas species for the three stratospheric surfaces noted above. Since these parameters can vary significantly with surface composition (e.g., the H_2SO_4/H_2O ratio for sulfate aerosol or the HNO_3/H_2O ratio for Type I PSC) the dependence of these parameters on surface composition is reviewed where sufficient data are available. Furthermore, data are also compiled for liquid water for several reasons. This surface is one asymptote of the H_2SO_4/H_2O aerosol continuum; the interactions of some trace species with liquid water and water ice (Type II PSC) surfaces are often similar; and the uptake of some trace species by water surfaces in the troposphere can play a key role in understanding their tropospheric chemical lifetimes and thus, the fraction which may be transported into the stratosphere. Finally, a few processes measured on solid inorganic salt surfaces, which may be relevant to the stratosphere perturbed by volcanic eruptions or solid rocket exhaust particles are also included. Heterogeneous processes on soot produced by high altitude aircraft or rockets using hydrocarbon propellants are not addressed in this tabulation but may be addressed in the future.

7.2 Temperature Dependence

A number of laboratory studies have shown that mass accommodation coefficients and, to some extent, surface reaction probabilities can be temperature dependent. While these dependencies have not been characterized for many systems of interest, temperature effects on kinetic data are noted where available. More work which fully separates heterogeneous kinetic temperature effects from temperature controlled surface composition is obviously needed.

7.3 Solubility Limitations

Experimental data on the uptake of some trace gases by various stratospherically relevant surfaces can be shown to be governed by solubility limitations rather than kinetic processes. In these cases properly analyzed data can yield measurements of trace gas solubility parameters relevant to stratospheric conditions. In general, such parameters can be strongly dependent on both condensed phase composition and temperature. Such parameters may be very important in stratospheric models since they can govern the availability of a reactant for a bimolecular heterogeneous process (e.g., the concentration of HCl available for the HCl + $ClONO_2$ reaction on sulfuric acid aerosols) or the gas/condensed phase partitioning of a heterogeneous reaction product (e.g., the HNO_3 formed by the reaction of N_2O_5 on sulfuric acid aerosols).

7.4 Data Organization

Data for trace gas heterogenous interactions with relevant condensed phase surfaces are tabulated in Tables 6, 7 and 8. These are organized into:

Table 6 - Mass Accommodation (Sticking) Coefficients
Table 7 - Surface Reaction Probabilities
Table 8 - Solubility Data

Mass accommodation coefficients (α), often called sticking coefficients, represent the probability of reversible uptake of a gaseous species colliding with the condensed surface of interest. For liquid surfaces this process is generally followed by bulk solvation. Examples include: simple surface absorption, absorption followed by ionic dissociation and solvation (e.g., $HCl + H_2O \leftrightarrow H^+(aq) + Cl^-(aq)$ and absorption followed by a reversible chemical reaction with a condensed phase substituent (e.g., $SO_2 + H_2O \leftrightarrow H^+ + HSO_3^-$). Processes involving liquid surfaces are subject to Henry's law which limits the fractional uptake of a gas phase species into a liquid. If the gas phase species is simply solvated a physical Henry's law restraint holds; if the gas phase species reacts with a condensed phase substituent, as in the sulfur dioxide/liquid water case noted above, a "chemically modified" or "effective" Henry's law constraint holds. It is presently unclear whether "surface solubility" effects govern the uptake on nominally solid water ice or HNO_3/H_2O ice surfaces in a manner analogous to bulk solubility effects for liquid substrates.

For some trace species on some surfaces experimental data suggest that mass accommodation coefficients untainted by experimental saturation limitations have been obtained. These are tabulated in Table 6. In other cases experimental data can be shown to be subject to Henry's law constraints, and Henry's law constants, or at least their upper limits, can be determined. These are tabulated for liquid surfaces in Table 8. Some experimental data sets are insufficient to determine if measured "uptake" coefficients are true accommodation coefficients or if the measurement values are lower limits compromised by saturation effects. These are currently tabulated, with suitable caveats, in Table 6.

Surface reaction probabilities (γ) are kinetic values for generally irreversible reactive uptake of trace gas species on condensed surfaces. Such processes are not subject to Henry's law constraints; however, the fate of the uptake reaction products may be subject to saturation limitations. For example, N_2O_5 has been shown to react with sulfuric acid aerosol surfaces. However, if the H_2SO_4/H_2O ratio is too high, the product HNO_3 will be insoluble and a large fraction will be expelled back into the gas phase. Surface reaction probabilities for substantially irreversible processes are presented in Table 7. Reaction products are identified where known.

The data in Tables 6 and 7 are organized by trace gas species, since some systematic variation may be expected for surface accommodation or reaction as the surface composition and/or phase is varied. Data presented for one surface may be judged for "reasonableness" by comparing with data for a "similar" surface. In some cases it is not yet clear if surface uptake is truly reversible (accommodation) or irreversibly reactive in nature. In such cases the available uptake coefficients are generally tabulated in Table 6 as accommodation coefficients, a judgement which will be subject to change if more definitive data become available.

Where a specific evaluated value for an accommodation coefficient or reaction probability has been obtained, an estimated uncertainty factor is also tabulated. However, when the data evaluation yielded only a lower or upper limit, no uncertainty factor can be reliably estimated and none are presented.

TABLE 6. MASS ACCOMMODATION COEFFICIENTS (α)

Gaseous Species	Surface Type	Composition	T(K)	α	Uncertainty Factor
HCl	Water Ice	H_2O(s)	191-211	0.3	3
	Liquid Water	H_2O(l)	274	0.2*	2
	Nitric Acid Ice	$HNO_3 \cdot 3H_2O$(s)	191-211	0.3	
	Sulfuric Acid	$H_2SO_4 \cdot nH_2O$(l)			
		($n \geq 8, \leq 40$ wt.% H_2SO_4)	283	0.15*	2
			218	>0.05*	
		(n < 8, >40 wt.% H_2SO_4)	(No data - all measurements limited by HCl solubility)		
HNO_3	Water Ice	H_2O(s)	200	0.03	3
	Liquid Water	H_2O(l)	268	0.2*	2
	Sulfuric Acid	$H_2SO_4 \cdot nH_2O$(l)			
		(73 wt.% H_2SO_4)	283	0.1	2
		(75 wt.% H_2SO_4)	230	$> 2 \times 10^{-3}$	
		(96.5 wt.% H_2SO_4)	295	$< 4 \times 10^{-3}$	
O_3	Water Ice	H_2O(s)	195-262	$< 1 \times 10^{-6}$‡	
	Liquid Water	H_2O(l)	292	$> 2 \times 10^{-3}$‡	
	Nitric Acid Ice	$HNO_3 \cdot 3H_2O$(s)	195	2.5×10^{-4}‡	3
	Sulfuric Acid	$H_2SO_4 \cdot nH_2O$(l)			
		(50 wt.% H_2SO_4)	195	$< 1 \times 10^{-6}$‡	
		(97 wt.% H_2SO_4)	196	$< 1 \times 10^{-6}$‡	
H_2O_2	Liquid Water	H_2O(l)	273	0.18*	2
	Sulfuric Acid	$H_2SO_4 \cdot nH_2O$(l)			
		(96 wt.% H_2SO_4)	298	$> 8 \times 10^{-4}$‡	
NO_2	Water Ice	H_2O(s)	195	$< 1 \times 10^{-4}$‡	
	Liquid Water	H_2O(l)	273	$> 6 \times 10^{-4}$‡	
	Sulfuric Acid	$H_2SO_4 \cdot nH_2O$(l)			
		(96 wt.% H_2SO_4)	298	$< 1 \times 10^{-6}$‡	
NO	Water Ice	H_2O(s)	195	$< 1 \times 10^{-4}$‡	
	Sulfuric Acid	$H_2SO_4 \cdot nH_2O$			
		(96 wt.% H_2SO_4)	298	$< 1 \times 10^{-6}$‡	
SO_2	Liquid Water	H_2O(l)	260-292	0.11	2
	Sulfuric Acid	$H_2SO_4 \cdot nH_2O$(l)			
		(96 wt.% H_2SO_4)	298	$< 1 \times 10^{-6}$‡	
HO_2	Liquid Water	H_2O(l)	275	> 0.02	
	Aqueous Salts	NH_4HSO_4(aq)	293	> 0.2	
		and $LiNO_3$(aq)			
	Sulfuric Acid	$H_2SO_4 \cdot nH_2O$(l)	275	>0.07	
		(28 wt.% H_2SO_4)			

Table 6 (Continued)

Gaseous Species	Surface Type	Composition	T(K)	α	Uncertainty Factor
	Liquid Water	$H_2O(l)$	275	$> 4 \times 10^{-3}$	
OH	Sulfuric Acid	$H_2SO_4 \cdot nH_2O(l)$			
		(28 wt.% H_2SO_4)	275	> 0.07	
		(96 wt.% H_2SO_4)	298	$> 5 \times 10^{-4}$‡	
O	Sulfuric Acid	$H_2SO_4 \cdot nH_2O(l)$			
		(96 wt.% H_2SO_4)	298	$< 1 \times 10^{-6}$‡	
HO_2NO_2	Sulfuric Acid	$H_2SO_4 \cdot nH_2O(l)$			
		(96 wt.% H_2SO_4)	298	$< 2.7 \times 10^{-5}$‡	
H_2O	Water Ice	$H_2O(s)$	200	0.5	2
	Sulfuric Acid	$H_2SO_4 \cdot nH_2O$			
		(96 wt.% H_2SO_4)	298	$> 2 \times 10^{-3}$‡	
CF_2O	Water Ice	$H_2O(s)$	192	$< 3 \times 10^{-6}$‡	
	Liquid Water	$H_2O(l)$	260-290	$< 1 \times 10^{-3}$‡	
	Nitric Acid Ice	$HNO_3 \cdot 3H_2O(s)$	192	$< 3 \times 10^{-6}$‡	
	Sulfuric Acid	$H_2SO_4 \cdot nH_2O(l)$	215-230		
		(60 wt.% H_2SO_4)		3×10^{-6}‡	3
		(40 wt.% H_2SO_4)		6×10^{-5}‡	2
CCl_2O	Liquid Water	$H_2O(l)$	260-290	$< 1 \times 10^{-3}$‡	
CF_3CClO	Liquid Water	$H_2O(l)$	260-290	$< 1 \times 10^{-3}$‡	
CF_3CFO	Liquid Water	$H_2O(l)$	260-290	$< 1 \times 10^{-3}$‡	
Cl_2	Water Ice	$H_2O(s)$	200	$< 1 \times 10^{-4}$‡	

* Varies with T.
‡ Measurement likely affected by saturation.

TABLE 7. GAS/SURFACE REACTION PROBABILITIES (γ)

Gaseous Species	Surface Type	Composition	T(K)	γ	Uncertainty Factor
ClO + Surface → Products					
ClO	Water Ice	H_2O(s)	190	> 0.01	
	Sulfuric Acid	$H_2SO_4 \cdot nH_2O$(l) (72 to 95 wt.% H_2SO_4)	221-296	8×10^{-5}	1 0
Cl + Surface → Products					
Cl	Sulfuric Acid	$H_2SO_4 \cdot nH_2O$(l) (72 to 95 wt.% H_2SO_4)	221-296	2×10^{-4}	1 0
$ClONO_2 + H_2O \rightarrow HOCl + HNO_3$					
$ClONO_2$	Water Ice	H_2O(s)	200-202	0.3	3
	Nitric Acid Ice	$HNO_3 \cdot 3H_2O$(s)	200-202	0.006	
	Sulfuric Acid	$H_2SO_4 \cdot nH_2O$(l)			
		(40 wt.% H_2SO_4)	218	6.4×10^{-2}	2
		(60 wt.% H_2SO_4)	215	3.1×10^{-3}	2
		(65 wt.% H_2SO_4)	215	1.2×10^{-3}	2
		(70 wt.% H_2SO_4)	220	3.9×10^{-4}	2
		(75 wt.% H_2SO_4)	230	1.9×10^{-4}	2
		(96 wt.% H_2SO_4)	295	3.2×10^{-4}	2
$ClONO_2 + HCl \rightarrow Cl_2 + HNO_3$					
$ClONO_2$/HCl	Water Ice	H_2O(s)	200-202	0.3	3
	Nitric Acid Ice Doped with HCl	$HNO_3 \cdot 3H_2O \cdot HCl$	200-202	0.3	3
	Sulfuric Acid	$H_2SO_4 \cdot nH_2O$(l) (H_2SO_4 wt.% > 60))			
$ClONO_2 + NaCl(s) \rightarrow Cl_2 + NaNO_3$					
$ClONO_2$	Sodium Chloride	NaCl(s)	300		
$ClONO_2 + NaBr(s) \rightarrow BrCl + NaNO_3$					
$ClONO_2$	Sodium Bromide	NaBr(s)	300		
$N_2O_5 + H_2O \rightarrow 2HNO_3$					
N_2O_5	Water Ice	H_2O(s)	195-200	0.03	1.5
	Liquid Water	H_2O(l)	270-275	0.08*	2
	Nitric Acid Ice	$HNO_3 \cdot 3H_2O$(s)	200	6×10^{-4}	3
	Sulfuric Acid	$H_2SO_4 \cdot nH_2O$(l)	210-230	0.1	2

Table 7. (Continued)

Gaseous Species	Surface Type	Composition	T(K)	γ	Uncertainty Factor
N_2O_5 + HCl → $ClNO_2$ + HNO_3					
N_2O_5	Water Ice	H_2O(s)	190-220	0.03	
	Nitric Acid Ice	$HNO_3 \cdot 3H_2O$(s)	200	0.003	2
N_2O_5 + NaCl(s) → $ClNO_2$ + $NaNO_3$(s)					
N_2O_5	Sodium Chloride	NaCl(s)	298	> 2.5×10^{-3}	
N_2O_5 + NaBr(s) → $BrNO_2$ + $NaNO_3$(s)					
N_2O_5	Sodium Bromide	NaBr(s)	298		
HOCl + HCl(s) → Cl_2 + H_2O					
HOCl/HCl	Water Ice	H_2O(s)	195-200	0.3	3
	Nitric Acid Ice	$HNO_3 \cdot 3H_2O$(s)	195-200	0.1	3

* γ is temperature dependent

TABLE 8. HENRY'S LAW CONSTANTS FOR GAS-LIQUID SOLUBILITIES

		H(T) (M/atm)	
HNO_3 in $H_2SO_4 \cdot nH_2O$			
		$H = A \exp(B/T)$	
T	wt. % H_2SO_4	A (M/atm)	B(K)
188-240	58	7.47×10^{-8}	7.16×10^{3}
	66	0.202	3.19×10^{3}
	74	8.54×10^{-3}	3.55×10^{3}
	87	3.56×10^{-3}	3.32×10^{3}
283	73	4×10^{3}	
HCl in $H_2SO_4 \cdot nH_2O$			
203	60	$> 8.6 \times 10^{3}$	
283	40	$> 1.0 \times 10^{4}$	
283	50	$> 1.0 \times 10^{3}$	
283	60	$> 1.0 \times 10^{2}$	
283	70	$> 1.0 \times 10^{1}$	
F_2CO in $H_2SO_4 \cdot nH_2O$			
215-230	60	> 5	

APPENDIX 1. GAS PHASE ENTHALPY DATA

SPECIES	ΔHf(298) (Kcal/mol)	SPECIES	ΔHf(298) (Kcal/mol)	SPECIES	ΔHf(298) (Kcal/mol)	SPECIES	ΔHf(298) (Kcal/mol)
H	52.1	CH_3OOH	-31.3	CH_3SH	-5.5	$CHCl_3$	-24.6
H_2	0.00	CH_3ONO	-15.6	CH_2SCH_3	36±3	$CHCl_2$	23±2
O	59.57	CH_3ONO_2	-28.6	CH_3SCH_3	-8.9	CH_2Cl	29±2
$O(^1D)$	104.9	$CH_3O_2NO_2$	-10.6±2	CH_3SSCH_3	-5.8	CH_2Cl_2	-22.8
O_2	0.00	C_2H	133±2	OCS	-34	CH_3Cl	-19.6
$O_2(^1D)$	22.5	C_2H_2	54.35	F	18.98	ClCO	-5±1
$O_2(^1\Sigma)$	37.5	C_2H_2OH	30±3	F_2	0.00	$COCl_2$	-52.6
O_3	34.1	C_2H_3	72±3	HF	-65.34	CHFCl	-15±2
HO	9.3	C_2H_4	12.45	HOF	-23.4±1	CH_2FCl	-63±2
HO_2	3±1	C_2H_5	28.4	FO	26±5	CFCl	7±6
H_2O	-57.81	C_2H_6	-20.0	F_2O	5.9±.4	$CFCl_2$	-22±2
H_2O_2	-32.60	CH_2CN	57±2	FO_2	6±1	$CFCl_3$	-68.1
N	113.00	CH_3CN	15.6	F_2O_2	5±2	CF_2Cl	-64±3
N_2	0.00	CH_2CO	-11±3	FONO	-15±7	CF_2Cl_2	-117.9
NH	85.3	CH_3CO	-5.8	FNO	-16±2	CF_3Cl	-169.2
NH_2	45.3	CH_3CHO	-39.7	FNO_2	-26±2	$CHFCl_2$	-68.1
NH_3	-10.98	C_2H_5O	-4.1	$FONO_2$	2.5±7	CHF_2Cl	-115.6
NO	21.57	CH_2CH_2OH	-10±3	CF_2	-44±2	COFCl	-102±2
NO_2	7.9	C_2H_5OH	-56.2	CF_3	-112±1	CH_3CH_2F	-63±2
NO_3	17±2	CH_3CO_2	-49.6	CF_4	-223.0	CH_3CHF	-17±2
N_2O	19.61	$C_2H_5O_2$	-6±2	CHF_3	-166.8	CH_2CF_3	-124±2
N_2O_3	19.8	CH_3COO_2	-41±5	CHF_2	-58±2	CH_3CHF_2	-120±1
N_2O_4	2.2	CH_3OOCH_3	-30.0	CH_2F_2	-107.2	CH_3CF_2	-71±2
N_2O_5	2.7±2	C_3H_5	39.4	CH_2F	-8±2	CH_3CF_3	-179±2
HNO	23.8	C_3H_6	4.8	CH_3F	-55.9±1	CF_2CF_3	-213±2
HONO	-19.0	n-C_3H_7	22.6±2	FCO	-41±14	CHF_2CF_3	-264±2
HNO_3	-32.3	i-C_3H_7	19±2	COF_2	-153±2	CH_3CF2Cl	-127±2
HO_2NO_2	-11±2	C_3H_8	-24.8	Cl	28.9	CH_2CF_2Cl	-75±2
C	170.9	C_2H_5CHO	-44.8	Cl_2	0.00	C_2Cl_4	-3.0
CH	142.0	CH_3COCH_3	-51.9	HCl	-22.06	C_2HCl_3	-1.9
CH_2	93±1	$CH_3COO_2NO_2$	-62±5	ClO	24.4	CH_2CCl_3	17±2
CH_3	35±.2	S	66.22	ClOO	23±1	CH_3CCl_3	-34.0
CH_4	-17.88	S_2	30.72	OClO	23±2	CH_3CH_2Cl	-26.8
CN	104±3	HS	34±1	$ClOO_2$	16.7	CH_2CH_2Cl	22±2
HCN	32.3	H_2S	-4.9	ClO_3	52±4	CH_3CHCl	17.6±1
CH_3NH_2	-5.5	SO	1.3	Cl_2O	19.5	Br	26.7
NCO	3 8	SO_2	-70.96	Cl_2O_2	31±3	Br_2	7.39
CO	-26.42	SO_3	-94.6	Cl_2O_3	34±3	HBr	-8.67
CO_2	-94.07	HSO	-1±3	HOCl	-18±3	HOBr	-19±2
HCO	10±1	HSO_3	-92±2	ClNO	12.4	BrO	3 0
CH_2O	-26.0	H_2SO_4	-176	$ClNO_2$	3.0	BrNO	19.7
COOH	-53±2	CS	67±2	ClONO	1 3	BrONO	25±7
HCOOH	-90.5	CS_2	28.0	$ClONO_2$	5.5	$BrNO_2$	17±2
CH_3O	4±1	CS_2OH	26.4	FCl	-12.1	$BrONO_2$	12±5
CH_3O_2	4±2	CH_3S	33±2	CCl_2	57±5	BrCl	3.5
CH_2OH	-6.2	CH_3SO_2	-57	CCl_3	18±1	CH_2Br	40±2
CH_3OH	-48.2			CCl_4	-22.9	$CHBr_3$	6±2

Gas Phase Enthalpy Data (Continued)

SPECIES	$\Delta H_f(298)$ (Kcal/mol)	SPECIES	$\Delta H_f(298)$ (Kcal/mol)	SPECIES	$\Delta H_f(298)$ (Kcal/mol)	SPECIES	$\Delta H_f(298)$ (Kcal/mol)
$CHBr_2$	45±2	CH_3CH_2Br	-14.8	I_2	14.92	IO	41.1
CBr_3	48±2	CH_2CH_2Br	32±2	HI	6.3	INO	29.0
CH_2Br_2	-2.6±2	CH_3CHBr	30±2	CH_3I	3.5	INO_2	14.4
CH_3Br	-8.5	I	25.52	CH_2I	52±2		

APPENDIX 2. PROFILES

The species profiles presented in these figures were generated by the LLNL 2-D model of the troposphere and stratosphere. The tropopause mixing ratios of key trace gases are as follows: total chlorine 3.4 ppb, methane 1.69 ppm, nitrous oxide 307 ppb, carbon dioxide 350 ppm, and total bromine 0. The kinetic parameters used were consistent, where possible, with the Evaluation Number 9 recommendations of the NASA Panel for Data Evaluation (JPL 90-1). The model was constrained by observational fields for temperature, ozone, methane, nitrous oxide, and water vapor. These fields of satellite data were obtained from the UARS program (Robert Seals, Jr., private communication, 1990) and incorporated into the model to produce distributions for other infrequently observed species. This version of the model did not incorporate the heterogeneous reaction of N_2O_5 with H_2O to form nitric acid, and the predicted nitric acid profiles are smaller than the available satellite distributions indicate.

The rate constants shown for various photolytic processes are derived from a version of the LLNL 2-D model developed for the 91/92 UNEP report and incorporated the temperature dependence of the absorption cross sections for all appropriate species in the calculation of both atmospheric transmission and absorption. This version of the model represents a 1990 ambient atmosphere. Further details on this model will appear in the UNEP report.

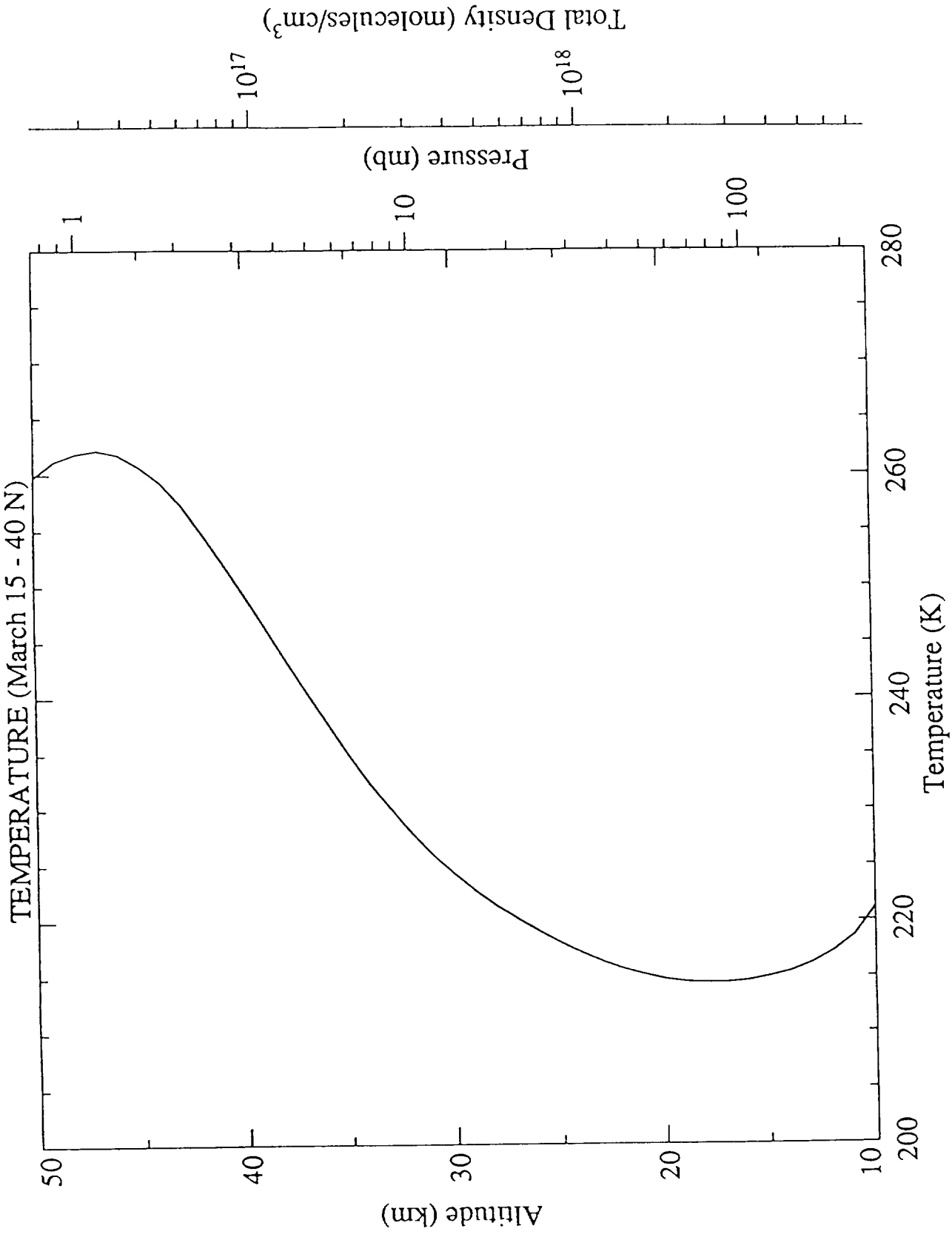
TEMPERATURE (March 15 - 40 N)
Altitude (km)
50
40
30
20
10
Temperature (K)
200
220
240
260
280
Pressure (mb)
1
10
100
Total Density (molecules/cm^3)
10^{17}
10^{18}

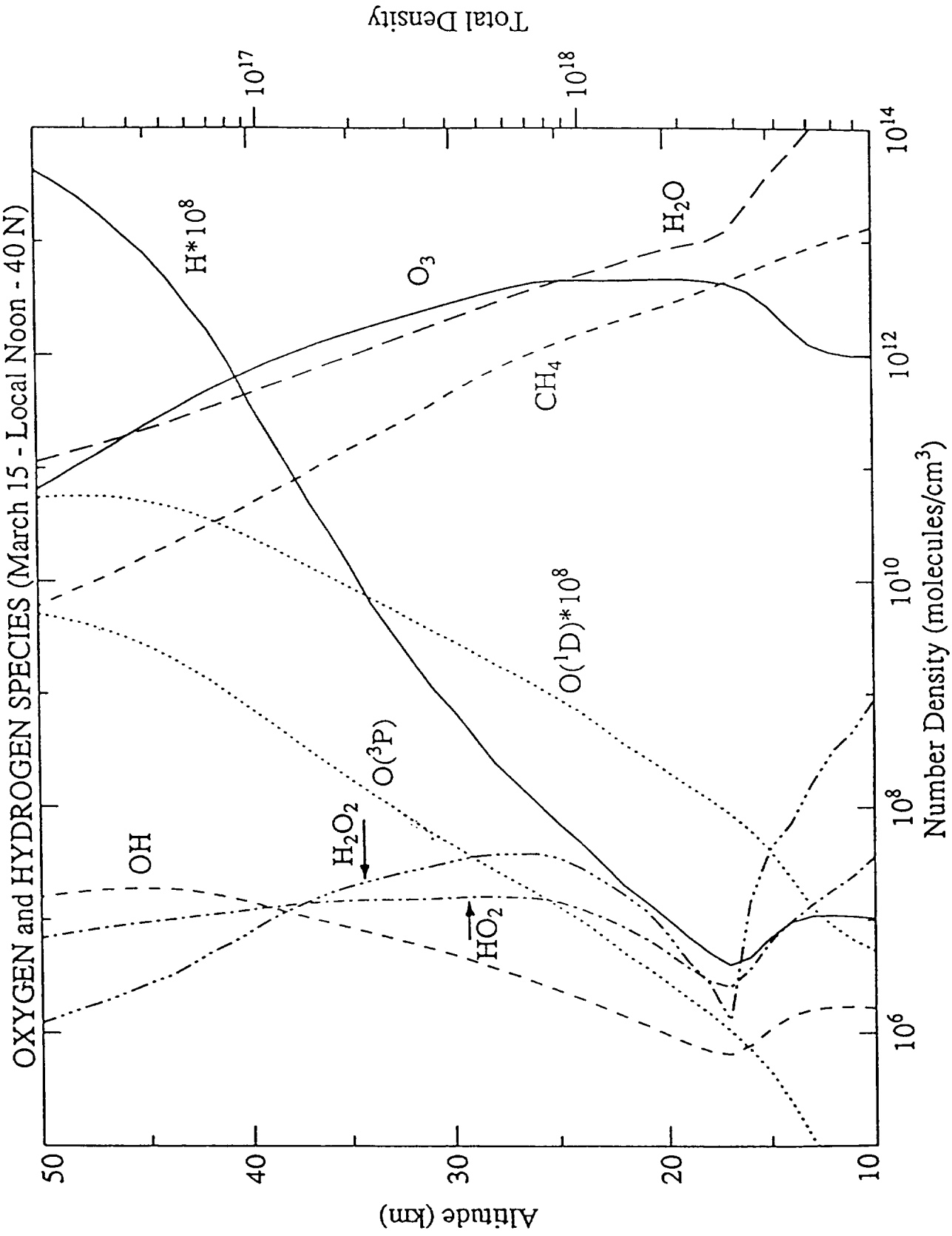
OXYGEN and HYDROGEN SPECIES (March 15 - Local Noon - 40 N)
Total Density
Altitude (km)
Number Density (molecules/cm^3)
H*10^8
O$_3$
H$_2$O
CH$_4$
O(^{1}D)*10^8
O(^{3}P)
OH
H$_2$O$_2$
HO$_2$
50
40
30
20
10
10^{17}
10^{18}
10^{14}
10^{12}
10^{10}
10^8
10^6

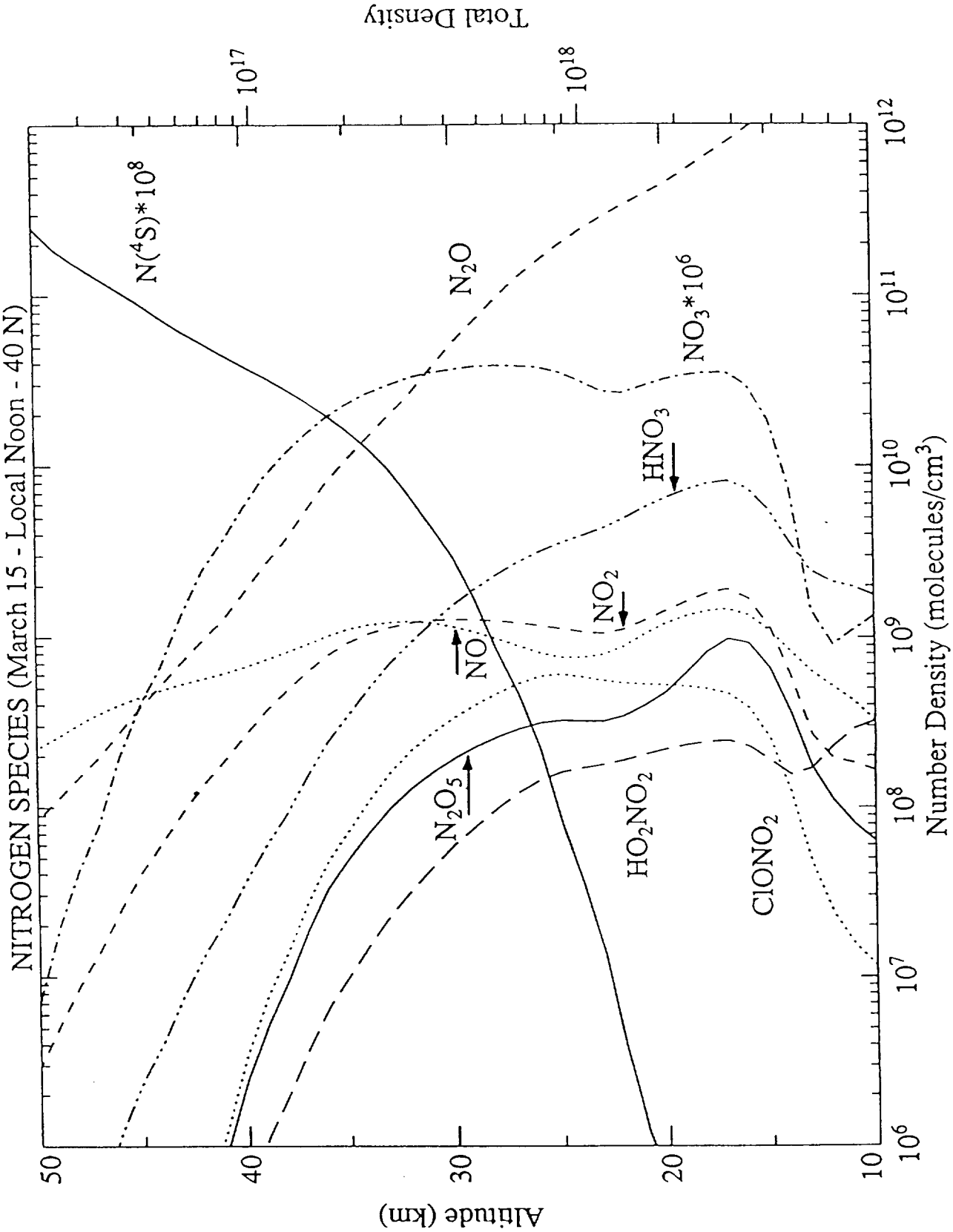
NITROGEN SPECIES (March 15 - Local Noon - 40 N)
Altitude (km)
Number Density (molecules/cm^3)
Total Density
$N(^4S)*10^8$
N_2O
NO_3*10^6
HNO_3
NO_2
NO
N_2O_5
HO_2NO_2
$ClONO_2$
50
40
30
20
10
10^6
10^7
10^8
10^9
10^{10}
10^{11}
10^{12}
10^{17}
10^{18}

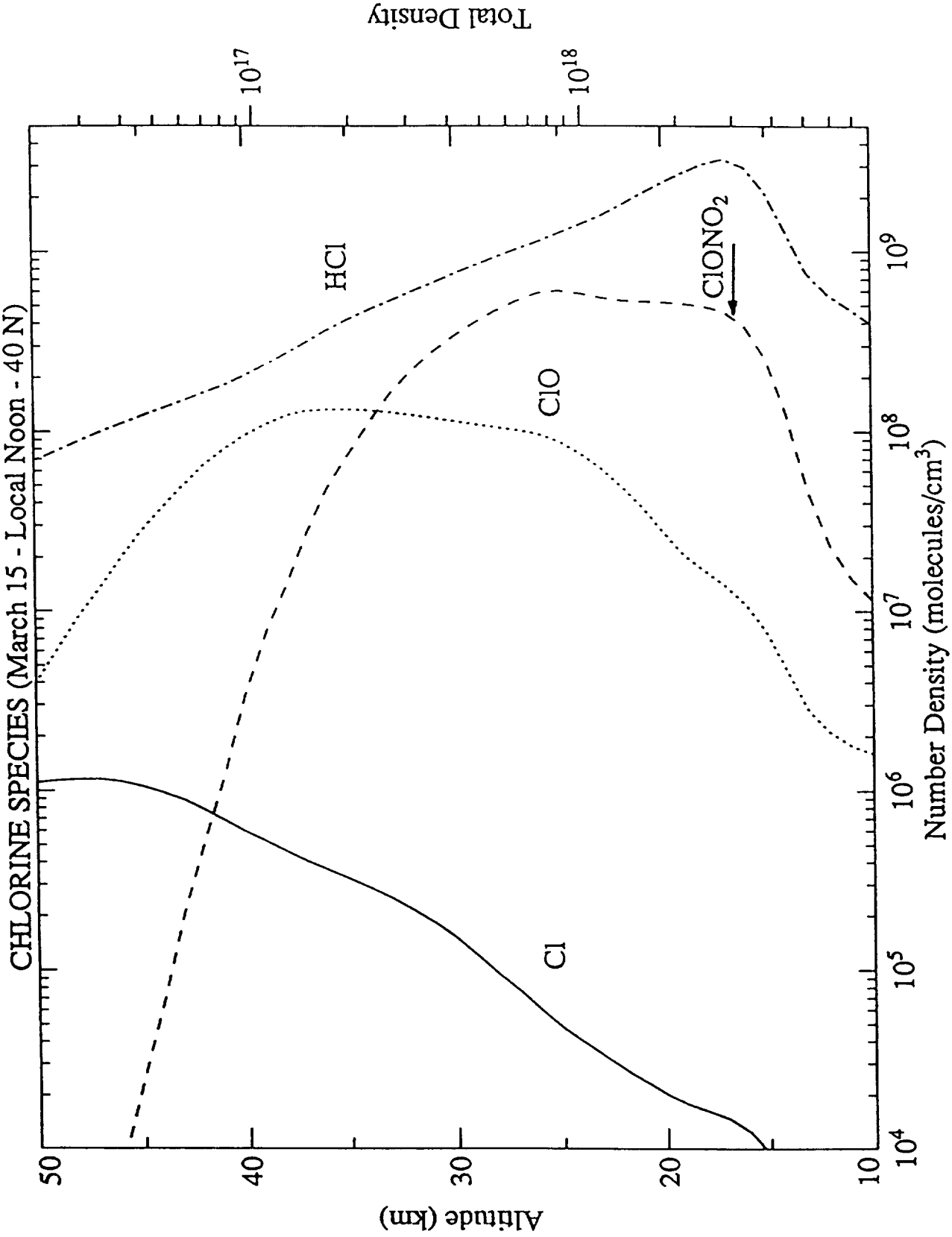
CHLORINE SPECIES (March 15 - Local Noon - 40 N)
Altitude (km)
Number Density (molecules/cm^3)
Total Density
HCl
ClONO$_2$
ClO
Cl
50
40
30
20
10
10^4
10^5
10^6
10^7
10^8
10^9
10^{17}
10^{18}

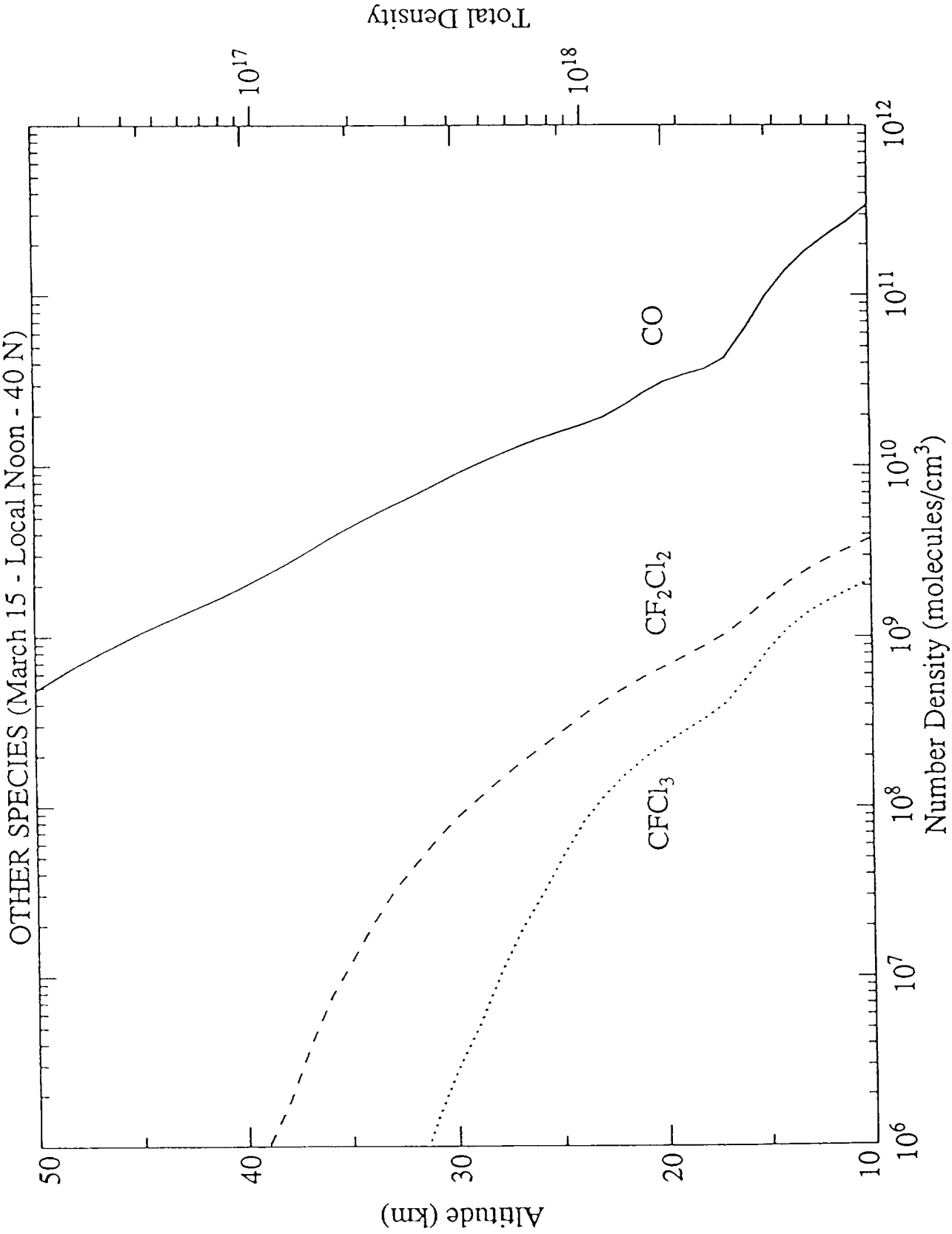
OTHER SPECIES (March 15 - Local Noon - 40 N)
Altitude (km)
Number Density (molecules/cm^3)
Total Density
CO
CF_2Cl_2
$CFCl_3$
50
40
30
20
10
10^{17}
10^{18}
10^{12}
10^{11}
10^{10}
10^{9}
10^{8}
10^{7}
10^{6}

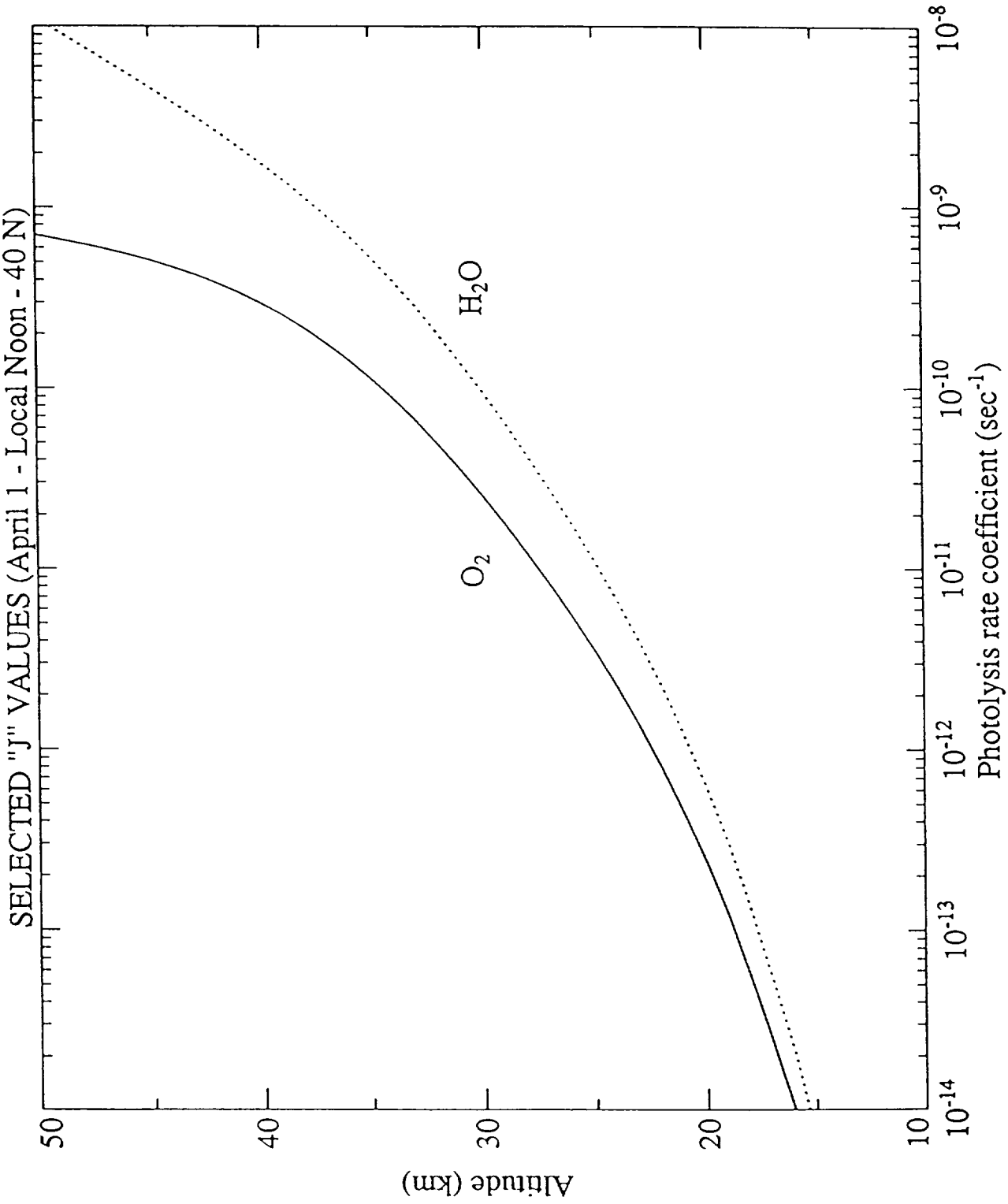
SELECTED "J" VALUES (April 1 - Local Noon - 40 N)
H_2O
O_2
Altitude (km)
50
40
30
20
10
10^{-14}
10^{-13}
10^{-12}
10^{-11}
10^{-10}
10^{-9}
10^{-8}
Photolysis rate coefficient (sec^{-1})

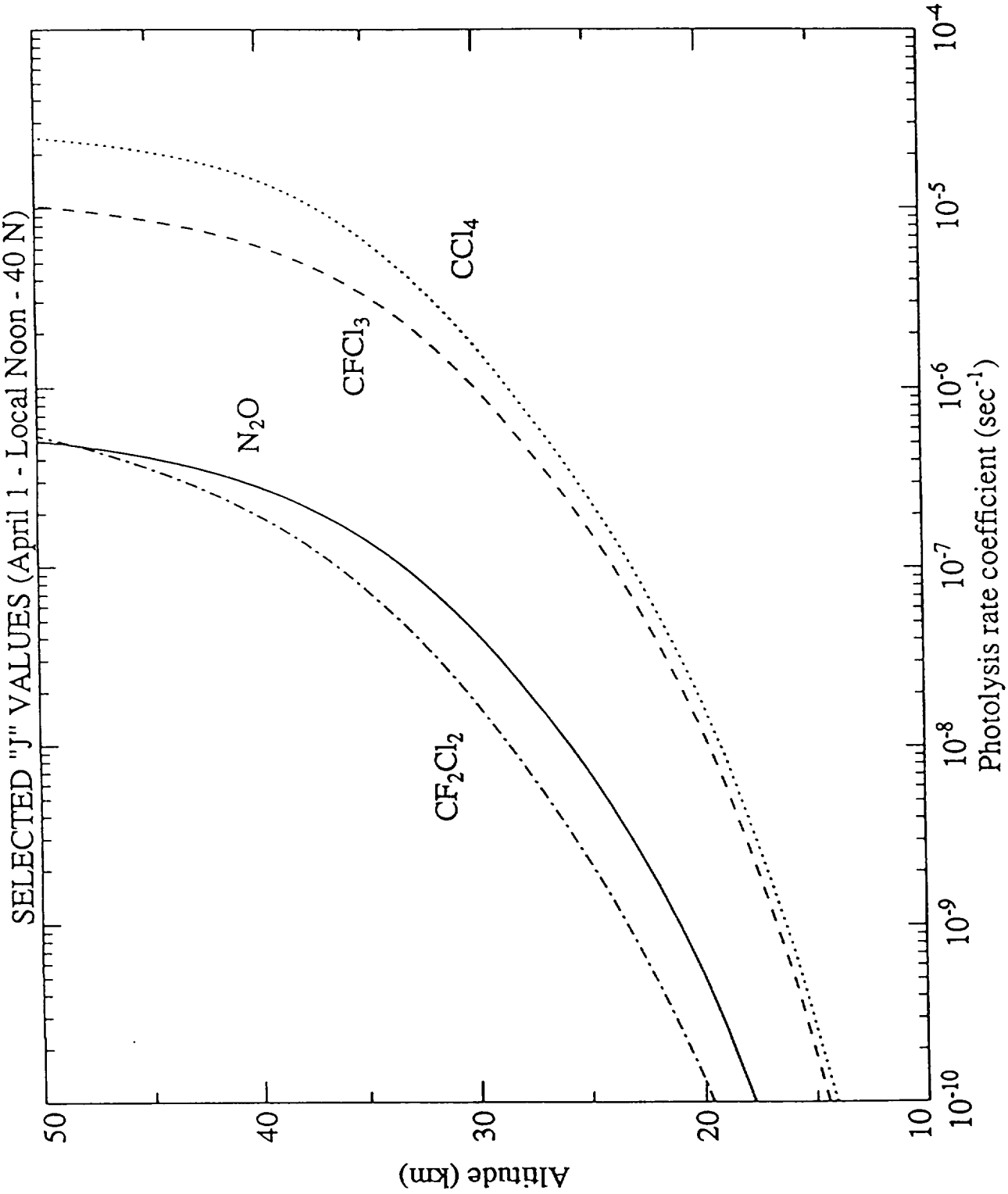
SELECTED "J" VALUES (April 1 - Local Noon - 40 N)
N_2O
$CFCl_3$
CCl_4
CF_2Cl_2
Altitude (km)
50
40
30
20
10
10^{-10}
10^{-9}
10^{-8}
10^{-7}
10^{-6}
10^{-5}
10^{-4}
Photolysis rate coefficient (sec^{-1})

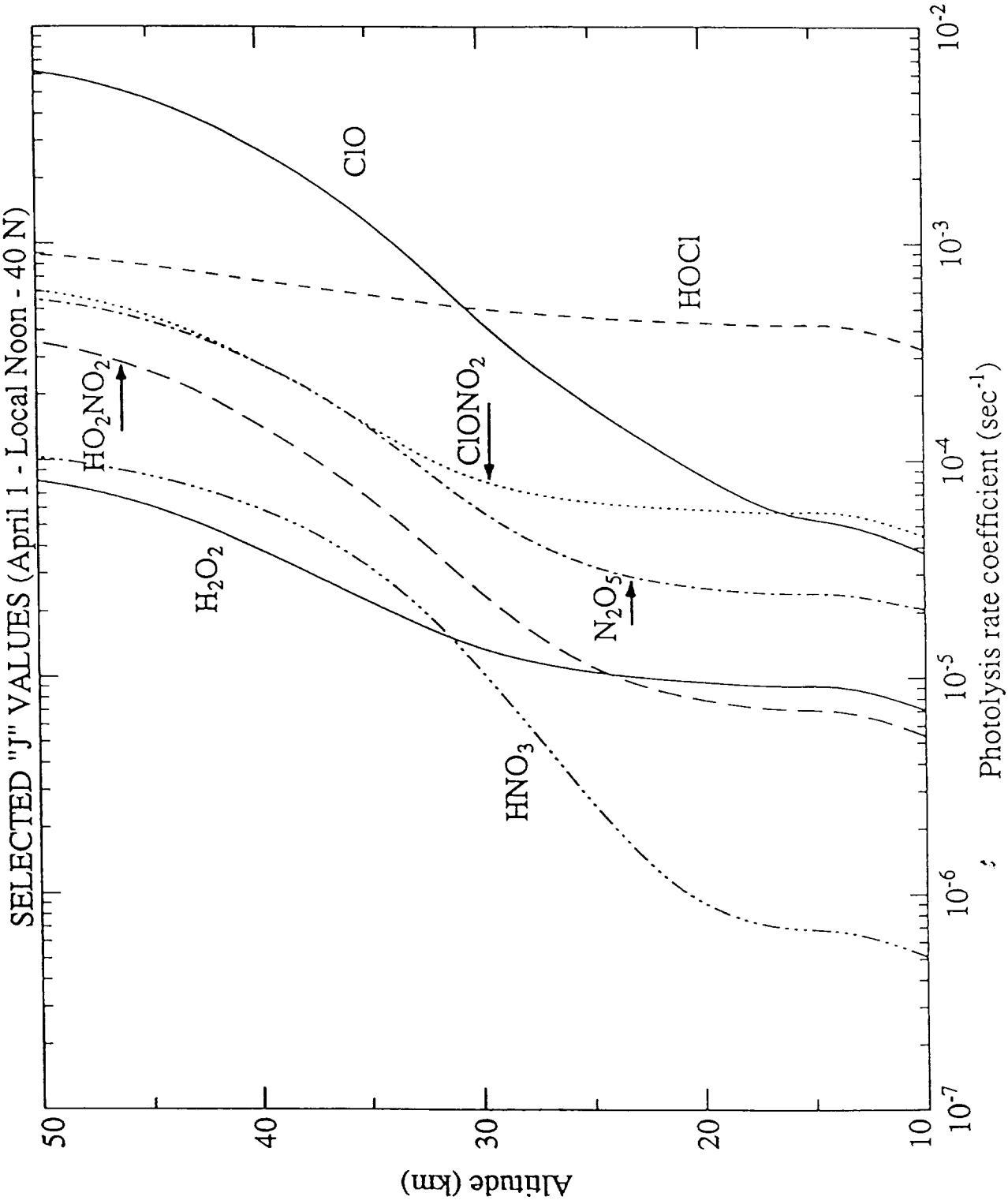
SELECTED "J" VALUES (April 1 - Local Noon - 40 N)
ClO
HOCl
HO_2NO_2
$ClONO_2$
H_2O_2
N_2O_5
HNO_3
Altitude (km)
50
40
30
20
10
10^{-2}
10^{-3}
10^{-4}
10^{-5}
10^{-6}
10^{-7}
Photolysis rate coefficient (sec^{-1})

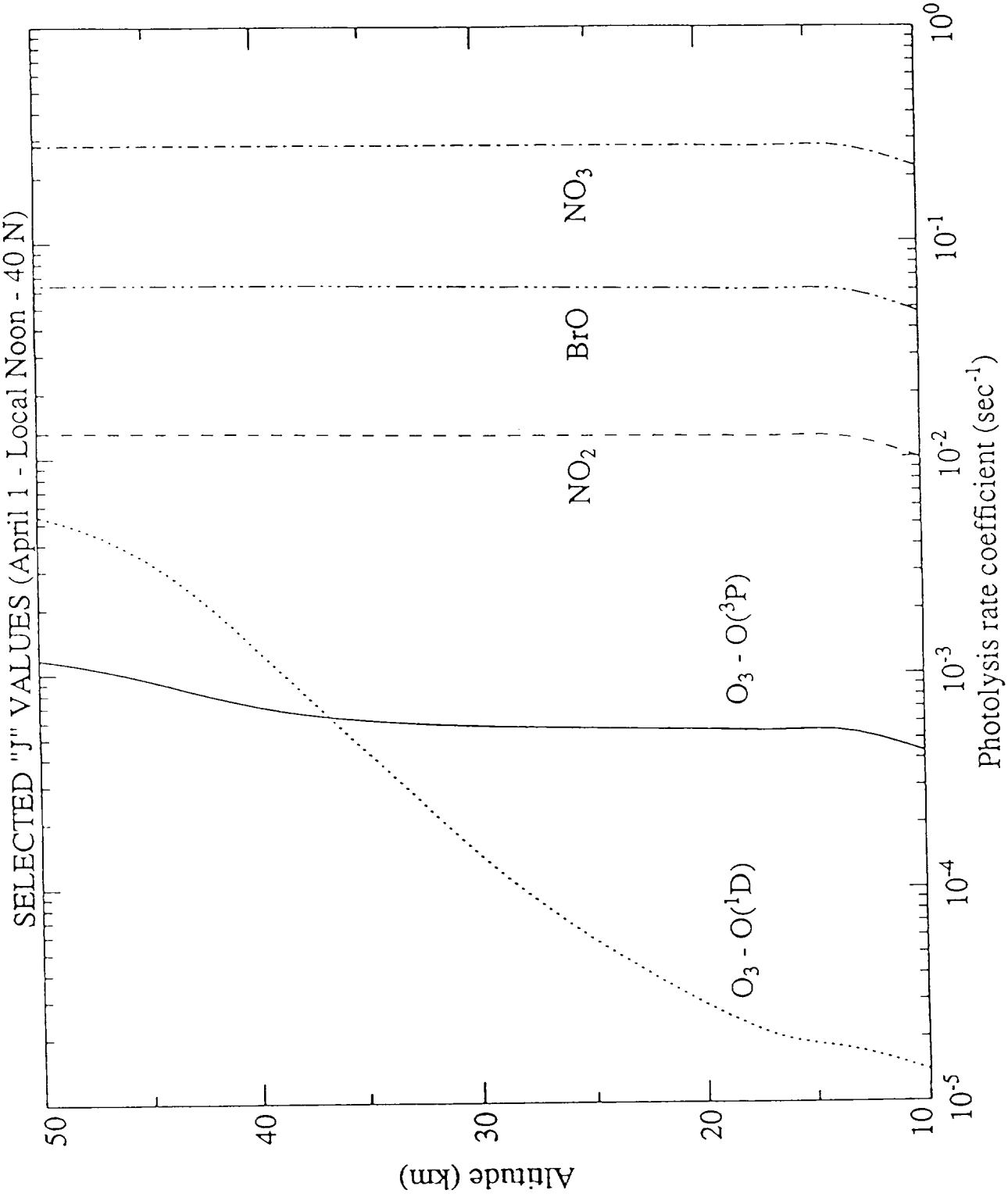
SELECTED "J" VALUES (April 1 - Local Noon - 40 N)
Altitude (km)
50
40
30
20
10
10^{0}
10^{-1}
10^{-2}
10^{-3}
10^{-4}
10^{-5}
Photolysis rate coefficient (sec^{-1})
NO_3
BrO
NO_2
O_3 - $O(^3P)$
O_3 - $O(^1D)$

SECTION G

CONTRIBUTORS AND REVIEWERS

SECTION B: Scientific Assessment of Ozone Depletion: 1991

CO-CHAIRS

Daniel L. Albritton	National Oceanic and Atmospheric Administration	USA
Robert T. Watson	National Aeronautics and Space Administration	USA

OZONE PEER-REVIEW MEETING
Les Diablerets, Switzerland
October 14-18, 1991

Daniel L. Albritton	NOAA Aeronomy Laboratory	USA
Roger Atkinson	Statewide Air Pollution Research Center	USA
Lane Bishop	Allied Signal Inc.	USA
Rumen D. Bojkov	World Meteorological Organization	Switzerland
William H. Brune	Pennsylvania State University	USA
Bruce Callander	Meteorological Office, IPCC Secretariat	UK
Daniel Cariolle	Meteorologie Nationale EERM/CNRM	France
Marie-Lise Chanin	Service d'Aèronomie du CNRS	France
R. Anthony Cox	Natural Environment Research Council	UK
Vitali Fioletov	Central Aerological Observatory	USSR
Paul J. Fraser	CSIRO	Australia
Sophie Godin	Service d'Aèronomie du CNRS	France
Robert S. Harwood	University of Edinburgh	UK
Abdel Moneim Ibrahim	Egyptian Meteorological Authority	Egypt
Ivar S. A. Isaksen	University of Oslo	Norway
Charles H. Jackman	NASA Goddard Space Flight Center	USA
Evgeny A. Jadin	Central Aerological Observatory	USSR
Colin Johnson	Harwell Laboratory	UK
Igor L. Karol	Main Geophysical Observatory	USSR
Jack Kaye	NASA Headquarters	USA
James B. Kerr	Atmospheric Environment Service	Canada
Dieter Kley	Kernforschungsanlage Jülich GmbH	Germany
Malcolm K. W. Ko	Atmospheric & Environmental Research, Inc.	USA
Michael J. Kurylo	National Institute for Standards and Technology and NASA Headquarters	USA
Jane Leggett	Environmental Protection Agency	USA
Conway B. Leovy	University of Washington	USA
Pak Sum Low	Ozone Secretariat, UNEP Headquarters	Kenya
Yoshihiro Makide	University of Tokyo	Japan
W. Andrew Matthews	DSIR Physical Sciences	New Zealand
Mack McFarland	E.I. DuPont de Nemours and Co., Inc.	USA

PRECEDING PAGE BLANK NOT FILMED

126 INTENTIONALLY BLANK

Richard L. McKenzie	DSIR Physical Sciences	New Zealand
Gèrard Mègie	Service d'Aèronomie du CNRS	France
P. Muthusubramanian	Madurari Kamaraj University	India
Michael Oppenheimer	Environmental Defense Fund	USA
D. C. Parashar	National Physical Laboratory	India
Stuart A. Penkett	University of East Anglia	UK
Lamont R. Poole	NASA Langley Research Center	USA
Michael J. Prather	University of California, Irvine	USA
Margarita Prendez	Universidad de Chile	Chile
Lian Xiong Qiu	Academica Sinica, Beijing	Peoples Republic of China
V. Ramaswamy	Princeton University	USA
A. R. Ravishankara	NOAA Aeronomy Laboratory	USA
Joan Rosenfield	NASA Goddard Space Flight Center	USA
Nelson Antonio Sabogal	Instituto Colombiano de Hidrologià	Colombia
Eugenio Sanhueza	Instituto Venezolano de Investigaciones Cientificas	Venezuela
Howard Sidebottom	University College Dublin	Ireland
Susan Solomon	NOAA Aeronomy Laboratory	USA
Johannes Staehelin	Atmosphärenphysik ETH	Switzerland
Richard S. Stolarski	NASA Goddard Space Flight Center	USA
Bhoganahalli Subbaraya	Physical Research Laboratory	India
Guido Visconti	Università degli Studi, L'Aquila	Italy
Andreas Wahner	KFA Jülich	Germany
Wei-Chyung Wang	State University of New York at Albany	USA
David A. Warrilow	Department of the Environment	UK
Robert T. Watson	NASA Headquarters	USA
Tom Wigley	University of East Anglia	UK
Donald J. Wuebbles	Lawrence Livermore National Laboratory	USA
Ahmad Zand	University of Teheran	Iran
Rudi J. Zander	University of Liege	Belgium
Joseph M. Zawodny	NASA Langley Research Center	USA
Christos Zerefos	Aristotelian University of Thessaloniki	Greece
Ya-Hui Zhuang	Asian Institute of Technology	Thailand
Sergei Zvenigorodsky	USSR Academy of Sciences	USSR

CHAPTER 1 - SOURCE GASES: CONCENTRATIONS, EMISSIONS, AND TRENDS

Chapter Coordinator

Paul Fraser	CSIRO	Australia

Lead Authors

Robert Harriss	University of New Hampshire	USA
Yoshihiro Makide	University of Tokyo	Japan
Stuart Penkett	University of East Anglia	UK
Eugenio Sanhueza	Instituto Venezolano de Investigaciones Cientificas	Venezuela

Contributors

Fred N. Alyea	Georgia Institute of Technology	USA
Don Blake	University of California, Irvine	USA
Derek M. Cunnold	Georgia Institute of Technology	USA
James W. Elkins	NOAA/CMDL	USA
Michio Hirota	Japan Meteorological Agency	Japan
Ronald G. Prinn	Massachusetts Institute of Technology	USA

Rei A. Rasmussen	Oregon Graduate Institute for Science & Technology	USA
F. Sherwood Rowland	University of California, Irvine	USA
Toru Sasaki	Meteorological Research Institute	Japan
H. Scheel	Fraünhofer Institute for Atmos. Env. Research	Germany
Wolfgang Seiller	Fraünhofer Institute for Atmos. Env. Research	Germany
P. Simmonds	University of Bristol	UK
Paul Steele	CSIRO	Australia
Ray F. Weiss	Scripps Institution of Oceanography	USA

Mail Reviewers

R. Anthony Cox	Natural Environment Research Council	UK
Jack Kaye	NASA	USA
Volker Kirchhoff	Atmospheric and Space Science, INPE	Brazil
Henning Rodhe	University of Stockholm	Sweden

CHAPTER 2 - OZONE AND TEMPERATURE TRENDS

Chapter Coordinator

Richard S. Stolarski	NASA Goddard Space Flight Center	USA

Lead Authors

Lane Bishop	Allied Signal Inc.	USA
Rumen D. Bojkov	World Meteorological Organization	Switzerland
Marie-Lise Chanin	Service d'Aèronomie du CNRS	France
Vitali Fioletov	Central Aerological Observatory	USSR
Sophie Godin	Service d'Aèronomie du CNRS	France
Volker Kirchhoff	Atmospheric and Space Science, INPE	Brazil
Joseph M. Zawodny	NASA Langley Research Center	USA
Christos Zerefos	Aristotelian University of Thessaloniki	Greece

Contributors

William Chu	NASA Langley Research Center	USA
John DeLuisi	NOAA/CMDL	USA
Anne Hansson	Atmospheric Environment Service	Canada
James Kerr	Atmospheric Environment Service	Canada
Evgeny Lysenko	Central Aerological Observatory	USSR
M. Patrick McCormick	NASA Langley Research Center	USA
Paul Newman	NASA Goddard Space Flight Center	USA
Margarita Prendez	Universidad de Chile	Chile
Johannes Staehelin	Atmosphärenphysik ETH	Switzerland
Bhoganahalli Subbaraya	Physical Research Laboratory	India

Mail Reviewers

Neil Harris	Department of the Environment	UK
William Hill	University of Wisconsin, Madison	USA
A. J. Miller	NOAA National Meteorological Center	USA

CHAPTER 3 - HETEROGENEOUS PROCESSES: LABORATORY, FIELD, AND MODELING STUDIES

Chapter Coordinator

Lamont R. Poole	NASA Langley Research Center	USA

Lead Authors

Rod L. Jones	University of Cambridge	UK
Michael J. Kurylo	National Institute of Standards and Technology and NASA Headquarters	USA
Andreas Wahner	KFA Jülich	Germany

Contributors

Jack G. Calvert	National Center for Atmospheric Research	USA
A. Fried	National Center for Atmospheric Research	USA
David J. Hofmann	NOAA/CMDL	USA
Leon F. Keyser	Jet Propulsion Laboratory	USA
Charles E. Kolb	Aerodyne Research, Inc.	USA
M.-T. Leu	Jet Propulsion Laboratory	USA
Mario J. Molina	Massachusetts Institute of Technology	USA
M. C. Pitts	Hughes STX	USA
A. R. Ravishankara	NOAA Aeronomy Laboratory	USA
L. W. Thomason	NASA Langley Research Center	USA
Margaret A. Tolbert	SRI, International	USA
Doug R. Worsnop	Aerodyne Research, Inc.	USA

Mail Reviewers

Robert F. Hampson	National Institute of Standards and Technology	USA
O. Brian Toon	NASA Ames Research Center	USA
Steve Wofsy	Harvard University	USA

CHAPTER 4 - STRATOSPHERIC PROCESSES: OBSERVATIONS AND INTERPRETATION

Chapter Coordinator

William H. Brune	Pennsylvania State University	USA

Lead Authors

Guy Brasseur	National Center for Atmospheric Research	USA
R. Anthony Cox	Natural Environment Research Council	UK
Anne Douglass	NASA Goddard Space Flight Center	USA
W. Andrew Matthews	DSIR Physical Sciences	New Zealand
Alan O'Neill	Robert Hooke Institute	UK
Margarita Prendez	Universidad de Chile	Chile
Jose M. Rodriguez	Atmospheric & Environmental Research, Inc.	USA
Bhoganahalli Subbaraya	Physical Research Laboratory	India
Richard Turco	University of California, Los Angeles	USA
Rudi J. Zander	University of Liege	Belgium
Xiuji Zhou	State Meteorological Administration	Peoples Republic of China

Contributors

J. Austin	Meteorological Office	UK
Malcolm K. W. Ko	Atmospheric & Environmental Research, Inc.	USA
Michael J. Prather	University of California, Irvine	USA
A. R. Ravishankara	NOAA Aeronomy Laboratory	USA
Mark R. Schoeberl	NASA Goddard Space Flight Center	USA
Susan Solomon	NOAA Aeronomy Laboratory	USA
Adrian F. Tuck	NOAA Aeronomy Laboratory	USA

Mail Reviewers

Daniel Cariolle	Meteorologie Nationale EERM/CNRM	France
Mack McFarland	E.I. DuPont de Nemours and Co., Inc.	USA
John A. Pyle	University of Cambridge	UK
Christos Zerefos	Aristotelian University of Thessaloniki	Greece

CHAPTER 5 - TROPOSPHERIC PROCESSES: OBSERVATIONS AND INTERPRETATION

Chapter Coordinator

Ivar S. A. Isaksen	University of Oslo	Norway

Lead Authors

Roger Atkinson	Statewide Air Pollution Research Center	USA
J. A. Fuglestvedt	University of Oslo	Norway
Colin Johnson	Harwell Laboratory	UK
Yuan-Pern Lee	National Tsing Hua University, Taiwan	Republic of China
Jos. Lelieveld	Max-Planck Institute for Chemistry, Mainz	Germany
Howard Sidebottom	University of Dublin	Ireland
Anne Thompson	NASA Goddard Space Flight Center	USA

Contributors

T. Berntsen	University of Oslo	Norway
William H. Brune	Pennsylvania State University	USA
Jack Kaye	NASA Headquarters	USA
Michael Oppenheimer	Environmental Defense Fund	USA

Mail Reviewers

Paul J. Crutzen	Max-Planck Institute for Chemistry, Mainz	Germany
Volker Kirchhoff	Atmospheric and Space Science - INPE	Brazil
Stuart Penkett	University of East Anglia	UK

CHAPTER 6 - OZONE DEPLETION AND CHLORINE LOADING POTENTIALS

Chapter Coordinator

Susan Solomon	NOAA Aeronomy Laboratory	USA

Lead Authors

John A. Pyle	University of Cambridge	UK
Donald J. Wuebbles	Lawrence Livermore National Laboratory	USA
Sergei Zvenigorodsky	USSR Academy of Sciences	USSR

Contributors

Peter Connell	Lawrence Livermore National Laboratory	USA
Donald A. Fisher	E.I. DuPont de Nemours and Co., Inc.	USA
Malcolm K. W. Ko	Atmospheric & Environmental Research, Inc.	USA
Frode Stordal	Norwegian Institute for Air Research	Norway
Debra Weisenstein	Atmospheric & Environmental Research, Inc.	USA

Mail Reviewers

Guy Brasseur	National Center for Atmospheric Research	USA
Michael J. Prather	University of California, Irvine	USA

CHAPTER 7 - RADIATIVE FORCING OF CLIMATE

Chapter Coordinator

V. Ramaswamy	Princeton University	USA

Lead Authors

Conway Leovy	University of Washington	USA
Henning Rodhe	University of Stockholm	Sweden
Keith Shine	University of Reading	UK
Wei-Chyung Wang	State University of New York at Albany	USA
Donald J. Wuebbles	Lawrence Livermore National Laboratory	USA

Contributors

M. Ding	State University of New York at Albany	USA
Jae A. Edmonds	Department of Energy	USA
Paul Fraser	CSIRO	Australia
Keith Grant	Lawrence Livermore National Laboratory	USA
Colin Johnson	Harwell Laboratory	UK
D. Lashof	National Resources Defense Council	USA
Jane Leggett	Environmental Protection Agency	USA
Jos. Lelieveld	Max-Planck Institute for Chemistry, Mainz	Germany
M. Patrick McCormick	NASA Langley Research Center	USA
Abraham Oort	NOAA Geophysical Fluid Dynamics Laboratory	USA
M. D. Schwartzkopf	NOAA Geophysical Fluid Dynamics Laboratory	USA
A. Sutera	University of Camerino	Italy
David A. Warrilow	Department of the Environment	UK
Tom Wigley	Meteorological Office	UK

Mail Reviewers

Jeffrey Kiehl	National Center for Atmospheric Research	USA
Joan Rosenfield	NASA Goddard Space Flight Center	USA

CHAPTER 8 - FUTURE CHLORINE- BROMINE-LOADING AND OZONE DEPLETION

Chapter Coordinator

Michael J. Prather	University of California, Irvine	USA

Lead Authors

Abdel Moneim Ibrahim	Egyptian Meteorological Authority	Egypt
Toru Sasaki	Meteorological Research Institute	Japan
Frode Stordal	Norwegian Institute for Air Research	Norway
Guido Visconti	Università degli Studi, L'Aquila	Italy

Model Contributors

Guy Brasseur	National Center for Atmospheric Research	USA
Christoph H. Brühl	Max-Planck Institute für Chemie	Germany
Donald A. Fisher	E.I. DuPont de Nemours and Co., Inc.	USA
Ivar S. A. Isaksen	University of Oslo	Norway

Charles H. Jackman	NASA Goddard Space Flight Center	USA
Evgeny A. Jadin	Central Aerological Observatory	USSR
Malcolm K. W. Ko	Atmospheric & Environmental Research, Inc.	USA
Toru Sasaki	Meteorological Research Institute	Japan
Susan Solomon	NOAA Aeronomy Laboratory	USA
Guido Visconti	Università degli Studi, L'Aquila	Italy
Donald J. Wuebbles	Lawrence Livermore National Laboratory	USA
Sergei Zvenigorodsky	USSR Academy of Sciences	USSR

Mail Reviewers

Daniel Cariolle	Meteorologie Nationale EERM/CNRM	France
Paul Fraser	CSIRO	Australia
Charles H. Jackman	NASA Goddard Space Flight Center	USA
Mack McFarland	E.I. DuPont de Nemours and Co., Inc.	USA
Susan Solomon	NOAA Aeronomy Laboratory	USA

CHAPTER 9 - PREDICTED AIRCRAFT EFFECTS ON STRATOSPHERIC OZONE

Chapter Coordinator

Malcolm K. W. Ko	Atmospheric & Environmental Research, Inc.	USA

Lead Authors

Evgeny A. Jadin	Central Aerological Observatory	USSR
Dieter Kley	Kernforschungsanlage Jülich GmbH	Germany
Steve Wofsy	Harvard University	USA

Contributors

Colin Johnson	Harwell Laboratory	UK
Michael J. Prather	University of California, Irvine	USA
D. Weisenstein	Atmospheric & Environmental Research, Inc.	USA
Donald J. Wuebbles	Lawrence Livermore National Laboratory	USA

Mail Reviewers

W. Andrew Matthews	DSIR Physical Sciences	New Zealand
K. Stamnes	University of Alaska	USA
Frode Stordal	Norwegian Institute for Air Research	Norway

CHAPTER 10 - PREDICTED ROCKET AND SHUTTLE EFFECTS ON STRATOSPHERIC OZONE

Chapter Coordinator

Charles H. Jackman	NASA Goddard Space Flight Center	USA

Lead Authors

Robert S. Harwood	University of Edinburgh	UK
Igor L. Karol	Main Geophysical Laboratory	USSR
Lian Xiong Qiu	Academia Sinica	Peoples Republic of China

Contributors

Michael J. Prather	University of California, Irvine	USA
John A. Pyle	Cambridge University	UK

Mail Reviewers

Ivar S.A. Isaksen	Univeristy of Oslo	Norway
Harold S. Johnston	Univeristy of California, Berkeley	USA
Michael Oppenheimer	Environmental Defense Fund	USA
Donald J. Wuebbles	Lawrence Livermore National Laboratory	USA

CHAPTER 11 - ULTRAVIOLET RADIATION CHANGES

Chapter Coordinator

Richard L. McKenzie	DSIR Physical Sciences	New Zealand

Lead Authors

V. Filyushkin	Central Aerological Observatory	USSR
John E. Frederick	University of Illinois, Chicago	USA
Mohammad Ilyas	University of Science of Malaysia	Malaysia

Contributors

M. Blumthaler	University of Innsbruck	Austria
Sasha Madronich	National Center for Atmospheric Research	USA
P. Muthusubramanian	Madurai Kamaraj University	India
Colin E. Roy	Australian Radiation Laboratory	Australia
K. Stamnes	University of Alaska	USA
Andreas Wahner	KFA Jülich	Germany

Mail Reviewers

Vyacheslav Khattatov	Central Aerological Observatory	USSR
Michael J. Prather	University of California, Irvine	USA
Frode Stordal	Norwegian Institute for Air Research	Norway

EDITORS

Daniel A. Albritton	Co-Chair - NOAA	USA
Robert T. Watson	Co-Chair - NASA	USA
Susan Solomon	Preprint - NOAA Aeronomy Laboratory	USA
Robert F. Hampson	National Institute of Standards & Technology	USA
Flo Ormond	NASA	USA

CONFERENCE COORDINATION AND DOCUMENTATION

Rumen D. Bojkov	WMO	Switzerland
Marie-Christine Charriere	WMO	France
Flo Ormond	NASA	USA
N. Plock	NOAA	USA
Shelagh Varney	Meteorological Office	UK
Jeanne Waters	NOAA	USA

SECTION C: Methyl Bromide And The Ozone Layer: A Summary Of Current Understanding

AUTHORS

Daniel L. Albritton	NOAA Aeronomy Laboratory	USA
Robert T. Watson	NASA Headquarters	USA
Tom Duafala	TriCal	USA
Ivar Isaksen	University of Oslo	Norway
Malcolm K. W. Ko	Atmospheric & Environmental Research Inc.	USA
Michael J. Kurylo	National Institute of Standards and Technology and NASA Headquarters	USA
Pak Sum Low	United Nations Environment Programme	Kenya
Mack McFarland	E.I. DuPont de Nemours and Co. Inc.	USA
Stuart A. Penkett	University of East Anglia	UK
F. S. Rowland	University of California, Irvine	USA
Eugenio Sanhueza	Instituto Venezolano de Investigaciones Cientificas	Venezuela
Susan Solomon	NOAA Aeronomy Laboratory	USA
Nien-Dak Sze	Atmospheric & Environmental Research Inc.	USA
David Warrilow	Department of the Environment	UK

WORKSHOP PARTICIPANTS WHO REVIEWED THE REPORT

James G. Anderson	Harvard University	USA
Bruno Carli	IROF-CNR	Italy
William B. DeMore	Jet Propulsion Laboratory	USA
Robert F. Hampson	National Institute of Standards and Technology	USA
Robert C. Harriss	University of New Hampshire	USA
Leroy E. Heidt	National Center for Atmospheric Research	USA
Jack Kaye	NASA Headquarters	USA
Andrew Matthews	Department of Scientific and Industrial Research	New Zealand
Pauline Midgely	ICI	Germany
Mario J. Molina	Massachusetts Institute of Technology	USA
Ira Nolt	NASA/Langley Research Center	USA
J. H. Park	NASA/Langley Research Center	USA
Walter Pollock	National Center for Atmospheric Research	USA
Michael Prather	University of California, Irvine	USA
A. R. Ravishankara	NOAA Aeronomy Laboratory	USA
Daniel Reible	Louisiana State University	USA
Jose M. Rodriguez	Atmospheric & Environmental Research Inc.	USA
Tsuneo Sakurai	Teijin Chemicals, Ltd.	Japan
Hanwant B. Singh	NASA Ames Research Center	USA
D. W. Toohey	University of California, Irvine	USA
Wesley A. Traub	Smithsonian Institution Astrophysical Observatory	USA
Steven C. Wofsy	Harvard University	USA
Yuk L. Yung	California Institute of Technology	USA

NON-WORKSHOP PARTICIPANTS WHO REVIEWED THE REPORT

Ralph J. Cicerone	University of California, Irvine	USA
R. A. Cox	Natural Environment Research Council	UK
Paul Crutzen	Max-Planck-Institute for Chemistry	Germany
Mohammad Ilyas	University of Science of Malaysia	Malaysia
P. Liss	University of East Anglia	UK
Richard McKenzie	Department of Scientific and Industrial Research	New Zealand
John A. Pyle	University of Cambridge	UK
Ulrich Schmidt	KFA Julich	Germany
Donald Weubbles	Lawrence Livermore National Laboratory	USA

OTHER WORKSHOP PARTICIPANTS AND OBSERVERS

Catherine Adams	Grocery Manufacturers of America, Inc.	USA
David Bach	Ethyl Corporation	USA
Julie Bedford	Science and Policy Associates, Inc.	USA
David Bouchard	Great Lakes Chemical Corporation	USA
Rick Bruno	Diamond Walnut	USA
Thomas G. Brydges	Service de l'environement atmospherique	Canada
Eugene Chen	Advance International Co.	USA
Thomas A. Cortina	Cammer and Associates	USA
William D. Dorko	National Institute of Standards and Technology	USA
Michael Eldan	Ameribrom, Inc.	USA
James W. Elkins	National Oceanic and Atmospheric Administration	USA
Gary R. Evans	U.S. Department of Agriculture	USA
S. Fernando Figuerola	Instituto de Investigaciones Technologicas	Chile
Aram Golumbek	Israeli Institute for Biological Research	Israel
Roberto Gonzalez	Asociacion de Exportadores de Chile	Chile
Frank Handy	Great Lakes Chemical Corp.	USA
Igal Hanegbi	Ameribrom, Inc.	USA
Bill Hayes	Ameribrom, Inc.	USA
Rongmei Hu	Permanent Mission of China to UNEP	China
Nobuya Itoh	Fukui University	Japan
Charles E. Kolb	Aerodyne Research Inc.	USA
Bob Krieger	Technical Assessment Systems, Inc.	USA
Joel Levy	National Oceanic and Atmospheric Administration	USA
Jean-Marie Libre	European Methyl-Bromide Association	France
Ronald G. Prinn	Massachusetts Institute of Technology	USA
R. A. Rasmussen	Oregon Graduate Institute of Science and Technology	USA
George C. Rhoderick	National Institute of Standards and Technology	USA
Ralph T. Ross	U.S. Department of Agriculture	USA
David Shapiro	Dead Sea Bromine Group	Israel
Peter Sparber	Sparber and Associates, Inc.	USA
M. Spiegelstein	Bromine Compounds, Ltd.	Israel
Dean Storkan	TriCal, Inc.	USA
Robert Suber	RJR Nabisco	USA
Allen Tillman	Ameribrom, Inc.	USA
Stephen Vogt	Purdue University	USA
David Wardle	Atmospheric Environment Service	Canada
Rene Weber	Great Lakes Chemical Corp.	USA

SECTION D: Concentrations, Lifetimes, and Trends of Chlorofluorocarbons (CFCs), Halons, and Related Molecules in The Atmosphere

CO-CHAIRS

Jack Kaye	National Aeronautics and Space Administration	USA
Stuart Penkett	University of East Anglia	UK

CFC PEER-REVIEW MEETING
BLAKENEY, U.K., January 20-24, 1992

Peter Bloomfield	North Carolina State University	USA
Byron Boville	National Center for Atmospheric Research	USA
Peter Connell	Lawrence Livermore National Laboratory	USA
Tom Duafala	TRICAL	USA
Donald Fisher	E.I. DuPont de Nemours and Company	USA
Paul Fraser	CSIRO	Australia
Amram Golombek	Israel Institute for Biological Research	Israel
Michael Gunson	Jet Propulsion Laboratory	USA
Charles Jackman	NASA Goddard Space Flight Center	USA
Jack Kaye	National Aeronautics and Space Administration	USA
Malcolm Ko	Atmospheric and Environmental Research, Inc.	USA
Joel Levy	National Oceanic and Atmospheric Administration	USA
Hillel Magid	Allied-Signal Corporation	USA
Arjun Makhijani	Institute for Energy and Environmental Research	USA
Pauline Midgley	ICI, Inc.	UK
Ole-John Nielsen	Riso National Laboratory	Denmark
Carol Niemi	Dow Chemical Company	USA
Stuart Penkett	University of East Anglia	UK
Michael Prather	University of California, Irvine	USA
Ronald Prinn	Massachusetts Institute of Technology	USA
Sherwood Rowland	University of California, Irvine	USA
Ulrich Schmidt	KFA Jülich	Germany
Paul Simon	Institut d'Aeronomie Spatiale	Belgium
Hanwant Singh	NASA Ames Research Center	USA
Ray Weiss	Scripps Institution of Oceanography	USA

CHAPTER 1 - MEASUREMENTS

Chapter Coordinator

Paul Fraser	CSIRO	Australia

Lead Authors

Michael Gunson	Jet Propulsion Laboratory	USA
Stuart Penkett	University of East Anglia	UK
Sherwood Rowland	University of California, Irvine	USA
Ulrich Schmidt	KFA Jülich	Germany
Ray Weiss	Scripps Institution of Oceanography	USA

Additional Contributors

Fred Alyea	Georgia Institute of Technology	USA
Don Blake	University of California, Irvine	USA
E. Brunke	CSIR	Rep. South Africa
James Butler	National Oceanic and Atmospheric Administration/CMDL	USA
Derek Cunnold	Georgia Institute of Technology	USA
James Elkins	National Oceanic and Atmospheric Administration/CMDL	USA
Michio Hirota	Japan Meteorological Agency	Japan
F. Irion	California Institute for Technology	USA
Yoshino Makide	University of Tokyo	Japan
Ronald Prinn	Massachusetts Institute of Technology	USA
Rei Rasmussen	Oregon Graduate Institute for Science & Technology	USA
Toru Sasaki	Meteorological Research Institute	Japan
H. Scheel	Fraunhofer Institute for Atmos. Env. Research	Germany
Wolfgang Seiler	Fraunhofer Institute for Atmos. Env. Research	Germany
P. Simmonds	University of Bristol	UK
Hanwant Singh	NASA Ames Research Center	USA

Mail Reviewers

Shyam Lal	Physical Research Laboratory	India
Curtis Rinsland	NASA Langley Research Center	USA
Jochen Rudolph	KFA Jülich	Germany

CHAPTER 2 - PRODUCTION AND EMISSION OF CFCS, HALONS, AND RELATED MOLECULES

Chapter Coordinator

Donald Fisher	E.I. DuPont de Nemours and Company	USA

Lead Authors

Tom Duafala	TRICAL	USA
Pauline Midgley	ICI, Inc.	UK
Carol Niemi	Dow Chemical Company	USA

Additional Contributors

Steven Seidel	Environmental Protection Agency	USA
Arjun Makhijani	Institute for Energy and Environmental Research	USA

Mail Reviewers

Stuart Gaffin	Environmental Defense Fund	USA
Dana Hartley	Georgia Institute of Technology	USA
Archie McCullogh	ICI Chemicals and Polymers, Ltd.	UK

CHAPTER 3 - INFERRED LIFETIMES

Chapter Coordinator and Lead Author

Peter Bloomfield	North Carolina State University	USA

Additional Contributors

Martin Heimann	Max-Planck Institut für Meteorologie	Germany
Michael Prather	University of California, Irvine	USA
Ronald Prinn	Massachusetts Institute of Technology	USA

Mail Reviewers

Lane Bishop	Allied-Signal, Inc.	USA
Margaret Brown	University of Washington	USA
Ian Enting	CSIRO	Australia
J. Mulquiney	Australian National University	Australia
Xufeng Niu	Florida State University	USA
Greg Reinsel	University of Wisconsin	USA

CHAPTER 4 - LABORATORY STUDIES OF HALOCARBON LOSS PROCESSES

Chapter Coordinator and Lead Author

Stanley Sander	Jet Propulsion Laboratory	USA

Additional Contributors

D. Gillotay	Institut d'Aeronomie Spatiale	Belgium
Robert Hampson, Jr.	National Institute for Standards and Technology	USA
Hillel Magid	Allied-Signal Corporation	USA
Ole-John Nielsen	Riso National Laboratory	Denmark
A. Ravishankara	NOAA Aeronomy Laboratory	USA
Paul Simon	Institute d'Aeronomie Spatiale	Belgium

Mail Reviewers

Roger Atkinson	University of California, Riverside	USA
R. Anthony Cox	National Environment Research Council	UK
William DeMore	Jet Propulsion Laboratory	USA
J. A. Kerr	EAWAG	Switzerland
Michael Kurylo	National Institute for Standards and Technology	USA
Robert Lesclaux	Universite de Bordeaux	France
V. Orkin	Russian Academy of Sciences	Russia
Andreas Wahner	KFA Jülich	Germany
Paul Wine	Georgia Institute of Technology	USA

CHAPTER 5 - MODEL CALCULATIONS OF ATMOSPHERIC LIFETIME

Chapter Coordinator

Malcolm Ko	Atmospheric and Environmental Research, Inc.	USA

Lead Author

Charles Jackman	NASA Goddard Space Flight Center	USA

Additional Contributors

Byron Boville	National Center for Atmospheric Research	USA
C. Brüehl	Max Planck Institut für Chemie	Germany
Peter Connell	Lawrence Livermore National Laboratory	USA
Amram Golombek	Israel Institute for Biological Research	Israel
Joel Levy	National Oceanic and Atmospheric Administration	USA
Jose Rodriguez	Atmospheric and Environmental Research, Inc.	USA
Toru Sasaki	Meteorological Research Institute	Japan
Ka Kit Tung	University of Washington	USA

Mail Reviewers

Richard Derwent	UK Department of the Environment	UK
Lesley Gray	Rutherford Appleton Laboratory	UK
Evgeny Jadin	Central Aerological Observatory	Russia
Hans Schneider	CSIRO	Australia
Susan Solomon	NOAA Aeronomy Laboratory	USA

ADDITIONAL CONTRIBUTORS

William. Hill	Allied-Signal, Inc.	
Helene LeTexier	Service d'Aeronomie du CNRS	France
Nien-Dak Sze	Atmospheric and Environmental Research, Inc.	USA
Robert Watson	National Aeronautics and Space Administration	USA

SECTION E: The Atmospheric Effects of Stratospheric Aircraft: Interim Assessment Report of the NASA High Speed Research Program

PRINCIPAL AUTHORS

Daniel L. Albritton	NOAA Aeronomy Laboratory	USA
William H. Brune	Pennsylvania State University	USA
Anne R. Douglass	NASA Goddard Space Flight Center	USA
Frederick L. Dryer	Princeton University	USA
Malcolm K. W. Ko	Atmospheric and Environmental Research, Inc.	USA
Charles E. Kolb	Aerodyne Research, Inc.	USA
Richard C. Miake-Lye	Aerodyne Research, Inc.	USA
Michael J. Prather	University of California, Irvine	USA
A. R. Ravishankara	NOAA Aeronomy Laboratory	USA
Richard B. Rood	NASA Goddard Space Flight Center	USA
Richard S. Stolarski	NASA Goddard Space Flight Center	USA
Robert T. Watson	NASA Headquarters	USA
Donald J. Wuebbles	Lawrence Livermore National Laboratory	USA

OTHER CONTRIBUTORS

Linnea Avallone	University of California, Irvine	USA
Steven L. Baughcum	Boeing Commercial Airplane Group	USA
James E. Dye	National Center for Atmospheric Research	USA
Dieter H. Ehhalt	Institute for Atmospheric Chemistry, KFA Julich	Germany
David W. Fahey	NOAA Aeronomy Laboratory	USA
William L. Grose	NASA Langley Research Center	USA
David R. Hanson	NOAA Aeronomy Laboratory	USA
James R. Holton	University of Washington	USA
Randy Kawa	NASA Goddard Space Flight Center	USA

Michael J. Kurylo	National Institute of Standards and Technology and NASA Headquarters	USA
Max Loewenstein	NASA Ames Research Center	USA
Michael B. McElroy	Harvard University	USA
Munir Metwally	McDonnell Douglas Corporation	USA
Daniel M. Murphy	NOAA Aeronomy Laboratory	USA
Paul A. Newman	NASA Goddard Space Flight Center	USA
Leonhard Pfister	NASA Ames Research Center	USA
R. Alan Plumb	Massachusetts Institute of Technology	USA
Lamont R. Poole	NASA Langley Research Center	USA
Philip J. Rasch	National Center for Atmospheric Research	USA
Jose M. Rodriguez	Atmospheric and Environmental Research, Inc.	USA
Mark R. Schoeberl	NASA Goddard Space Flight Center	USA
Robert K. Seals, Jr.	NASA Langley Research Center	USA
Henry B. Selkirk	NASA Ames Research Center	USA
Margaret A. Tolbert	University of Colorado, Boulder	USA
Darin W. Toohey	University of California, Irvine	USA
Adrian Tuck	NOAA Aeronomy Laboratory	USA
Richard P. Turco	University of California, Los Angeles	USA
Christopher R. Webster	Jet Propulsion Laboratory	USA
James C. Wilson	University of Denver	USA

REVIEWERS

James G. Anderson	Harvard University	USA
Robert E. Anderson	NASA Headquarters	USA
Steven L. Baughcum	Boeing Commercial Airplane Group	USA
Darrel Baumgardner	National Center for Atmospheric Research	USA
Guy P. Brasseur	National Center for Atmospheric Research	USA
William H. Brune	Pennsylvania State University	USA
Ralph J. Cicerone	University of California, Irvine	USA
Estelle Condon	NASA Ames Research Center	USA
Willard J. Dodds	GE Aircraft Engines	USA
Frederick L. Dryer	Princeton University	USA
James E. Dye	National Center for Atmospheric Research	USA
Dieter H. Ehhalt	Institute for Atmospheric Chemistry, KFA Julich	Germany
James W. Elkins	NOAA Environmental Research Laboratories/CMDL	USA
Randall R. Friedl	Jet Propulsion Laboratory	USA
Edwin J. Graber	NASA Lewis Reserch Center	USA
William L. Grose	NASA Langley Research Center	USA
Donald E. Hagen	University of Missouri, Rolla	USA
Neil Harris	British Antarctic Survey	UK
Michael H. Henderson	Boeing Commercial Airplane Group	USA
Richard Hines	Pratt and Whitney	USA
James R. Holton	University of Washington	USA
Ivar S. A. Isaksen	University of Oslo	Norway
Charles H. Jackman	NASA Goddard Space Flight Center	USA
Thomas A. Jackson	Wright Laboratory	USA
Harold S. Johnston	University of California, Berkeley	USA
Jack A. Kaye	NASA Headquarters	USA
Kenneth Kelly	NOAA Aeronomy Laboratory	USA
Nicholas P. Krull	Federal Aviation Administration	USA
Richard L. Kurkowski	NASA Ames Research Center	USA

Michael J. Kurylo	National Institute of Standards and Technology and NASA Headquarters	USA
James G. Lawless	NASA Ames Research Center	USA
James D. Lawrence, Jr.	NASA Langley Research Center	USA
Ming-Taun Leu	Jet Propulsion Laboratory	USA
Joel M. Levy	NOAA Office of Oceanic and Atmospheric Research	USA
Max Loewenstein	NASA Ames Research Center	USA
Nicole Lousinard	Office National d'Etudes et Recherches Aerospatiales	France
Donald L. Maiden	NASA Langley Research Center	USA
James J. Margitan	Jet Propulsion Laboratory	USA
Richard C. Miake-Lye	Aerodyne Research, Inc.	USA
Mario J. Molina	Massachusetts Institute of Technology	USA
Alan K. Mortlock	McDonnell Douglas Corporation	USA
Jarvis Moyers	National Science Foundation	USA
Paul A. Newman	NASA Goddard Space Flight Center	USA
Richard W. Niedzwiecki	NASA Lewis Research Center	USA
Robert C. Oliver	Institute for Defense Analyses	USA
Michael Oppenheimer	Environmental Defense Fund	USA
R. Alan Plumb	Massachusetts Institute of Technology	USA
Michael J. Prather	University of California, Irvine	USA
Michael H. Proffitt	NOAA Aeronomy Laboratory	USA
John A. Pyle	University of Cambridge	UK
A. R. Ravishankara	NOAA Aeronomy Laboratory	USA
David H. Rind	NASA Goddard Institue for Space Studies	USA
F. Sherwood Rowland	University of California, Irvine	USA
Arthur L. Schmeltekopf	NOAA Aeronomy Laboratory (retired)	USA
Stephen Seidel	Environmental Protection Agency	USA
Richard S. Stolarski	NASA Goddard Space Flight Center	USA
Margaret A. Tolbert	University of Colorado, Boulder	USA
Owen B. Toon	NASA Ames Research Center	USA
Adrian F. Tuck	NOAA Aeronomy Laboratory	USA
Richard P. Turco	University of California, Los Angeles	USA
Guido Visconti	Università degli Studi, L'Aquila	Italy
Robert T. Watson	NASA Headquarters	USA
Christopher R. Webster	Jet Propulsion Laboratory	USA
Howard L. Wesoky	NASA Headquarters	USA
Philip D. Whitefield	University of Missouri, Rolla	USA
Allen H. Whitehead, Jr.	NASA Langley Research Center	USA
James C. Wilson	University of Denver	USA
Steven C. Wofsy	Harvard University	USA
Douglas R. Worsnop	Aerodyne Research, Inc.	USA
Donald J. Wuebbles	Lawrence Livermore National Laboratory	USA

SECTION F: Chemical Kinetics and Photochemical Data For Use in Stratospheric Modeling

NASA PANEL FOR DATA EVALUATION

W. B. DeMore, Chairman	Jet Propulsion Laboratory	USA
David M. Golden	SRI International	USA
Robert F. Hampson	National Institute for Standards and Technology	USA
Carleton J. Howard	NOAA Environmental Research Laboratory	USA
Charles E. Kolb	Aerodyne Research, Inc.	USA
Michael J. Kurylo	National Institute for Standards and Technology	USA
Mario J. Molina	Massachusetts Institute of Technology	USA
A. R. Ravishankara	NOAA Environmental Research Laboratory	USA
Stanley P. Sander	Jet Propulsion Laboratory	USA

NASA

Report Documentation Page

1. Report No.	2. Government Accession No.	3. Recipient's Catalog No.
NASA RP-1337		

4. Title and Subtitle	5. Report Date
Present State of Knowledge of the Upper Atmosphere 1993: An Assessment Report Report to Congress	January 1994
	6. Performing Organization Code YSE
7. Author(s) M. J. Kurylo, J. A. Kaye, R.F. Hampson, and A. M. Schmoltner	8. Performing Organization Report No.
	10. Work Unit No.
9. Performing Organization Name and Address NASA Office of Mission to Planet Earth Science Division	11. Contract or Grant No.
	13. Type of Report and Period Covered Reference Publication
12. Sponsoring Agency Name and Address National Aeronautics and Space Administration Washington, DC 20564	14. Sponsoring Agency Code

15. Supplementary Notes

16. Abstract

This document is issued in response to the Clean Air Act Amendment of 1990, Public Law 101-549, which mandates that the National Aeronautics and Space Administration (NASA) and other key agencies submit triennial reports to Congress and the Environmental Protection Agency. NASA is charged with the responsibility to report on the state of our knowledge of the Earth's upper atmosphere, particularly the stratosphere. Part I of this Report, summarizes the objectives, status, and accomplishments of the research tasks supported under NASA's Upper Atmosphere Research Program and Atmospheric Chemistry Modeling and Analysis Program in the years 1990-1991 and 1992-1993.

Part II (this document) presents summaries of several scientific assessments of our current understanding of the chemical composition and physical structure of the stratosphere, in particular how the abundance and distribution of ozone is predicted to change in the future. These reviews include: (Section B) "Scientific Assessment of Ozone Depletion: 1991"; (Section C) "Methyl bromide and the Ozone Layer: A Summary of Current Understanding", published in 1992; (Section D) "Concentrations, Lifetimes, and Trends of Chlorofluorocarbons (CFCs), Halons, and Related Molecules in the Atmosphere"; (Section E) "The Atmospheric Effects of Stratospheric Aircraft: Interim Assessment Report of the NASA High-Speed Research Program"; (Section F) "Chemical Kinetics and Photochemical Data for Use in Stratospheric Modeling"; and (Section G) a list of the contributors to this Report.

17. Key Words (Suggested by Author(s))	18. Distribution Statement
Ozone, Polar Ozone, chloroflurocarbons, CFCs, model results, stratosphere, assessment, PSCs, Montreal Protocol, chemical kinetics, photochemistry, methlbromide	Unclassified-Unlimited Subject Category 46

19. Security Classif. (of this report)	20. Security Classif. (of this page)	21. No. of pages	22. Price
Unclassified	Unclassified	144	A07